# HUMAN EXPOSURE AND ASSOCIATED RISKS DUE TO NATURAL RADIOACTIVITY AND HEAVY METALS IN ORTUM, WEST POKOT COUNTY, KENYA

**WANJALA FELIX OMONYA (M.SC)**

**REG NO. I84/37350/2017**

**PHYSICS DEPARTMENT, KENYATTA UNIVERSITY**

**A THESIS SUBMITTED IN FULFILLMENT OF THE REQUIREMENTS FOR THE AWARD OF THE DEGREE OF DOCTOR OF PHILOSOPHY IN PHYSICS (NUCLEAR PHYSICS) IN THE SCHOOL OF PURE AND APPLIED SCIENCES OF KENYATTA UNIVERSIT*Y***

**MAY 2021**

## DECLARATION

**This thesis is my original work and has not been presented for the award of a degree or any other award in any University**

**Mr. Wanjala Omonya Felix**
Kenyatta University
Physics Department,
P.O. Box 43844,
**Nairobi, Kenya**

**Signature** 29/04/2021 **Date**

**This thesis has been submitted for examination with the approval of Supervisors;**

**Dr. Nadir Hashim**
Kenyatta University
Physics Department,
P.O. Box 43844,
**Nairobi, Kenya**

**Signature** 29/04/2021 **Date**

**Dr. Otwoma David**
Technical University of Kenya
Department of Physics,
P.O. Box 52428-00200,
**Nairobi, Kenya**

Signature 29/04/2021 **Date**

## DEDICATION

This thesis is dedicated to my beloved wife Carmen Atieno, daughter Flavia Atyang and my sons Allan Emukule and Adrian Omonya. I also dedicate this work to my beloved parents Julius Omonya and Bibiana Atyang, Peter Amei and Victorina Naliaka and Michael Makari and Joyce Nafuna for your support.

## ACKNOWLEDGEMENTS

I wish to thank my research project supervisors Dr. Nadir Hashim and Dr. David Otwoma for their professional support, guidance and encouragement that I received from the start to the end of this thesis work. I also extend my gratitude to the entire staff members of the physics department, Kenyatta University for their guidance, corrections, ideas and encouragement during the tenure of this research project.

Special thanks to Kenyatta University, the Institute of Nuclear Science and Technology, University of Nairobi, Kenya Nuclear Regulatory Aurhority, Kenya Bureau of Standards, IAEA Seibersdorf laboratory and Karlsruhe Institute of Technology for their assistance in providing the equipment used for analysis in this research work. I wish to recognize the special assistance I recieved from Mr. Mudimba, Mr. Wataka, Mr. Bartilol, Mr. Keter, Mr. Mauring, Mr. Bojan, Ms. Sibylle, Ms. Susanne, Dr. Kebwaro, Ms. Nyambura, Dr. Chege, Mr. Tollah, Mr. Kiragu, Mr. Ariteluk, Mr. Ndege, Mr. Keter, Ms. Tanya and Mr. Mangala.

I am grateful to the African Development Bank and the Kenya National Research Fund for funding this work. To this end, all the praise and glory goes to God for granting me good health and strength during the entire period of my research work.

## ABSTRACT

The background radiation in air, the activity concentration of selected radionuclides in soil and rock samples, the radon and thoron concentration in selected mud houses and elemental concentration of heavy metals in soil and water samples from Ortum, West Pokot County in Kenya was determined in this study. Ortum was chosen due to the presence of granitic and silicon rocks which are associated with high levels of background radiation. The activity concentration of $^{238}U$, $^{232}Th$ and $^{40}K$ in soil was determined using the High Purity Germanium detector (HPGe) and the average values were 40 ± 3 Bq/kg, 56 ± 4 Bq/kg and 425 ± 19 Bq/kg respectively which is within the world average range. The activity concentration of $^{238}U$ and $^{232}Th$ in soil samples reduced with increasing depth while that of $^{40}K$ increased slightly with increase in depth. The average activity concentration of $^{238}U$, $^{232}Th$, and $^{40}K$ in soil samples was higher than in the rock samples implying that the soils originate from other regions. The average outdoor absorbed dose rate in air at 1 m above the ground was found to be 112 ± 30 nGy/h which is almost double the world average value of 60 nGy/h. The average $Ra_{eq}$ was 153 ± 49 Bq/kg which is less than the limit of 300 Bq/kg and the external hazard indices ($H_{ex}$) and the internal hazard index ($H_{in}$) were 0.41 ± 0.13 and 0.52 ± 0.16 respectively which is below the limit values of unity (>1). This implies that soil and rocks in Ortum poses low radiological risk and they can therefore, be used for construction of houses, industrial and agricultural purposes. The average radon and thoron concentration in mud houses was determined using RADUET detector and found to be 40 ± 19 Bq/m$^3$ and 54 ± 30 Bq/m$^3$ respectively which is below the ICRP recommended lower and upper limit of 100 Bq/m$^3$ and 300 Bq/m$^3$ respectively. The elemental concentration of Ni, Cu, Zn, Pb, K, Ca, Fe, Ti, Mn, Rb, Sr, Zr and Nb in soil was determined using the Energy dispersive X-Ray Fluorescence Spectrometer (EDXRF) and found to be below the WHO recommended limits. The mean concentration of trace elements Pb, Zn and Cu in soil samples reduced with increasing depth while that of Ni increased with increasing depth. The Geoaccumulation Index ($I_{geo}$), Potential Ecological Risk Index ($E_i$) and synthesized potential ecological risk index ($E_r$) were evaluated and found to be -0.40, 4.92 and 19.69 respectively. The results show that soil from Ortum is moderately polluted and the risk associated with exposure to heavy metals in soil is low. The concentration of Ni, Cu, Pb, Zn, Ag, Al, As, Ba, Ca, Cd, Co, Cr, Fe, K, Mg, Mn, Mo, Na and Se in water samples was determine using Agilent-5100 Inductively Coupled Plasma-Optical Emission Spectrometry (ICP-OES). The elemental concentrations in water samples from the two rivers was found to be lower than the WHO permissible limits, except for calcium (Ca) which was higher than the permissible levels in borehole water. Hence, water from rivers in Ortum is unpolluted and fit for use except for borehole water which has high calcium levels. The lifetime cancer risk due to background radiation ($LTCR_{BR}$) and elemental pollution in water ($LTCR_{EP}$) was found to be 1.47 x $10^{-3}$ and 1.92 x $10^{-6}$ respectively which is within the recommended safe limits. The lifetime cancer risk due to exposure to background radiation evaluated using RESRAD programme for a resident farmer in Ortum was found to be 0.011 or 1.1%. This implies that cancer risk due to exposure to background radiation in Ortum is low.

**TABLE OF CONTENTS**

## LIST OF TABLES

## LIST OF FIGURES

## LIST OF PLATES

## ABBREVIATIONS AND ACRONYMS

| | |
|---|---|
| ADRA | Absorbed Dose Rate in Air |
| AEDE | Annual Effective Dose Equivalent |
| ADC | Analog Digital converter |
| ALARA | As Low As Reasonably Achievable |
| ALARP | As Low As Reasonably Practicable |
| AXIL | Analysis of X-ray Spectra by Iterative Least squares fitting |
| Bq/kg | Becquerels per kilogram |
| DNA | Deoxyribonucleic Acid |
| EETC | Equivalent Equilibrium Thoron Concentration |
| EDXRF | Energy Dispersive X-Ray Fluorescence |
| FPM | Fundamental Parameter Method |
| GPS | Global Positioning System |
| HBRA | High Background Radiation Area |
| HPGe | High Purity Germanium |
| IAEA | International Atomic Energy Agency |
| ICP-OES | Inductively Coupled Plasma-Optical Emission Spectrometry |
| ICRP | International Commission on Radiological Protection |
| LTCR | Lifetime Cancer Risk |
| MI | Metal Index |

| | |
|---|---|
| MCA | Multichannel Analyzer |
| MPI | Metal Pollution Index |
| mSv | Millisievert |
| nGy/h | Nano Gray per hour |
| NORM | Natural Occurring Radioactive Material |
| REE | Rare Earth Elements |
| OECD | Organization for Economic Cooperation and Development |
| QAES | Quantitative Analysis of Environmental Samples software |
| RESRAD | RESidual RADioactivity |
| UNSCEAR | United Nations Scientific Committee on Effects of Atomic Radiation |
| U.S. NRC | United States Nuclear Regulatory Commission |
| WHO | World Health Organization |
| WNA | World Nuclear Association |
| XRF | X-Ray Fluorescence |

# CHAPTER ONE: INTRODUCTION

## 1.1 Background information

The level of background radiation, concentration of radon and thoron in mud houses and elemental concentration in soil, rocks and water was determined in ortum region which is located in West-Pokot County in Kenya. Radiation is the energy that travels in space in the form of particles (alpha (α), Beta (β) and neutrons (n)) and rays (cosmic, gamma (γ) and X-rays) which may be able to penetrate matter. Radiation on earth comes from artificial and natural sources which include the sun, rocks, soil, food, water and air as shown in Figure 1.1.

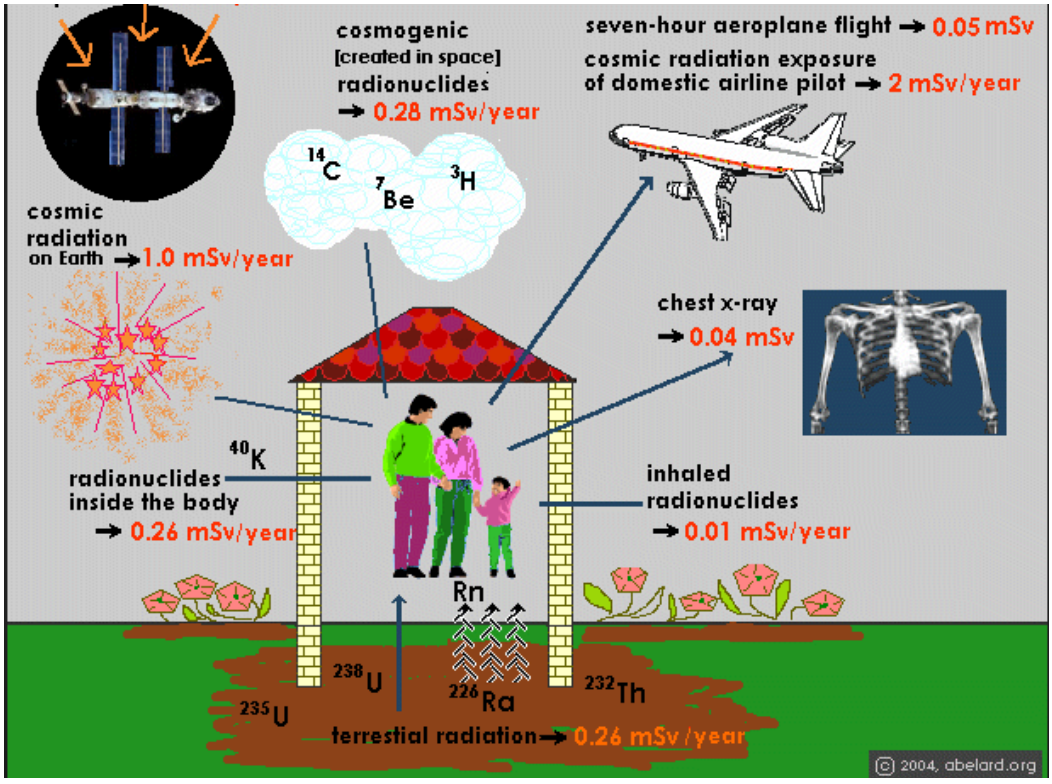


Figure 1.1: Radiation sources on earth (Abelard, 2004)

A relatively small amount of radiation in the environment comes from artificial sources including medical irradiating devices like x-ray machines, nuclear power plants and nuclear medicine (radiopharmaceuticals). Natural background radiation is everywhere on earth and varies from one point to another mainly due to the geological differences on earth, (Kumar *et al.*, 2003). Some places on earth have very high levels of radiation from the normal levels due to abundance of primordial radionuclides and minerals that contain $^{238}$U, $^{235}$U, $^{234}$U, $^{232}$Th and $^{40}$K and their decay products, (UNSCEAR, 2000; Mohanty *et al.*, 2004).

Radioactivity and radiation monitoring in the environment is important for analysing the radiation impact on environment and occupationally exposed persons. (Stochioiu *et al*., 2004). Radioactivity measurement in the environment helps in determining and setting standards and guidelines for the use of soil, rocks, water and vegetation and in assessing the radiation doses, risks and hazard associated with radiation exposure (Krieger, 1981 and OECD, 1979). The potential health effects associated with exposure to high levels of ionizing radiations have made it necessary for continuous environmental monitoring to ascertain the radiation levels in the environment so as to inform and create awareness to the public and policy makers on the surrounding environment in regard to radiation levels.

When man is exposed to ionizing radiation above the threshold levels, living tissue and cells may be damaged causing deterministic and stochastic effects. Deterministic effects are also called non-stochastic effects and they are responses which when the radiation dose increases, the effect or severity of radiation also increases with no threshold dose

below which exposure has no effect as shown in Figure 1.2. Deterministic effects of radiation include skin injury, hair loss and eye cataract. Stochastic effects are chances or probability that the effect will occur (cancer and genetic effects) increases with increase in dose. Stochastic effects have no threshold value.

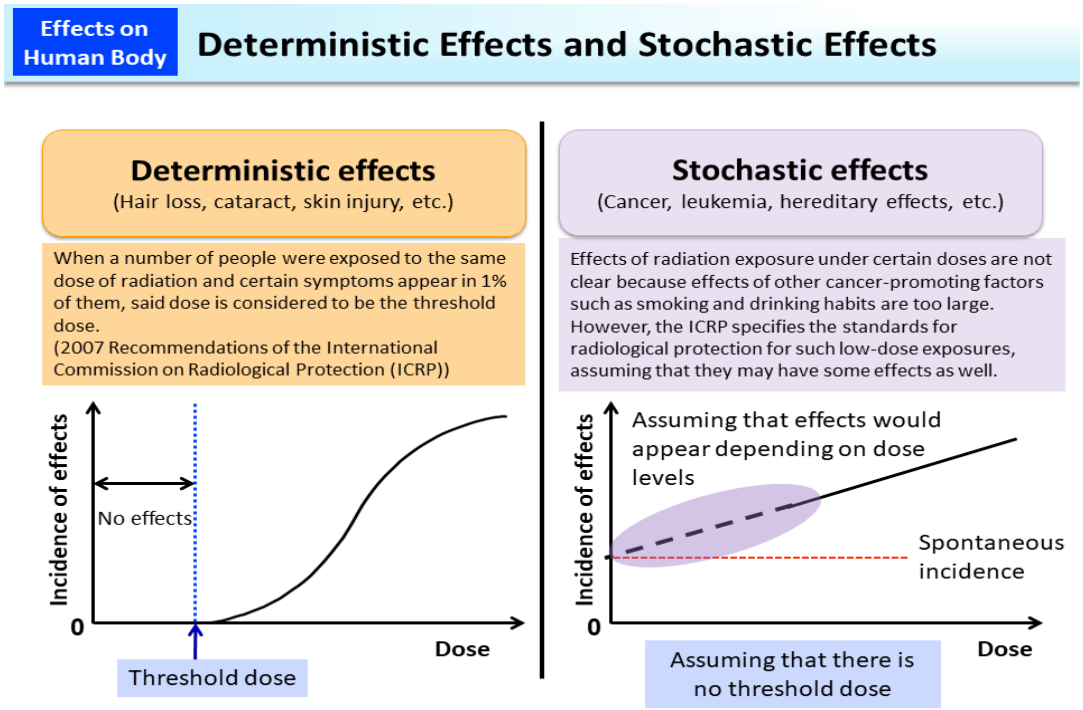


Figure 1.2: Deterministic and stochastic effects of radiation (Holmes-Siedle and Adams., 1993)

Exposure to radiation results to increased probability of getting cancer, leukemia, eye cataracts and sterility or genetic effect which leads to destruction of the germ cells in the reproductive organ causing birth defects, mental retardation, limb deformities and other deformities in offspring's.

Radon and thoron are radioactive colourless and odourless gas found naturally in the environment. Radon accounts to about 55% of the total radiation exposure in the environment (Nazir *et al.,* 2020). Outdoor radon and thoron are not a major risk because they disperses easily in the environments but indoor radon and thoron which is a result of the use of uranium and thorium rich soil and rocks as building materials is major health concern. This is because radon and thoron emanating from soil and rocks which is used as building material is strapped in houses and accumulates to high concentrations especially in houses that are not well ventilated. Hence, monitoring of radon and thoron in houses is important in understanding the levels of radon and thoron so as to take necessary measures due to the associated health risk including lung cancer.

Soil and water are very important resources that supports growth and development of plants and animals on earth. Elemental concentration in soils and water vary from one place to another on earth due to the local geology, agricultural, inductrial and anthropogenic activities. Major and trace element analysis is important in determining the presence of pollutants and for setting standards and guidelines for use of soil and water resources.

Soil and water contains nutrient element required by plants and animals at a certain optimum concentration. Some of these metals include calcium, iron, zinc, cobalt, magnesium, nickel and manganese and if it is less or exceeded, it will lead to deficiency or toxicity symptoms which consequently affect the survival and growth of plants and

animals. Deficiency of some heavy metals in man causes insomnia and chronic pain especially in joints while high levels of some elemental like Pb, Zn, Cd, As, Cr and Ni results to adverse health effects including cancer and damage of the liver, kidney and brain (Austin C. and Vincent S., 2017). Elemental pollution has increased due industrialization and poor disposal of waste containing high levels of heavy metals in the environment. Rocks containing rare earth elements (REE) including granite, niobium and alkaline-silicate found in some parts of Ortum are important raw materials that can lead to mining and technological advancement (Elliott *et al*., 2018). This research aims at determining the concentration of heavy metals in soil and water to give baseline data on elemental concentration, determine the soil and water quality and find possible opportunities for mining important heavy metal in Ortum.

### 1.2 Problem statement

Studies on background radiation and elemental concentration have been carried out in several parts of the world including some parts of Kenya but this has not been done in Ortum region. Man depends on the environment for his livelihood and hence he is continuously exposure to background radiation and intake of heavy metals in the environment (Mohanty *et al.,* 2004). The presence of granitic, silicon and carbonatite rocks in Ortum makes Ortum a possible high background radiation area (HBRA) (Fereira and and Pecequilo, 2019).

Soil, air, water and vegetation are the major human resources which when they are contaminated with high levels of radiation and heavy metals, it can lead to adverse health effects to both plants and animals. Exposure to high levels of radiation may result to eye cataract, leukemia and cancer while deficiency or excess intake of heavy metals like Pb, Cd and Ni in soil and water may results to adverse health effects including cancer and damage of the liver, kidney and brain (Austin C. and Vincent S., 2017).

More focus has recently been directed to radioactivity levels in the environment for the purpose of establishing baseline data to be used for impact and health risk assessment, exploration and radiation protection assessment, (Ramli *et al.,* 2004). There have been several cases of cancer reported in Ortum and this might be associated radiation exposure from the surrounding environment including radon and thoron exposure in mud houses. The cancer statistics report from Moi Teaching and Referral Hospital in Eldoret show that there were 57 cancer cases from West-Pokot in 2019 as shown in Appendix 7. The National Cancer Control Strategy 2011-2016, reported that cancer is caused by abnormal changes due to interactions between genetic and environmental factors including physical carcinogens like ionizing radiation.

The data obtained on radiation levels and elemental concentration will be used as baseline data to compute the dose and associated cancer risks. The data will help to create awareness to the public and policy makers so as to put in place measures to minimize radiation exposure and heavy metal intake if the sources are anthropogenic and for setting standards and guidelines for use of soil and water resources.

## 1.3 Justification

Radiation exposure in the environment varies from one place to another and depends on the geology of the place which includes abundance of uranium and thorium in the soil and rock in the region. The geology of Ortum indicates the presence of granitic, silicon and carbonatite rocks which are associated with high background radiation area (Fereira and & Pecequilo, 2019). Soil and water are essential for the growth of plants and animals. Several places on earth including some parts of Kenya including Mrima hills, Homa Mountains and Nairobi river have been found to have high levels of background radiation and elemental concentration in soil and water (Kebwaro *et al*., 2011, Otwoma *et al*., 2013 and Njuguna *et al*., 2017).

The potential health risks associated to exposure to high background radiation and heavy metals in soil and water have not received adequate attention in terms of research in Kenya. Cancer is ranked as the third cause of death in Kenya and is closely linked to exposure of radiation in the environment which caused damage to the Deoxyribonucleic Acid (DNA) (National Cancer Institute, 2015 and Republic of Kenya, 2011). Globocan 2020 (Bray *et al*., 2020) reported that there are 42,116 new cases of cancer and 27,092 deaths reported annually in Kenya as shown in Appendix 6.

The good agricultural soils and mineral rocks from Ortum hills and Cheranganyi mountains have resulted to settlement and increased human activities in the region like agriculture, mining of gold and quarry which have increased exposure to radiation and heavy metals through ingestion, inhalation and absorption. High levels of some heavy

metal like Pb, Cd and Ni in soil and water results to adverse health effects including cancer, and damage of the liver, kidney and brain. Environmental monitoring is therefore very important in determining the presence of pollutants, setting standards and guidelines for use of soil, rocks and water resources and for providing baseline data for radiation exposure and heavy metal concentration in soil and water ortum.

The data generated will be used to assess the dose and health risks and also create awareness to the public and policy makers to ensure mitigation measures are put in place for protection and safety of the general public. The information on doses and risks will also help to ensure that exposure is as low as reasonably practicable (ALARP) or As Low as Reasonable Achievable (ALARA) by applying the radiation protection principles of reducing exposure time, keeping distance from the source and using radiation shielding. Kenya anticipated to include nuclear energy in its energy mix by 2031. The concentration of uranium in the soil and rocks is therefore important for possibility of uranium mining to provide raw materials for making nuclear fuel.

Studies on levels of radionuclides have not been extensive in Kenya in terms of covering different geographical areas. Therefore, this study will contribute in generating comprehensive baseline data on the levels of background radiation and elemental concentration in soil and water in order to assess associated health risks for residents in Ortum region. The data may be used by the Kenya Nuclear Regulatory Authority to establish the NORM reference levels for compliance with the laws and regulations in Kenya.

## 1.4 Research hypotheses

i. Ortum is a High Background Radiation Area (HBRA)

ii. Rocks and soils in Ortum have high levels of uranium ($^{238}U$) and thorium ($^{232}Th$)

iii. Residents of Ortum have high risks of suffering from radiation and elemental pollution related illnesses

## 1.5 Objectives

### 1.5.1 General objective

The main objective of this study was to determine the levels of background radiation and elemental concentration in soil, rocks and water so as to evaluate the associated dose and risk due to exposure to natural background radiation and hevy metals in Ortum.

### 1.5.2 Specific objectives

i. To determine the levels of naturally occurring radionuclides $^{238}U$, $^{232}Th$ and $^{40}K$ in soil and rocks in Ortum region

ii. To determine the levels of radon and thoron in mud houses in Ortum

iii. To determine the concentration of selected heavy metals in rocks, soil and water in Ortum

iv. To compute the annual effective dose and lifetime risk due to exposure to background radiation and selected heavy metals in Ortum

## 1.6 Scope

The target area of this research is Ortum in West Pokot county covering and area of about 5 $km^2$ which is surrounded by Ortum and Cheranganyi hills. The research focused on determining the background radiation in air, determining the level of $^{238}U$, $^{232}Th$ and $^{40}K$ in soil and rocks, determining the level of radon and thoron concentration in mud houses, determing the elemental concentration in rocks, soil and water and computing the associated annual effective dose and lifetime cancer risk due to exposure to background radiation and heavy metal intake in Ortum.

## 1.7 Limitations of the study

The limitations of this study include limited access to geological data for Ortum region, lack of previous research on background radiation and heavy metal concentration in soil, rocks and water and inaccessibility of some places in Ortum due to the steep terrain and poor access roads. Soil sampling with depth was also affected due to presence of bedrocks which prevented soil sampling with depth at some sampling points.This limitations favoured the choice of purposive sampling method for choosing sampling points for air, soil, rock and water.

# CHAPTER TWO: LITERATURE REVIEW

## 2.1 Radiation exposure

Radiation is the energy that comes from a nuclear reaction and travels in space in form of waves, rays or particles. Radiation with high energy which can ionize atoms when they interact with matter is referred to as ionizing radiation while radiation with low energies which can only excite the atom to higher energy level is referred to as non-ionizing radiation (Campbell and Norman, 1998). The types of ionizing radiation are; alpha (α) particles which can be stopped by a thin piece of paper, beta (β) particles which can be stopped by an aluminium plate and gamma rays (γ), X-rays which have high penetrating power and can be stopped by a thick lead shield and neutrons which can be stopped by water or concrete (Kolb *et al*., 2012) as shown in figure 2.1. Non-ionizing radiation in the environment include radio waves, microwaves and visible light. Radiation exposure in the environment can originate from natural and/or man-made sources as shown in Figure 2.2. Radiation exposure to workers who handle radioactive materials is a major concern today.

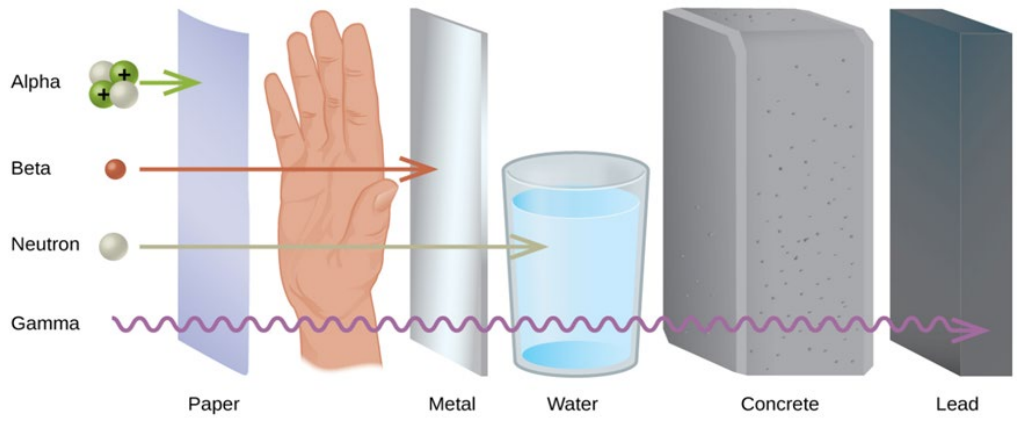


Figure 2.1: Stopping power of ionizing radiation (Kolb *et al*., 2012)

Inhalation of radon and thoron in mines and houses which are not well ventilated is one of the major source of exposure to natural radiation followed by external terrestrial radiation. Man-made exposure to radiation is mainly from the use of radioactives sources in medicine during diagnosis and treatment, scientific research, agriculture, industry, processing and fabrication of nuclear fuel and from radiation released from nuclear power plants and radioactive waste (UNSCEAR, 2000).

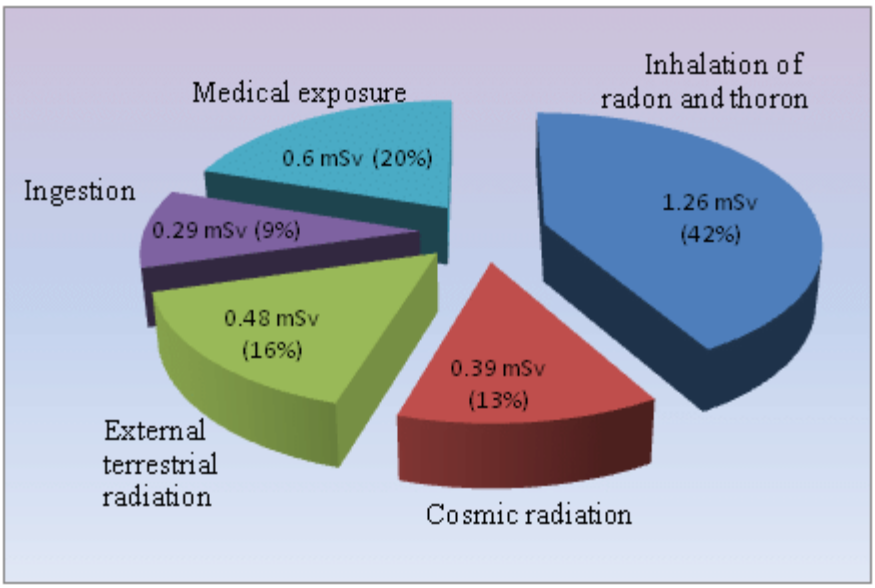


Figure 2.2: Annual radiation exposure from natural and man-made sources (UNSCEAR 2000)

**2.2 Peaceful uses of radiation technology**

Man is continuously exposed to radiation from natural and artificial radiation sources in the environment. Radiation can be good due to its many uses in nuclear science and technology and can also be bad if it is used to develop weapons of mass destruction like atomic bombs which lead to acute exposure to radiation leading to adverse health effects

and death. Man has been using radiation and radioactive materials since its discovery in different fields of peaceful uses like medicine, food and agriculture, industry, water resource management, environment monitoring, education and research and energy.

### 2.2.1 Medicine

There are several uses of radiation in medicine and they include diagnostic and therapeutic uses whereby radiation can be administered either externally or internally. The use of radiation ranges from X-rays to the use of radioactive tracers to diagnose thyroid glands or bone problems, (Waterstram-Rich and Gilmore, 2016). Most commonly, X-rays are used to check for bone fractures and sterilization of medical equipment. Radiation is also used in the treatment of cancers whereby cancerous cells are exposed and killed selectively by radiation beam directed to the cancerous cells. The use of radiation in medicine for diagnosis and treatment has saved many lives (Zanzonico and Stabin, 2009).

### 2.2.2 Food and agriculture

The agricultural sector is key to global economic growth and food security. Nuclear technology like mutation breeding has helped to improve agricultural production and hence contributing to food security through enhanced crop varieties with high yields and resistant to biotic stress or diseases, increased livestock and crop production, improved soil and water management practices, and improved food quality safety.

Nuclear techniques have been used to improve reproductive techniques, breeding, diagnosis and treatment of zoonotic diseases and tracking the transmission pathways of

infectious diseases. The Sterile Insect Techniques (SIT) uses irradiation technique to irradiate male tsetse flies making them infertile and hence mating of released sterile males with female tsese flies in the environment results to production of infertile eggs leading to a drastic reduction of the tsetse flies in the region. The four strategic actions used in SIT are; suppression, eradication, containment and prevention. The sterile insect technique (SIT) has been used to reduce or eradicate tsetse flies and other insects like mosquitos and fruit flies have been also reduced using the same method (Hendrichs *et al*., 2005). This technique has worked in Lambwe Valley in Kenya, Zanzibar, and California to eliminate flies.

Foods that need to be exported like beef, chicken and vegetables are also subjected to radiation to sterilize them, increase their shelf life and kill germs and bacteria, (Molins, 2001).

### 2.2.3 Environmental monitoring

Nuclear techniques are used to understand sources and sinks of pollutants, their transport pathways and their fate in the environment which helps us to manage air, water and soil quality through environmental monitoring by use of radiotracers. The movement of pollutants in the environment can be accurately measured using radioactive tracers, (Hughes *et al*., 2004).

Additionally, radiation processing technology, with other nuclear techniques, are used to killing germs through irradiating of wastewater and support the reuse of treated wastewater for urban irrigation and industrial purposes.

### 2.2.4 Nuclear energy

Nuclear power plants generate abundant, reliable, clean and safe electricity through nuclear fission which involves splitting of atoms. Uranium act as fuel in nuclear power plants. During the fission process, it emits huge amounts of heat energy which is used to boil water into steam that powers the generator to produce electricity. There are over 440 nuclear plants around the world and they contribute to about 16% of the world's electrical energy needs. 109 power plants are in operation in the United states of America and they contributed to about 19% of the United States electricity in 2018, US Energy Information Administration (2019).

### 2.2.5 Industrial application

There are many industrial applications of radiation in the world today. The most common is the non-destructive testing by use of radiography which is used to check the quality of metal parts joints and cracks without destroying the material being checked. Gauges that contain radioactive substances are also used to measure paper thickness, fluid level in oil or chemical tanks and moisture of materials including soil. Well logging equipment use radioactive sources to study formations in deep boreholes for exploration of oil, minerals, gas and groundwater.

The properties of plastics or polymers are modified using radiation without any damage as opposed to the use of heat for example in the manufactuture of car dashboards. Nuclear irradiation facilities utilize gamma radiation and X-rays for varied applications, including

wastewater treatment, sterilization of medical products and irradiation of food products and cultural heritage artefacts, (Hain *et al*., 2005).

### 2.2.6 Water resources management

Nuclear science and technology through isotope hydrology techniques are used to manage and ensure proper utilization of water resources in a sustainable manner. Isotopic nuclear techniques are used to identify and study the sources, extent, transport, quality and interactions of the different components of the water cycle, and to support the development of the national water resource plans for sustainable water management, (Ehleringer *et al*., 2016).

### 2.2.7 Education and research

Radiation equipment and materials are used for education and research purposes in many science fields to enhance our knowledge and understanding necessary to further technological innovation, which brings about changes and new benefits to the society. Nuclear applications and research contribute in many ways to development in many areas including health, power production, food and agriculture, safety and security, industry, environment, and water management.

## 2.3 Non peaceful uses of radiation

Radiation can be used for non peaceful purposes like manufacturing of nuclear bombs like those used in Hiroshima and Nagasaki in Japan on $6^{th}$ and $9^{th}$ August 1945 respectively can have a great negative impact on man and the environment (Ozasa *et al*., 2019).

Radiation exposure can result to adverse health effects including skin and tissue burns, eye cataract, leukemia, cancer, death and genetic effects to offsprings like down syndrome. Nuclear technology can be used to manufacture nuclear weapons which can lead to nuclear insecurity if used in war. This can lead to death of many people and log term health effect to man and the environment due to exposure to high radiation doses as a result of the nuclear explosions. The Nuclear Non-Proliferation Treaty ( NPT ) of 1968 is an agreement signed by several IAEA Member States of the major nuclear and non-nuclear powers to enhance cooperation in stemming the spread of nuclear technology by monitoring movement of nuclear materials so that they are not diverted from their intended peaceful uses (Ford, 2007).

**2.4 Natural background radiation exposure**

Natural background radiation comes from from the rocks and soil of the earth's crust and from cosmic radiation from outer space. The United Nations Scientific Committee on Effects of Atomic Radiation, (UNSCEAR, 2017) reported that natural background radiation which originates from the terrestrial environment, varies worldwide and is the highest contributor to mankind's exposure to radiation.

A high natural background radiation (HNBR) area is a region where the total radioactivity from different sources lead to chronic internal and external exposure to man and the environment. The annual effective dose in HNBR areas is classified into four levels reported by UNSCEAR (2017) as low for less than 5 mSv/y which is about twice the global average of 2.4 mSv/y, intermediate for 5-20 mSv/y; high for 20–50 mSv/y and

finally very high for >50 mSv/y. The Health Physics Society 2010, also reported that the human caused background radiation average exposure is about 5 μSv/y while that due to medical sources ranges from 0.4 μSv/y to 1 μSv/y. Recent studies have shown increased interest in mapping exposures in different places on earth and the data collected show the worldwide average values for $^{238}U$, $^{232}Th$ and $^{40}K$ concentrations in soil as 33 Bq/Kg for $^{238}U$, 32 Bq/Kg for $^{226}Ra$, 45 Bq/Kg for $^{232}Th$ and 420 Bq/Kg for $^{40}K$ and 60 nGy/h in air at 1m above the ground level, (UNSCEAR 2008).

Several studies on the levels of radionuclides have indicated that some regions in the world exhibit high levels of radiation exposure than the recommended threshold levels while other regions experience very low levels of radiation. The World Nuclear Association (WNA) 2021 reported that there are several places with high levels of background radiation and these include the Brazilian beach with the highest in the world at 800 mSv/y and others places like Ramsar (Iran) and Kerala (India) receiving 10 mSv/y and 15 mSv/y respectively.

Some places like the US Naval submarine reactor where the crew are a few meters from a nuclear reactor experience the lowest radiation level of 0.06 mSv/y exposure which is far much below the world average due to less natural background radiation reaching the ship because it is stopped by water and proper shielding of the reactor containment (US Naval data, 2013).

Study on levels of background radiation has been reported in several places in Kenya including Homa Mountains (470 nGy/y, Otwoma *et al.,* 2013) and in Mrima Hills (440

nGy/y by Kebwaro *et al*., 2011 and 106 mSv/y by Patel, 1991). Chronic or acute exposure to ionizing radiation can lead to harmful biological effects like cancer and abnormal growth or death of living cells (WHO, 2016). The common types of terrestrial radionuclides that will be investigated in this research include $^{238}U$, $^{232}Th$ and $^{40}K$.

## 2.5 Radiation exposure pathways

There are three main radiation exposure pathways through which radionuclides enter the human body. These pathways are external radiation, inhalation and ingestion as shown in the Figure 2.3.

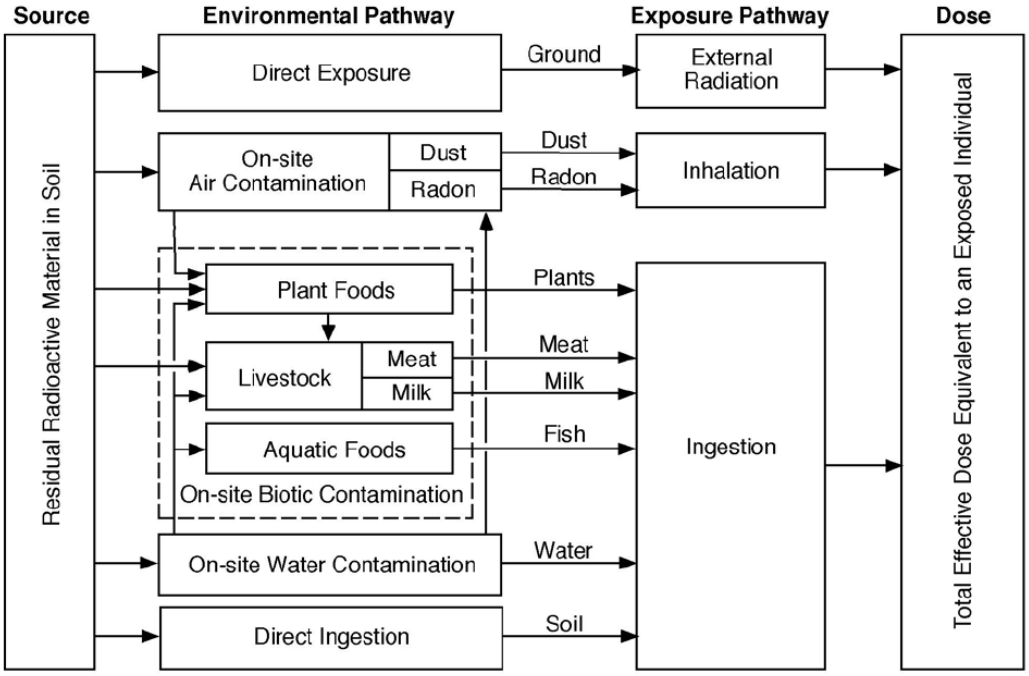


Figure 2.3: Schematic representation of RESRAD Pathways (Yu *et al*., 2001)

### 2.5.1 External radiation pathways

External radiation is due to direct exposure to gamma and beta radiations from radioactive materials in the environment. The dose received due to the external radiation exposure at a point in the environment is measured at 1 meter above the surface of the ground.

### 2.5.2 Inhalation pathways

Exposure due to Inhalation is mainly from radon, thoron and their decay products and dust containing radionuclides, (Yu, *et al.,* 2001). Exposure due to inhalation depends on the time an individual inhale the contaminated dust, the inhalation rate and the concentration of airborne radionuclides in the air at the exposure location.

### 2.5.3 Ingestion pathways

Man can be exposed to radiation through ingestion of food containing radionuclides. These foods include; plant food, meat, aquatic food, water and milk. Contaminated soil can also be directly ingested especially by small children and expectant mothers. The dose received due to soil ingestion depends on the concentration of radionuclides in the soil and the amount of soil ingested.

## 2.6 Exposure scenarios

Man is exposed to radiation naturally from the environment and from artificial sources. Exposure scenarios describe the human activities in the study area that affect the radiation dose received at a given area over a given period of time. In this study, RESRAD ONSITE computer code was used to evaluate and predict the dose and cancer risk due to exposure

to background radiation at different durations ranging from 1 year to 100 years in Ortum. The resident farmer scenario will be used to compute the radiation dose and the associated risks over a period of time ranging 1, 30, 70 and 100 years. The resident farmer is involved in farm activities including farming and taking care of livestock during the day for an average of 8 hours per day and has no protective gear like masks or gloves.

### 2.7 Biological effects of ionizing radiations

Radiations dose received by man depends on the activities that exposes him to radiation sources and the time of exposure which can be either chronic or acute exposure. Acute exposure occurs when one is exposed to very large amount of radiation in a short period of time which can cause sickness or death while chronic exposure is exposure to a small amount of radiation over a long period of time. The health effects associated to acute or chronic exposure to radiation is illustrated in Figure 2.4.

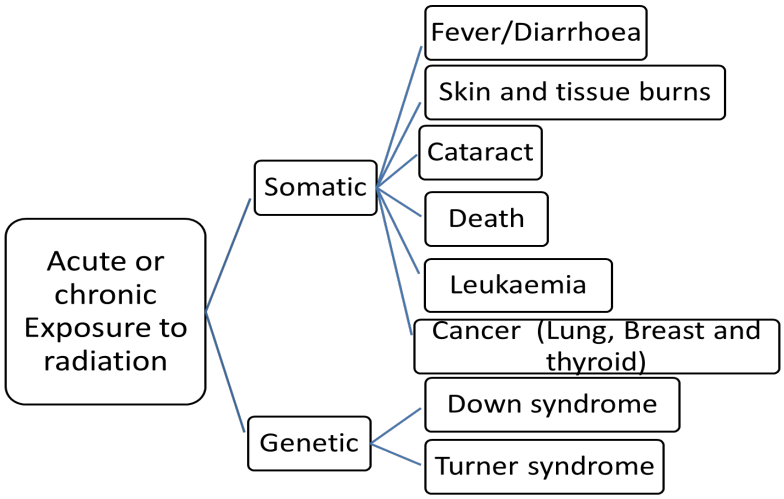


Figure 2.4: Radiation exposure health effects to man

Exposure to radiation doses above a given threshold dose can cause death to cells, organs and tissues and can lead to cancer or genetic effect which affects the person and the germ cells in the reproductive organ leading to birth defects in offspring's, mental retardation and limb deformities, (EPA, 2017).

Cancer risk due to ionizing radiation can be calculated from the radiation doses receive. Many studies have been carried out on the possible health effects caused by exposures to chronic or acute ionizing radiation. This include the study of Hiroshima and Nagasaki atomic bomb survivors in Japan and studies of workers exposed by artificial radiation in medical procedures (UNSCEAR, 2012). WHO, 2016 reported that epidemiological studies done on atomic bomb survivors in Japan or patients undergoing radiotherapy, showed an increase in cancer risk at doses above 100 mSv. Recent studies on pediatric Computer Tomography (CT) have also shown an increase in cancer risk at even lower doses between 50 mSv and 100 mSv.

However, radiation risks due to low-dose exposures is not well understood in terms of setting the safe levels of exposure to ionizing radiation. The risk of getting cancer from exposure to ionizing radiation depends on several factors including sex, age, the exposed organs, time of exposure, level of radiation and other factors like tobacco use.

## 2.8 Limiting radiation exposure

Artificial or natural radiation exposure can be reduced in three main standard ways which are; time, distance and shielding.

### i. Time

People working in areas with high levels of radiation can minimize exposure period or time to reduce the amount of dose received from radiation. This is because radiation dose absorbed is directly proportional to exposure time (Dose = Dose rate x time). Therefore to reduce the dose received, there is need to limit the time spent in the area. In case of a HBRA, the regulatory authorities may prevent access to such areas to avoid exposure of the public to high background radiation.

### ii. Distance

People working in a radiation environment should stay as far as possible from the radiation sources because absorbed radiation dose ($R_d$) received decreases sharply with increasing distance (d) according to the inverse square law ($R_d \propto 1/d^2$). Hence people staying close to a radiation source or HBRA are moved far from the source or area to reduce radiation exposure.

### iii. Shielding

Barriers like skin, aluminium sheet, air, paper, concrete block, lead blocks can be used to block or reduce the amount of radiation passing from one end to another. Shielding can be used to reduce the amount of radiation reaching a worker by creating a barrier to

attenuate the radiation. The thicker the material the more the amount of radiation is blocked. The thickness of the material that reduces the amount of radiation by half is called half-value thickness and half –value thickness depends on the shielding material and the type of radiation.

### 2.9 Research on radioactivity levels

Distribution of radioactive elements is not uniform on earth and hence different regions of the world experience different levels of radioactivity as shown in Table 2.1. Farai *et al*., 2006 reported high dose rate values of 273 mSv/y and 284 mSv/y in Abeokuta and Jose City respectively which are higher than the world's average value of 2.4 mSv as shown in Table 2.1. Research has also shown that high concentration of $^{40}K$, $^{238}U$ and $^{232}Th$ are associated with granitic and silicon rocks, (Brimhal and Adams, 1982) while sedimentary rocks are low emitters of radiations, (Tzortzis *et al.,* 2003).

### 2.10 Exposure to radon and thoron

Radon ($^{222}Rn$) and thoron ($^{220}Rn$) are radioactive gases originating from the decay of uranium and thorium respectively. The concentration of radon and thoron in houses depends on the geological materials like soil and rocks used for building houses. Many studies have been carried out in several places showing high levels of radon and throrn in mud housed including japan (Tokonami, 2010) and in Kenya (Chege, 2015). Inhalation of radon and thoron can cause adverse health effects and the WHO declared radon as the second leading cause of lung cancer after smoking of tobacco (WHO, 2009). Radon and

thoron is measured using a passive discriminative radon detectors called RADUET (Tokonami, 2010).

Measurement of radon and throron is important from a health point of view public. The data will provides recommendations on how best to reduce health risks associated to exposure from radon and thoron as well as policy options for preventing and mitigating radon and thoron exposure.

Table 2.1: World and selected countries average radiation levels

| **S/N** | **Reporter** | **Country** | **Place** | **Average level** |
|---|---|---|---|---|
| 1 | UNSCEAR, 2000 | World average | | 2.4 mSv/y |
| 2 | World Nuclear Association, 2015 | Brazil | Brazilian Beach | 800 mSv/y |
| 3 | World Nuclear Association, 2015 | Iran | Ramsar | 10 mSv/y |
| 4 | World Nuclear Association, 2015 | India | Kerala | 15 mSv/y |
| 5 | US Noval Submarine, 2013 | USA | Submarine | 0.06 mSv/y |
| 6 | Farai *et al*. 2006 | Nigeria | Abeokuta | 273 mSv/y |

In Kenya, previous research on levels of radionuclide have shown both high and low background radiation levels in different parts as shown in Table 2.2. Otwoma *et al.* (*2*013) investigated radiological hazard of naturally occurring radioactive material in Mount Homa in South Western Kenya and found the mean value of radiation levels for $^{226}Ra$, $^{232}Th$ and $^{40}K$ to be 195 Bq/kg, 409 Bq/kg and 915 Bq/kg respectively with the mean gamma radiation at 1 meter above the ground of 470.4 nGy/h. This is above the world

average values of 32 Bq/kg for $^{226}$Ra, 45 Bq/kg for $^{232}$Th and 420 Bq/kg for $^{40}$K and 60 nGy/h, (UNSCEAR 2008) for dose rate in air. Kebwaro *et al.,* (2011) also measured high levels of $^{238}$U, $^{232}$Th and $^{40}$K with the average concentration being 207.03 ± 11.3 Bq/kg, 500.7 ± 20.3 Bq/kg, 805.38 ± 20.7 Bq/kg and 440 nGy/h respectively around Mrima Hills.

Table 2.2: Radiation Levels in Kenya (Bq/kg)

| **Author** | **Place** | **Radiation in air (nGy/h)** | **$^{238}$U Bq/kg** | **$^{232}$Th Bq/kg** | **$^{226}$Ra Bq/kg** | **$^{40}$K Bq/kg** |
|---|---|---|---|---|---|---|
| Kebwaro *et al*., 2011 | Mrima Hills | 440.7 | 207.0 | 500.7 | - | 805.4 |
| Otwoma *et al*., 2013 | Homa mountains | 470 | - | 409 | 195 | 915 |
| UNSCEAR, 2008 | World Average | 60 | 33 | 45 | 32 | 420 |

The two research studies conducted in Kenya in Mrima Hills and Homa mountains show that the levels of radionuclides $^{238}$U, $^{226}$Ra, $^{232}$Th and $^{40}$K were higher than the world average levels given by UNSCEAR (2008). In this study, the levels of radionuclides $^{238}$U, $^{232}$Th and $^{40}$K in soil and rocks from Ortum was determined and the ingestion, inhalation and external radiation pathways were consider under the resident farmer exposure scenario to compute the dose and cancer risks associated to the exposure to background radiation in Ortum using RESRAD ONSITE computer code.

## 2.11 Heavy metals in soil and rock samples

Soil is formed as a result of weathering of rocks and it is a mixture of minerals, water, air and organic matter. The typical soil is composed of approximately 45% mineral, 20 - 30% water, 20 - 30% air and 5% organic matter, (McClellan *et al*., 2013). Soil contains nutrient elements required by both plants, animals and man at a certain optimum concentration, which if it is less or exceeded, it will lead to deficiency or toxicity symptoms which consequently affect the survival and growth of plants, animals and human beings. Some of these elements include; macronutrients potassium (K), calcium (Ca), magnesium (Mg), nitrogen (N), phosphorus (P), and Sulphur (S) and the micronutrients copper (Cu), zinc (Zn), nickel (Ni), chlorine (Cl), boron (B), iron (Fe), manganese (Mn) and molybdenum (Mo) as stated by White and Brown, (2010). The composition of these elements in the soil is critical for plant survival and enables us to classify the soils as fertile, infertile or poor for plant growth and more so if they are polluted.

Most of the soils especially in cities, industrial and mining areas have been polluted through dumping and settling of dust containing high levels of metal pollutants especially those in the lower land which are contaminated due to runoff and leaching (Ribeiro *et al*., 2019). This study will help determine elemental concentration in soils and rocks in Ortum to determine if the soil is polluted by comparing the levels of heavy metals in soils and rocks. This will enable necessary action to be taken in case the soil is polluted through anthropogenic sources to ensure the safety of man and the environment.

## 2.12 Heavy metals in water samples

Clean water is very essential for human, animal and plant life. However, due to industrialization and increased population, human activities like mining and dumping of waste into rivers and other water sources have resulted to water pollution. Most of the surface and underground water sources in most parts of the cities and towns have been polluted making it not fit for human consumption, (Ntengwe, 2005). Njuguna *et al*., 2017, found very high levels of heavy metals in nairobi river above the recommended levels by WHO. When water is contaminated with heavy metals, it becomes a health risk to people and the environment (Johri *et al*., 2010) and hence the need for this research to determine the levels of heavy metals in the water from Ortum to inform the public on how well to use and manage water resources to reduce heavy metal pollution so as to improve water quality.

# CHAPTER THREE: MATERIALS AND METHODS

## 3.1 Study area

The study covered an area of 5 $km^2$ of the larger Ortum region, which is in the Rift Valley, West Pokot County, Kapenguria constituency about 450 km North West of Nairobi City as shown in Figure 3.1 and 3.2. Ortum lies between longitude $35^O$ 15' E and $35^O$ 20' E and latitude $1^O$ 10' N and $1^O$ 30' N in a broad depression at an altitude of about 1550 m above the sea level surrounded by Cheranganyi hills to the Eastern side and Ortum hills to the Western and Northern part. The main economic activities of the people of Ortum include; agriculture, gold mining, quarrying and building and construction.

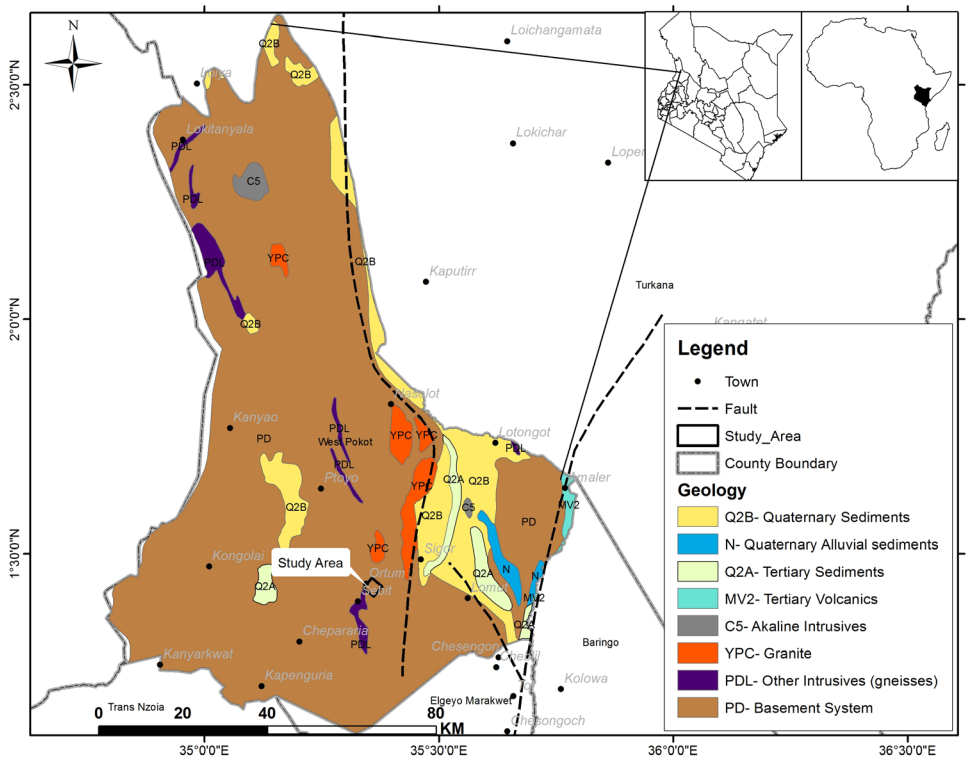


Figure 3.1: Geological map of Ortum in West Pokot County

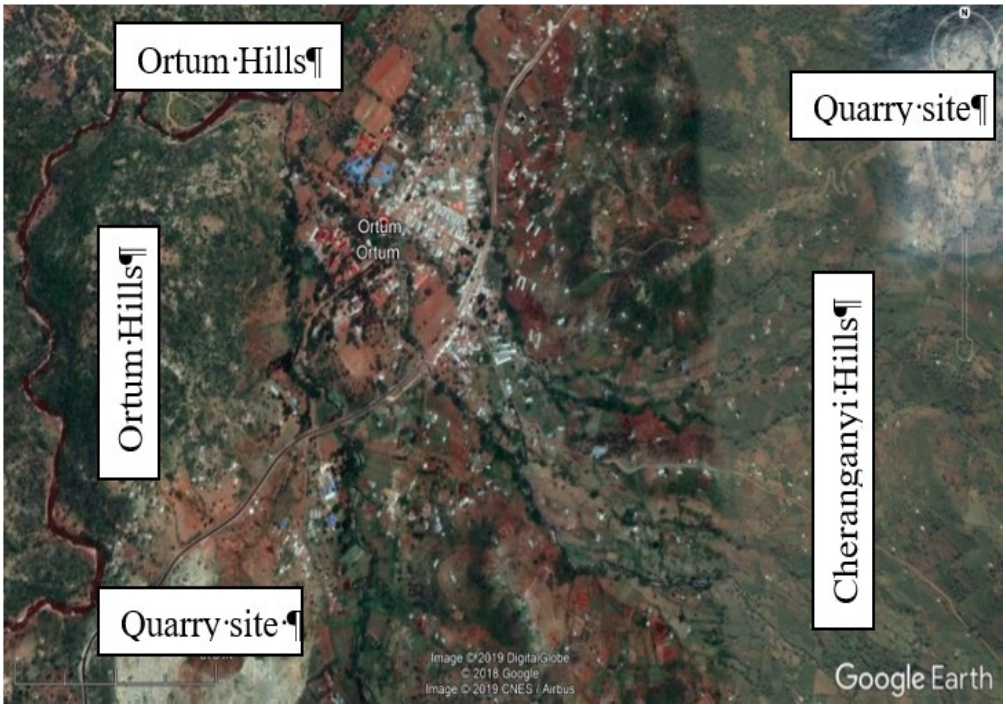


Plate 3.1: Arial map of Ortum (Scale 1cm = 200 m)

Plate 3.2: Rock harvesting in Ortum quarry area

Several companies harvest rocks from the quarry sites from Ortum and Cheranganyi hills as shown in plates 3.1 and 3.2. The residents of Ortum get their water from Kerelwa and Tipagh rivers which flows from South-East to North-West of Ortum passing through Ortum Hospital and Ortum Centre. The water from the two rivers is of great importance to the people of Ortum since it is used for drinking and irrigation purposes. Hence the need to take good care so that it is not polluted as a result of disposal of domestic and mining waste. Some of the major institutions in Ortum like Ortum Secondary School, Holy Rosary Girls Secondary School, Ortum Primary School and Ortum Hospital have piped water coming from the two rivers and by gravity from the springs on top of the hills. Ortum Secondary School gets its water which is not treated from the two boreholes in school and from piped water originating from the two rivers.

### 3.2 Research design

This study used descriptive experimental design method to study radiation exposure levels in air, soil and rocks and elemental concentration in soil, rocks and water in Ortum. The study used purposive sampling method to identify sampling point for soil, rock, and water sample according to the terrain, accessibility and ease of collecting samples at the study area. Measurements of radiation levels in air and water pH at different points was done directly in the field (*insitu*) while the radiation levels and elemental concentration in soil, rocks and water was determined in at different laboratories in Kenya.

### 3.3 Soil and rock sample collection

Proper sample collection, preparation and storage methods are critical and very important in ensuring that the research results obtained from the experiment are credible and reliable to establish background levels and determining the nature of the contamination for a specific site (IAEA, 2019). During sampling, great care was taken into consideration to avoid contamination of samples collected for analysis. A total of 35 soil samples of about 1 kg each were taken from the surface soils at different locations as shown in Plate 3.3 and ten (10) rock samples were also collected for analysis of levels of radionuclides and elemental concentration as shown in Plate 3.4.

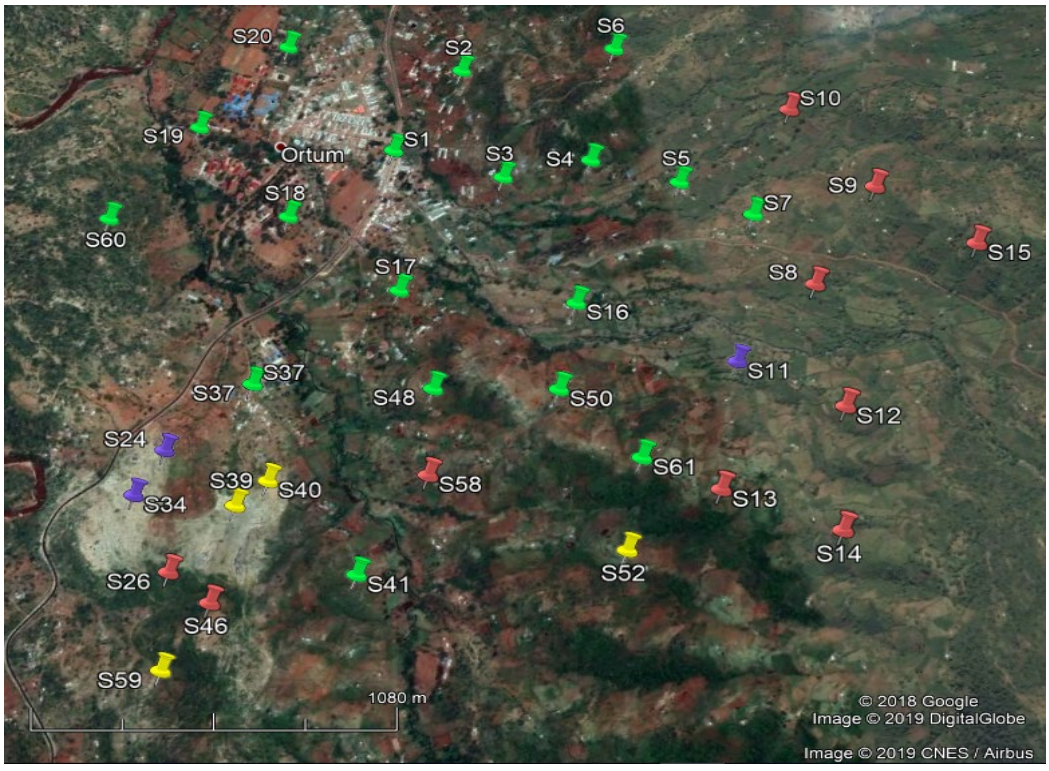


Plate 3.3: Surface soil sampling points in Ortum

The collected soil samples were enclosed in transparent polythene bags and labeled according to sampling location. The 10 rock samples were collected from different points in Ortum as shown in Plate 3.4, packed in a polythene bag and labelled from Rock-01 to Rock-10 as shown in Plate 3.5.


Plate 3.4: Rock sampling points in Ortum (scale 1cm = 200m)

The sampling locations for the soil and rocks was recorded using a hand held Global Positioning System (GPS) model etrex Venture HC Garmin as shown in Plate 3.6 in degree-minute-second (latitude and longitude position) and the level of radiation in air was measured using the Hand-Held Radiation meter (RadEye) shown in Plate 3.7 and the RADOS RDS-110 Plate 3.8.


Plate 3.5: Rock samples in a polythene bag


Plate 3.6: etrex Garmin GPS


Plate 3.7: Handheld RadEye


Plate 3.8: Handheld Rados RDS-110

A total of 24 Soil samples were collected with depth from 8 locations (S1, S13, S15, S22, S23, S37, S46 and S50) as shown in plate 3.9 in Ortum at a depth of 0 cm to 5 cm (surface soil), 10 cm to 20 cm and 30 cm to 40cm using the soil auger, hoe and a panga. The collected soil samples were then labeled according to the sampling location and depth.

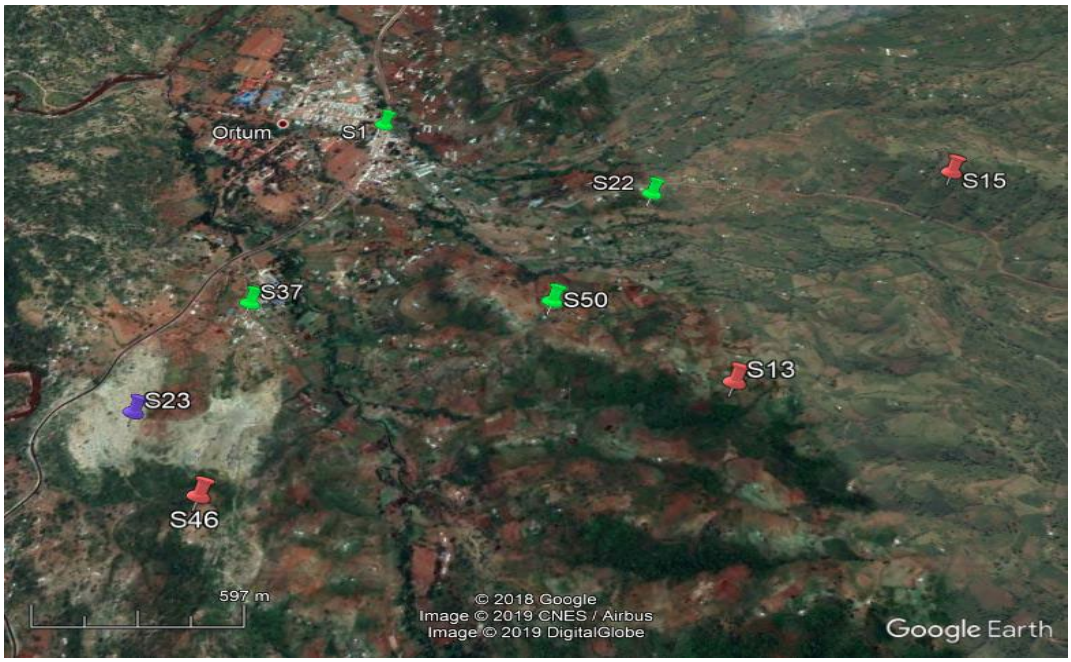


Plate 3.9: Soil sampling points with depth

### 3.4 Soil and rock sample preparation

The soil and rock samples collected from different sampling points were cleaned by removing small stones and grass. The soil and rock samples were then oven dried for 24 hours at 110 ºC and crushed to fine powder using a Herzog grinder, homogenized and sieved by passing them through 100 µm sieve shown in Plate 3.10 and 3.11. About 350 grams of each of the soil and rock samples were then put in a leak- proof and air tight plastic containers (Plate 3.12), mixed well using a mixer (Plate 3.13) and stored for one

month to ensure secular equilibrium between radiam-226 ($^{226}$Ra), thorium-232 ($^{232}$Th), the noble gas radon-222 ($^{222}$Ra) and their decay products, (Nwankwo *et al*., 2015).

Plate 3.10: 100 µm soil sieve

Plate 3.11: Sieved rock and soil samples

Plate 3.12: Packed and stores soil samples

Plate 3.13: Soil sample mixer

Secular equilibrium is reached when the daughter radionuclide has the same activity as the parent radionuclide ($A=\lambda_p N_p = \lambda_d N_d$) as shown in Figure 3.2. where A is the activity of the sample, $\lambda_p$ and $\lambda_d$ are the decay constants for the parent and daughter radionuclides

and $N_p$ and $N_d$ are the number of atoms of the parent and daughter radionuclides present at a given time.

The soil samples were then subjected to HPGe Detector and EDXRF analysis to determine the level of radioactivity and elemental concentration of selected metals in the soil and rock samples respectively.

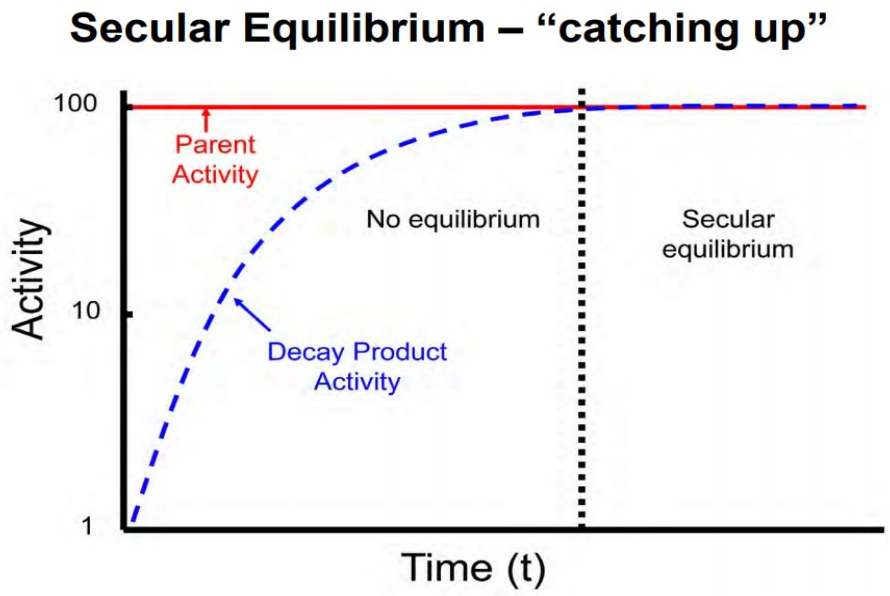


Figure 3.2: Secular equilibrium graph for parent and daughter radionuclides (Cetnar, 2006)

### 3.5 Water sample collection and preparation for heavy metal analysis

A total of 10 water samples of 1 liter each was collected from the rivers, boreholes and taps whose water originates from the 2 rivers in Ortum for analysis. The water sampling points were recorded using etrek Garmin Global Positioning System (GPS). Three water samples WS1, WS2 and WS3 were collected from different points along Kerelwa River which originates from Koporoch springs, three water samples WS4, WS5 and WS6 were also collected at different points along Tipagh river, two water samples WS7 and WS8

were collected from the taps at Ortum shopping center and lastly two water samples WS9 and WS10 were collected from 2 boreholes at Ortum Secondary school as shown in Table 3.1 and Plate.3.14.

Table 3.1: Ortum water sampling points

| | **Places** | **No of samples and labels** |
|---|---|---|
| 1. | Kerelwa river | 3 (WS1, WS2 and WS3) |
| 2. | Tipagh river | 3 (WS4, WS5 and WS6) |
| 3. | Ortum Town tap water | 2 (WS7 and WS8) |
| 4. | Ortum Secondary School Borehole | 2 (WS9 and WS10) |

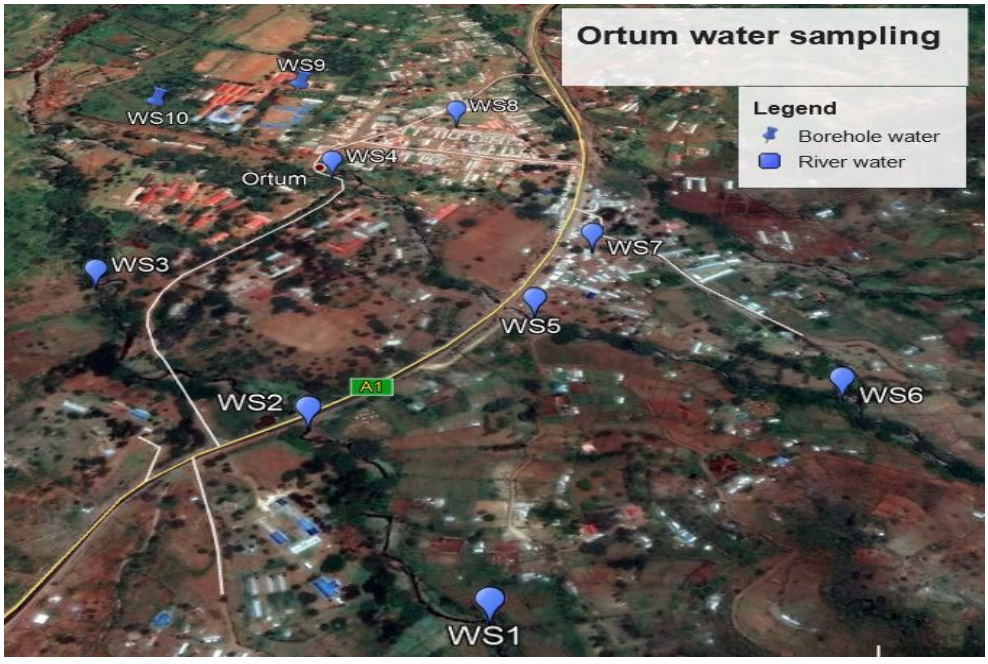


Plate 3.14: Ortum water sampling points (Scale 1cm =200m)

### 3.6 Water sample preparation and analysis

Water sample analysis was done both in situ and at the Kenya Bureau of Standards laboratory in Nairobi. The Hydrogen Ion Concentration (pH) was measured in the field using a portable pH meter. The collected water samples were then taken to the laboratory and filtered using a 4.5 µm pore size filter, acidified with concentrated nitric acid to a pH of 2 to avoids precipitation and adsorption on the container walls. Elemental concentration of the selected 19 elements (Cu, Ni, Pb, Zn, Ag, Al, As, Ba, Ca, Cd, Co, Cr, Fe, K, Mg, Mn, Mo, Na and Se) was determined using Agilent-5100 Inductively Coupled Plasma-Optical Emission Spectrometry (ICP-OES) at the Kenya Bureau of Standards, Nairobi, Kenya.

### 3.7 Measurement of external gamma radiation dose rate in air

Measurement of radiation in air at 1m above the ground was done in the field at 61 different locations in Ortum as shown in Plate 3.15 using the hand-held multi-purpose survey meters (RadEye B20 and the RADOS RDS-110) obtained from the Kenya Nuclear Regulatory Authority (KNRA). The energy range of the RadEye B20 is 17 keV to 1.3 MeV while that of RADOS RDS-110 is 50 keV to 3 MeV respectively. The RadEye and the RADOS-110 are advanced handheld instruments used for measuring radiation in a given area by measuring gamma dose rates in µSv/h or counts per second (CPS). The average values from the reading of both instruments was taken and recorded against the sampling point. Calibration of the survey meters was done at Tanzania Atomic Energy Commission's Secondary Standards Dosimetry Laboratory to check on the sensitivity, accuracy and reliability of the radiation survey meters.

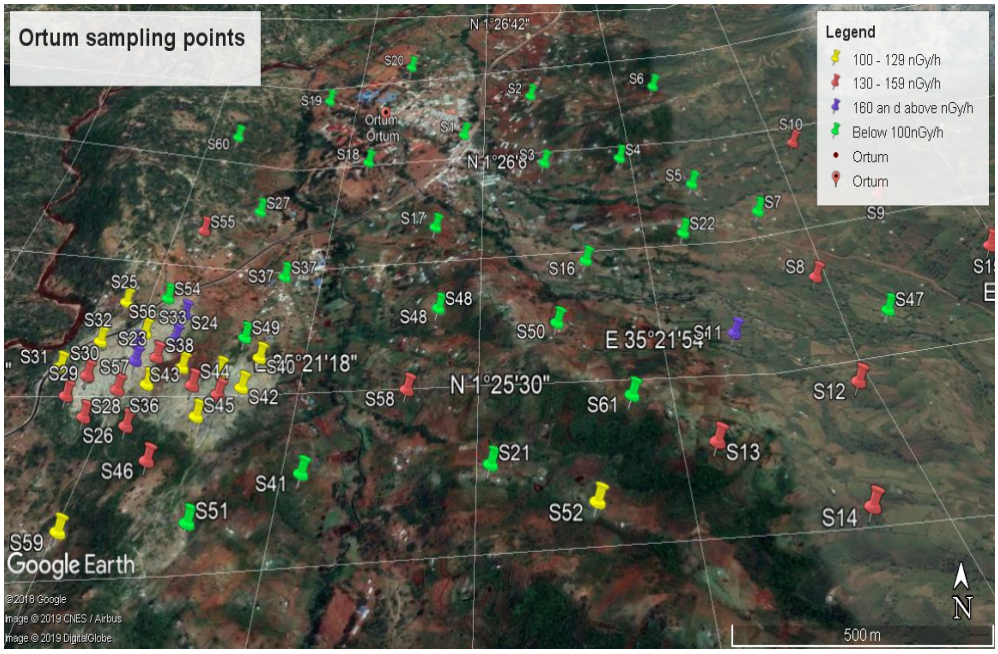


Plate 3.15: Radiation in air measurement points (Scale 1cm = 150m)

### 3.7.1 Annual effective dose equivalent (AEDE)

The annual effective dose equivalent (AEDE) received from terrestrial gamma radiation in Ortum region was calculated using Equation 3.2, (UNSCEAR, 2000) and the results are shown in table 4.4 and 4.6.

$$AEDE = D_{Air} \times F \times T \qquad 3.2$$

Where $D_{air}$ is the annual dose rate in air, F is the conversion factor which is 0.7 Sv/Gy and converts the absorbed dose rate in air to human effective dose rate and T is the outdoor occupancy time of 1 year.

### 3.8 High Purity Germanium (HPGe) detector

The gamma ray spectrometry employs the principal of direct proportionality between the energy of the incoming gamma ray and the pulse amplitude at the outputs of the detector to identify and quantify the activity of radionuclides in a sample (IAEA, 2003). The High Purity Germinium detector (HPGe) at INST-UoN was use to measures the activity of radionuclides $^{238}U$, $^{232}Th$, and $^{40}K$ in soil and rock sample collected from Ortum.

#### 3.8.1 HPGe detector instrumentation

The concentration of the radionuclides in the soil and rock sample was determined using the High Purity Germanium detector (HPGe) model No. CPVDS30-30185 at the Institute of Nuclear Science and Technology, University of Nairobi shown in Plate 3.16. The detector is housed in a cylindrical lead shield with inside diameter of 57.4 mm and outside diameter 76 mm, length 56.9 mm with an active volume of 144 $mm^3$.The detector has an efficiency of 31.6% and a resolution of 1.8 KeV at 662 keV line of Ceasium-137 ($^{137}Cs$). The background activity in the laboratory was determined prior to the sample activity measurement using an empty plastic beaker with the same geometry under the same measurement conditions as the sample using the HPGe detector for a period of 10 hours. The measured background gamma radiation was then subtracted from each of the samples gamma spectra to obtain the spetra due to the activity of the sample.


Plate 3.16: HPGe detector at the INST-University of Nairobi.

### 3.8.2 Efficiency calibration for HPGe detector

Instrument calibration is an important process that helps in checking the quality and reliability of the results obtained. In this research, efficiency calibration for HPGe detector was performed using a standard reference material RGU-1, RGTh-1 and RGK-1 supplied by the International Atomic Energy Agency (IAEA). with known activity concentrations using Equation 3.3 given by Al-Zahrani, 2017.

$$\varepsilon = \frac{N}{A\ x\ \varepsilon \times P_{\gamma} \times M \times T} \qquad 3.3$$

Where, $\varepsilon$ is detector efficiency, A is activity concentration of the isotope measured in Bq/kg, N is the net area under the photo peak, T is the counting time (10 hours), $P\gamma$ is the emission probability of the energy of interest as shown in Appendix 5 and M is mass of the sample in Kg.

### 3.8.3 Energy calibration for HPGe detector

The HPGe detector energy calibration was done by relating the channel number with the photon energy using the Gamma lines $^{214}$Pb, $^{214}$Bi, $^{228}$Ac, $^{40}$K and $^{214}$Bi with energies 351 KeV, 609 KeV, 911 KeV, 1460 KeV and 1765 KeV respectively (Wanjala *et al*., 2019 and Otwoma *et al*., 2013) using the Equation 3.4.

$$E = a\,x\,(Ch) + b \qquad 3.4$$

Where E is the energy, a and b are constants and Ch is the channel number.

Activity concentration of $^{238}$U, $^{232}$Th and $^{40}$K in soil samples was determined using the counts under the gamma line of 351 KeV ($^{214}$Pb) and 609 KeV ($^{214}$Bi) for $^{238}$U, 911 KeV ($^{228}$Ac) for $^{232}$Th and 1461 KeV (40K) for $^{40}$K as shown in figure 3.3.

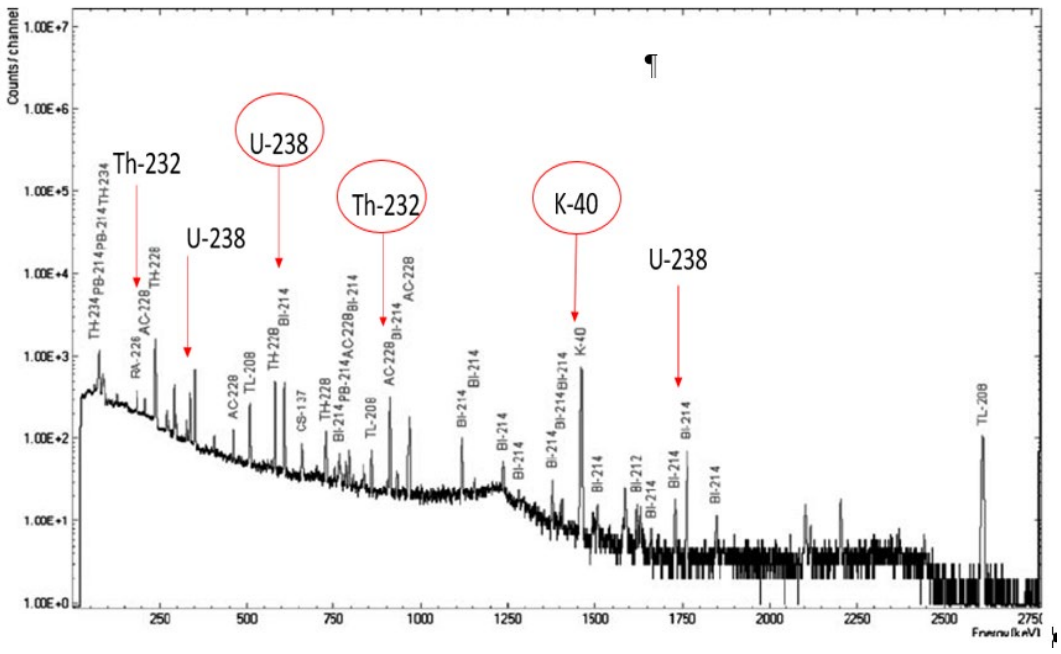


Figure 3.3: Typical NORM spectrum (Kumar, 2011)

MAESTRO Multichannel Analyzer Emulation Software was used for spectrum acquisition. The time used for spectrum acquisition for each soil sample was 10 hours. An empty container with the same geometry as the one used for soil sample analysis was analyzed under similar conditions to obtain the background net counts (background correction). The net counts from sample analysis was then found by subtracting the background counts as described by Mustapha *et al*., 1997.

### 3.8.4 Radioactivity analysis in soil sample

The soil samples were stored for one month in an identical plastic container to ensure secular equilibrium between $^{226}$Ra and its decay products. The soil sample was then analysed using HPGe detector for radionucuclide identification and qauntification. The sample matrix and detector geometry for the reference sample and the soils were the same. The standard reference samples and the soil and rock samples were analysed for 10 hours and the results of the intensity obtained were used in the comparative formula to determine the activity concentrations of the radionuclides in the sample given in the Equation 3.5.

$$\frac{M_S A_S}{I_S} = \frac{M_r A_r}{I_r} \qquad 3.5$$

Where, $M_s$ is the mass of the soil sample material, $M_r$ is the mass of the standard reference material, $I_s$ is the intensity of the sample, $I_r$ is the intensity of the reference material, $A_s$ is the activity of the sample and $A_r$ is the activity of the reference material.

### 3.8.5 Absorbed dose rate in air (ADRA)

The absorbed dose rate in air (ADRA) at 1m above the ground was calculated using the Equation 3.6 by UNSCEAR, 2000 and the results displayed in table 4.6.

$$ADRA = 0.462\ A_{Ra} + 0.621A_{Th} + 0.0417\ A_K \qquad 3.6$$

Where $A_{Ra}$, $A_{Th}$ and $A_K$ are the activity concentration of $^{226}$Ra, $^{232}$Th and $^{40}$K respectively in the soil samples expressed in Bq/kg.

### 3.8.6 Radium equivalent

Radium equivalent activity is the activity level of $^{226}$Ra, $^{232}$Th, and $^{40}$K which considers the associated radiation hazards of each of the radionuclides. This was calculated using Equation 3.7 given by Beretka and Mathew 1985 and the results are shown in table 4.4 and 4.6.

$$Ra_{eq} = A_U + 1.43A_{Th} + 0.077A_K \qquad 3.7$$

Where $A_U$, $A_{Th}$ and $A_k$ are the specific activities of $^{238}$U, $^{232}$Th, and $^{40}$K respectively. The Equation 3.7 assumes that 10 Bq/kg of $^{238}$U, 7 Bq/kg of $^{232}$Th, and 130 Bq/kg of $^{40}$K produce the same gamma radiation doses. OECD (1979) and Beretka and Mathew (1985) stated that the allowed $Ra_{eq}$ using the Equation 3.37 should be less than 370 Bq/kg for safe use of building materials.

### 3.8.7 External radiation hazard index ($H_{ex}$)

The risk due to exposure to gamma radiation from natural radionuclides $^{238}U$, $^{232}Th$ and $^{40}K$ in soil is termed as external radiation hazard index ($H_{ex}$) The allowed value for $H_{ex}$ should be less than unity (<1). The external hazard index is calculated using the Equation 3.8, (Krieger 1981).

$$H_{ex} = \frac{A_U}{370} + \frac{A_{Th}}{259} + \frac{A_K}{4810} \qquad 3.8$$

Where $A_u$, $A_{Th}$ and $A_K$ are the activity concentration of $^{226}Ra$, $^{232}Th$ and $^{40}K$ respectively. The extent of radiation effect associated with exposure to natural radionuclides present in soil and rocks samples was evaluated using $H_{ex}$ since the soil and rocks from the region are used as buildings materials for dwellings in Ortum.

### 3.8.8 Internal radiation hazard index ($H_{in}$)

Radon ($^{222}Rn$) is a short lived and hazardous gas especially to the respiratory organs. The internal exposure to $^{222}Rn$ and its daughter products doubles the risk of exposure and hence the Internal Hazard index ($H_{in}$) is calculated using Equation 3.9, (Krieger 1981) and the results are displayed in table 4.4 and 4.6.

$$H_{In} = \frac{A_U}{185} + \frac{A_{Th}}{259} + \frac{A_K}{4810} \qquad 3.9$$

Where $A_u$, $A_{Th}$ and $A_K$ are the activity concentration of $^{238}U$, $^{232}Th$ and $^{40}K$ respectively Internal Hazard ($H_{in}$) index determines the hazard to respiratory organs caused by radon

emanating from the soil and rocks used to build house in Ortum. For safe use of soil and rock materials for construction of houses, $H_{ex}$ and $H_{in}$ should be less than unity (<1).

### 3.8.9 Dose to risk conversion

The dose to risk conversion was used to estimate the number of people who are likely to die due to Annual effective dose (E) received from background radiation in Ortum. The dose to risk conversion factor was estimated using Equation 3.10 below.

$$\mathrm{NP} = \mathrm{D} \times \mathrm{E} \times \mathrm{P} \qquad 3.10$$

Where NP is the number of people likely to die, D is the dose to risk conversion factor, E is the dose conversion factor, and P is the population of Ortum.

### 3.8.10 Lifetime cancer risk ($LTCR_{BR}$)

The lifetime cancer risk ($LTCR_{BR}$) due to external exposure to background radiation was calculated using equation 3.11 below (Ahmad *et al*., 2019)

$$LTCR_{BR} = \mathrm{AEDE}(Sv/y) \times AL \times RF \qquad 3.11$$

where AEDE is the annual effective dose equivalent from the results in Ortum (0.42 mSv/y), AL is the average life expectancy which in Kenya is estimated at 70 years and RF is the associated risk factor which is 0.05 given by Yu *et al*., 2001.

## 3.9 Energy dispersive X-Ray Fluorescence Spectrometer (EDXRF)

### 3.9.1 EDXRF instrumentation

All elements emit characteristic radiations when they are subjected to a substantial amount of external energy through impact with fast moving particles like electrons, neutrons, protons, alpha-particles, and gamma rays. The interaction of γ-rays with matter may results to photoelectric effect, Compton scattering, and pair production.

Two EDXRF systems were used to identify and quantify the elements in the soil and rock samples. The Energy Dispersive X-ray Fluorescence (EDXRF) Spectrometry and the Amptek XRF Kit are analytic technique which are non-destructive, fast, simple and enables determination of many elemental and their concentration simultaneously with very high sensitivity (Wanjala *et al*., 2020 and Moussa and Mounia, 2015). The EDXRF consists of $^{109}$Cd radioactive source which is used for excitation of the sample to produce characteristic X-rays. The Silicon Lithium detector (Si(Li)) is used to detect x-rays with energy resolution between 170 eV to 200 eV at 5.9 KeV, $M_nK\alpha$-lines. Figure 3.4 shows the schematic diagram of the EDXRF detector.

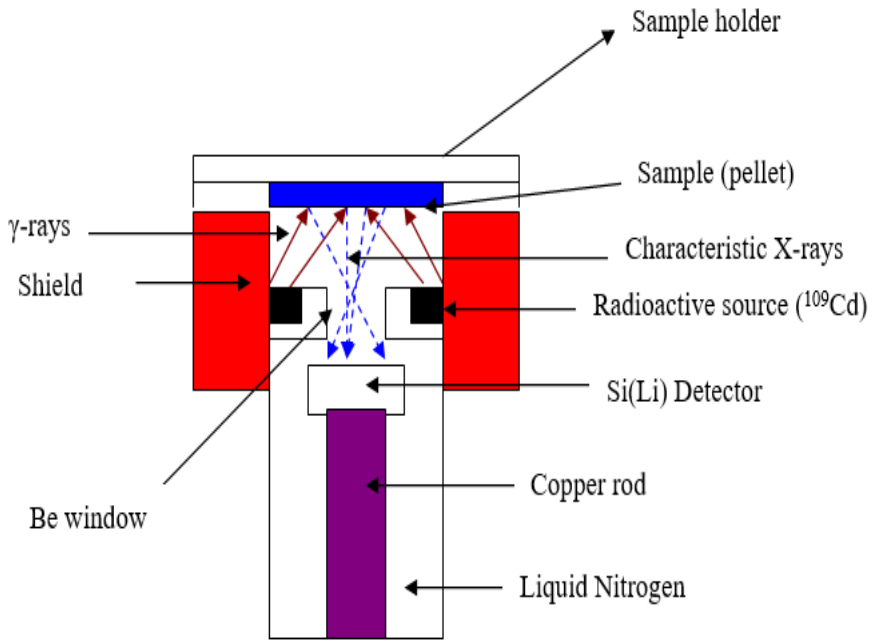


Figure 3.4: Schematic diagram of the EDXRF detector (Wanjala, 2016)

The EDXRF contains a gamma ray detector, the pre-amplifier, the linear amplifier, the multi-channel analyzer (MCA), personal computer (PC) and the printer as shown in Figure 3.5. The initial and final energy of the photon provides the means of identifying elements in the sample since specific characteristic X-ray energies emitted are associated with individual elements, the gamma ray spectra can hence be used to identify and quantify the elements in the sample. The elemental concentration is determined by the measure of the gamma-ray photo-peaks emitted by the radionuclides.

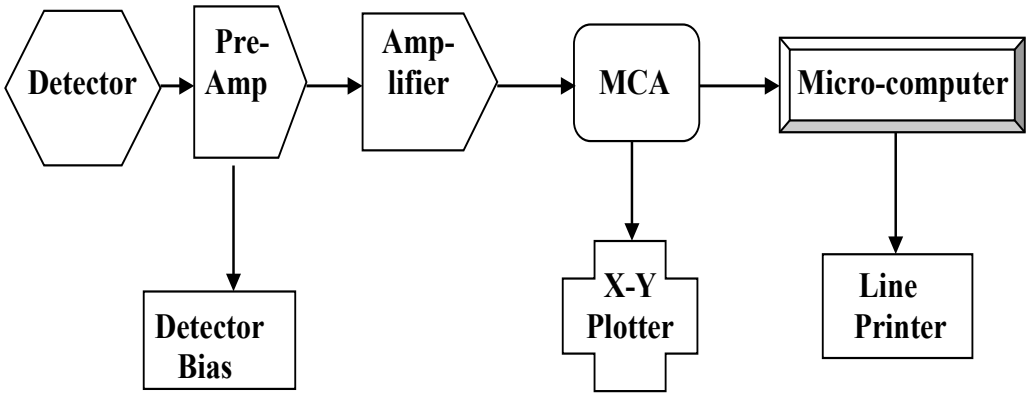


Figure 3.5: Schematic flow chart of the EDXRF detector (Wanjala *et al.,* 2009)

### 3.9.2 Calibration and quality assurance for the EDXRF spectrometer

Efficiency Calibration for the EDXRF spectrometer was done using the IAEA Reference material called Soil 7 (IAEA, 1987). Elemental concentration analysis was done using the EDXRF analytical procedure as described by Kinyua, 1982 and IAEA, 1997. The results of the elemental concentration obtained from the soil samples and those from the reference material were used in the comparative formula to determine the concentrations of the elements in the sample.

For energy calibration of EDXRF system, four peaks of known energy for metals Chromium (Cr), Iron (Fe), Nickel (Ni) and Molybdenum (Mo) Kα peaks in stainless steel 316 standard source was used. The region of interest (RoI) of the peaks was marked and the calibration dialog opened and the energies of the centroids inputted. The fluorescent energy and the characteristic peaks locations were then determined from the energy calibration equation for the detector using the Equation 3.12.

$$E = B + A \times Ch \quad 3.12$$

Where E is the X-ray energy and Ch is the channel number or counts and A is a constant.

The accuracy of the energy calibration function depends on the linearity of the Analog Digital Converter (ADC) and the associated electronic systems. The energy calibration curve is used to find the energy of unknown x-ray lines while the x-ray emission table is used to identify the unknown elements. The resolution of the detector was determined prior to analysis to monitor the systems performance. This was found to be ranging from 170 eV to 190 eV determined from the FWHM of Mn Kα lines.

Experimental measurements with reference material are necessary for comparison with the manufacturer's specification to determine the performance of the detector. The data obtained was used to develop a calibration and efficiency data of the detector.

### 3.9.3 Soil and rock sample preparation and EDXRF analysis

A small amount of about 0.4 g of the pulverize soil samples was weighed using an electronic weighing balance model Mettler Toledo AT460, shown in Plate 3.17. The soil sample was homogenized using a mixer and pelletized using a pellet dice with a pressure of 100,000 $N/m^2$ from a hydraulic press machine shown in Plate 3.18 to form a pellet of 2.5 cm in diameter using a pellet steel die shown in Plate 3.19. The pellet was then put in a clean petri dish and later analyzed using EDXRF spectrometer and the Amptek XRF Kit shown in plate 3.20. Three Pellets were prepared for each soil sample and weighed again before analysis using the EDXRF spectrometer.


Plate 3.17: Weighing balance with sample


Plate 3.18: Hydraulic press machine

Plate 3.19: pellet dice, mortar and pestle

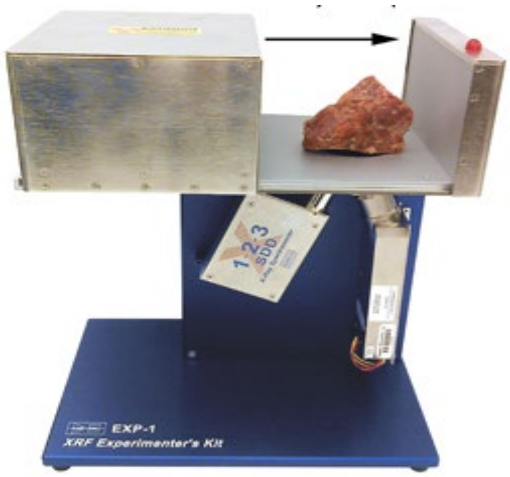


Plate 3.20: Amptek XRF Kit

The Amptek Experimenters XRF Kit was also used to obtaing soil and rock sample spectra. It contains an X-ray tube, which is the source of X-rays with a silver target and a Silicon Drift Detector (SDD). The operating current and voltage were optimized at 80 µA and 30 KV respectively (Finestone *et al*, 2020). The soil sample pellets were irradiated for 200 seconds and the spectral data obtained was analysed for elemental content using Analysis of X-ray Spectra by Iterative Least squares fitting (AXIL) software and the

Quantitative Analysis of Environmental Samples (QXAS) software. The concentration of 13 elements Ni, Cu, Zn, Pb, K, Ca, Fe, Ti, Mn, Rb, Sr, Zr and Nb in the soil was then determined using the Fundamental Parameter Method (FPM), Equation 3.13 (Shaltout *et al*., 2020). The average results of elemental concentration obtained from the EDXRF and the Amptek Experimenters XRF Kit was then recorded as shown in table 4.11.

$$I_i(E_i) = G_o\, K_i\, \varepsilon(E_i)\alpha_i \frac{(1-exp(-a\rho d))}{a\rho d} \qquad 3.13$$

Where $I_i(Ei)$, is the intensity of the primary radiation, $G_o$ is the geometric constant, $K_i$ is the ratio of the intensity of a given $K_i$ line to the intensity of the whole series, $\varepsilon(E_i)$ is the relative efficiency of the detector for a photon energy $E_i$, and $\alpha_i$ is the mass absorption coefficient for primary and fluorescent radiation in the sample, ρ is the density of the sample and d is the thickness of the sample.

### 3.9.4 Metal pollution indices

The three metal pollution indices geoaccumulation assessment (Igeo), potential ecological risk ($E_i$) and synthetic pollution estimation ($E_r$] for the soil samples collected from Ortum were calculated to check on the degree of soil pollution for selected heavy metals Ni, Cu, Zn and Pb.

#### 3.9.4.2 The geoaccumulation assessment

The $I_{geo}$ index is used to evaluate metal pollution levels for selected heavy metals Ni, Cu, Zn and Pb in soils. It is calculated using the equation 3.14 given by Wu *et al*., 2018.

$$I_{geo} = \log_2 (C^i/(1.5 \times B^i)) \quad 3.14$$

Where $C^i$ is the measured concentration of the metal i and $B^i$ is the concentration of Huize background value of element i. The coefficient of 1.5 is used to make even small anthropogenic effect detectable. The metals pollution level obtained ($I_{geo}$) were classified as shown in table 3.2

Table 3.2: Metal pollution level classification for Igeo (Wu *et al.,* 2018)

| | **Level** | **Classification** |
|---|---|---|
| 1 | <0 | Unpolluted |
| 2 | 0–1 | unpolluted to moderately polluted |
| 3 | 1–2 | moderately polluted |
| 4 | 2–3 | moderately to seriously polluted |
| 5 | 3–4 | seriously polluted |
| 6 | 4–5 | seriously to extremely polluted |
| 7 | >5 | extremely polluted |

### 3.9.4.2 Potential ecological risk index ($E_i$)

The potential ecological risk ($E_i$) index reveals the level of contamination risk for each of the selected heavy metal Ni, Cu, Zn and Pb to the environment. This was calculated using the equation 3.15 below by Wu *et al.,* 2018.

$$E_i = \sum_{i=1}^{n} T^i \times C^i/B^i \quad 3.15$$

where $C^i$ is the obtained concentration of metal i in the soil samples, $B^i$ is the Huize background value of element i, $T^i$ is the biological toxic factor of metal i. The relevant biological toxic factors for Ni, Cu, Zn and Pb are 5, 5, 1 and 5 respectively.

### 3.9.4.3 Synthesized potential ecological risk index ($E_r$)

the synthesized potential ecological risk index ($E_r$) reveal the overall ecological hazard of all selected heavy metals Ni, Cu, Zn and Pb in soils and it is the sum total of the potential ecological risk index $E_i$ for all metals of interest and is given by the equation 3.16 below by Wu *et al.,* 2018.

$$E_r = \sum_{i=1}^{n} E_i \qquad 3.16$$

The potential ecological risk level of the selected metals Ni, Cu, Zn and Pb is classified according to the table 3.3.

Table 3.3: Classification of Ei and Er risk index

| **Sn** | **Level $E_i$ index** | **Classification ($E_i$)** | **$E_r$ index** | **Classification ($E_r$)** |
|---|---|---|---|---|
| 1 | <40 | low risk | <150 | low risk |
| 2 | 40–80 | moderate risk | 150–300, | moderate risk |
| 3 | 80–160 | high risk | 300–600 | high risk |
| 4 | 160–320 | serious risk | 600–1200 | serious risk |
| 5 | >320 | severe risk | >1200 | severe risk |

### 3.10 ICP-OES Spectrometer

#### 3.10.1 ICP-OES instrumentation

Elemental analysis of the 10 water samples collected from Ortum, Kenya was nalysed using Agilent-5100 Inductively Coupled Plasma-Optical Emission Spectrometry (ICP-OES) at the Kenya Bureau of Standards in Nairobi, Kenya as shown in Plate 3.21. ICP-OES uses the emission spectra to identify and quantify multiple elements simultaneously as shown in Figure 3.5.


Plate 3.21: The ICP-OES at Kenya Bureau of Standards

The method is fast, accurate, highly sensitive and capable of determining several metals and non-metals in water samples (Sereshti *et al*., 2012). In this study the elemental concentration of 19 elements (Cu, Ni, Pb, Zn, Ag, Al, As, Ba, Ca, Cd, Co, Cr, Fe, K, Mg,

Mn, Mo, Na and Se) in water samples was determined. Heavy metals like Pb, Ni and Cu are not essential for plants and animals and their presence in the soil can lead to accumulation to toxic levels leading to adverse health effects (Wheal *et al.,* 2011).

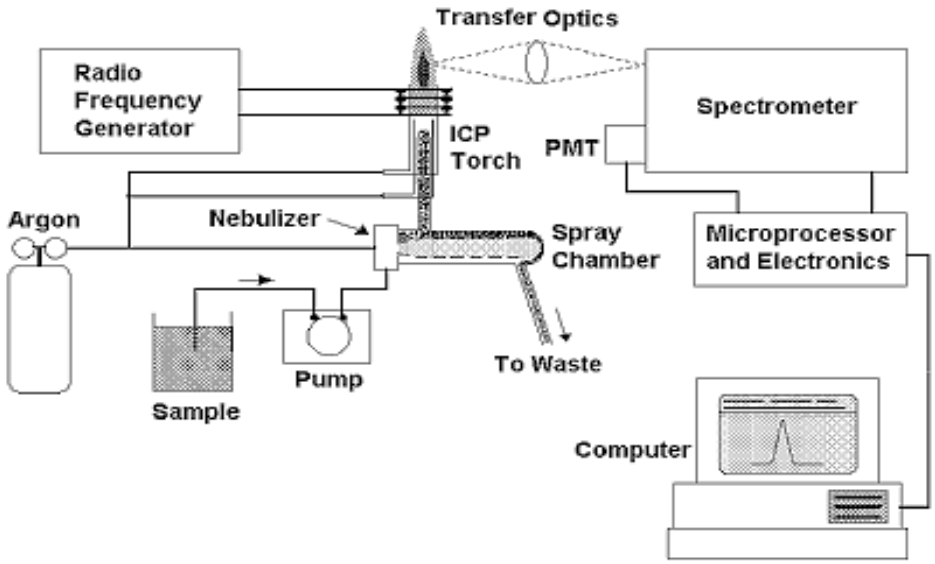


Figure 3.6: Schematic diagram of the ICP-OES

The water sample in the glass is pumped to the nebulizer and spray chamber which then mixes with high temperature argon gas to vapourize, atomize and desolve the compound in the liquid sample. The spray chamber and torch injection help in removing large aerosols and only allow small ones to pass the chamber. The atoms of the sample then absorb heat from the plasma generated by the radio frequency generator which makes them excited. The excited atoms then return back to their stable state by emission of energy of wavelength corresponding to a particular element of the atom. The emitted photon or light energy is then collected and reflected through a set of mirrors and passed through a prism onto a planar diffraction grating.which then allows the photons to be

detected through the photosensitive detector (PMT) as shown in figure 3.6. The element type is then determined based on the wavelength of the photon rays as shown in table 3.4, while the quantity of each element is determined based on the rays intensity.

Calibration curves for all the 19 elements were obtained by running high-purity single element standard solutions. Background correction for all wavelengths and spectral interferences were applied using software algorithms (Wheal *et al*., 2011). The analysis showed 19 elements with some having two wavelengths as shown in the Table 3.4

Table 3.4: Table of elements and observed atomic and ionic wavelengths (Wheal *et al*., 2011).

| **Element** | **Wavelength lines λ (nm)** | **Element** | **Wavelength lines λ (nm)** |
|---|---|---|---|
| Ag | 328.06, 338.29 | K | 766.49 |
| Al | 396.15 | Mg | 280.27 |
| As | 188.98, 193.70 | Mn | 257.61 |
| Ba | 455.67 | Mo | 202.03 |
| Ca | 422.67 | Na | 589.59 |
| Cd | 226.50 | Ni | 230.30 |
| Co | 230.79 | Pb | 220.35 |
| Cr | 267.72 | Se | 196.03 |
| Cu | 327.40 | Zn | 213.86 |
| Fe | 238.20 | | |

ICP Multi-Element Standard Solution with known elemental concentrations was used for quality control and testing the performance of the ICP-OES spectrometer. 1 blank and 6 standard solutions were prepared and analyzed using the same procedure and the results compared with the reference values.

### 3.10.2 Annual effective radiation dose due to water intake

The annual effective radiation dose that enters the body through ingestion of water was calculated using the Equation 3.17 by Ali *et al*., 2015.

$$E = K \times C_{Rn} \times KM \times t \qquad 3.17$$

Where E is the effective dose from ingestion in Sv, K is the ingestion dose conversion factor of $^{222}Rn$ which is 2 x $10^{-8}$ for children and 1 x $10^{-8}$ for Adults, (Fakhri *et al.,* 2016). $C_{Rn}$ is the radon concentration in Bq/l, KM is the average water consumption per day (21.5 L/day) and t is the time of consumption in one year (365 days), (WHO, 2004).

### 3.10.3 Heavy metal pollution index (MPI).

Heavy Metal Pollution Index (MPI) was evaluated so as to give the overall status of heavy metal contamination in the 10 water samples collected from Ortum as shown in Equation 3.18 by Koki *et al.,* 2015 and Poshtegal *et al.,* 2019.

$$MPI = (C_1 \times C_2 \times - - - \times C_n)^{1/n} \qquad 3.18$$

Where $C_1$, $C_2$, and $C_n$, are the heavy metal concentrations of metals of interest (Ni, Cu, Zn, Pb, Cr and As) in ppm or mg/L and n is the number of elements.

### 3.10.4 Heavy metal index (MI)

The overall water quality was evaluated using the Heavy Metal Index (MI) which is determined by the heavy metals present in the water samples using Equation 3.19, (Balakrishnan and Ramu, 2016 and Ojekunle *et al.,* 2016).

$$MI = \sum \frac{C_i}{MAC} \quad 3.19$$

Where MAC is the maximum permissible concentration of the metal in water given by WHO and $C_i$ is the heavy metal concentration in the water samples.

### 3.10.5 Cancer risks due to heavy metals in water

The probability of the population getting cancer due to intake of carcinogenic heavy metals Ni, Cd, Pb, Cr and As in water was calculated using the equation 3.20 a and 3.20 b provided by Koki *et al*., 2015 and Markovic *et al*., 2020)

$$\text{CDI} = \frac{\text{C}_\text{i} \text{ x WIR x T x ED}}{\text{BW x AT}} \quad 3.20\text{ a}$$

$$LTCR_{Wp} = CDI_{Cd} \text{ x } CSF_{Cd} + CDI_{Ni} \text{ x } CSF_{Ni} + CDI_{Pb} \text{ x } CSF_{Pb} + CDI_{Cr} \text{ x } CSF_{Cr} \quad 3.20\text{ b}$$

Where CDI is the chronic daily intake of the carcinogen (mg/Kg Bw/day), $C_i$ is the concentration of heavy metal in mg/L, WIR is the water ingestion rate (1.5 L/day for adults); T is the time in one year (365 days), ED is the exposure period (70 years), BW is the average body weight (70 kg for adults); AT is the average exposure time (ED x 365 days for adults) and CSF is the Cancer slope factor ((Pb = 0.0085. Cr = 0.0041, Cd = 0.0061, Ni = 0.00084, As = 1.5). The permissible limits for $LTCR_{WP}$ are between $10^{-6}$ and less than $10^{-3}$ for a single and multi-element carcinogens (Mohammadi *et al*., 2019).

Water from Ortum was classified in terms of Heavy Metal Pollution Index (MPI) and Heavy metal index (MI) using the classification provided in Table 3.5 and 3.6 (Balakrishnan and Ramu 2016; Ojenkunle *et al.,* 2016; Singh *et al.,* 2019)

Table 3.5: Water quality classification indices MI and MPI (Ojekunle *et al*., 2016)

| **Metal pollution index (MI)** | | | **Heavy metal Pollution index (MPI)** | |
|---|---|---|---|---|
| **MI** | **Characteristics** | **Class** | **MPI** | **MPI rating** |
| <0.3 | Very pure | I | < 0.01 | Very lightly polluted |
| 0.3-1.0 | Pure | II | 0.01-1 | Lightly polluted |
| 1.0-2.0 | Slightly affected | III | 1-5 | Moderately polluted |
| 2.0-4.0 | Moderately affected | IV | 5-10 | Highly polluted |
| 4.0-6.0 | Strongly affected | V | >10 | Very highly polluted |
| >6 | Seriously affected | VI | | |

Table 3.6: Water quality classification according to elemental concentration (Singh *et al.*, 2019)

| **S.No.** | **Parameters** | **Unit** | **Classes** | | | | |
|---|---|---|---|---|---|---|---|
| | | | **Excellent** | **Good** | **Fair** | **Poor** | **Heavily polluted** |
| 1. | pH | – | 7 | 6.8 – 8.0 | 6.5–6.8 and 8.0–8.5 | 5.5–6.5 and 8.5–9.5 | < 5.5 and > 9.5 |
| 2. | Aluminium (Al) | mg/L | 0–0.01 | 0.01–0.03 | 0.03–0.2 | 0.2–0.5 | > 0.5 |
| 3. | Calcium (Ca) | mg/L | 0–40 | 40–150 | 150–200 | 200–600 | > 600 |
| 4. | Copper (Cu) | mg/L | 0–0.05 | 0.05–1 | 1–1.5 | 1.5–3 | > 3 |
| 5. | Iron (Fe) | mg/L | 0–0.05 | 0.05–0.10 | 0.10–0.30 | 0.30–1.0 | > 1.0 |
| 6. | Magnesium (Mg) | mg/L | 0–30 | 30–50 | 50–100 | 100–500 | > 500 |

| S.No. | Parameters | Unit | Classes | | | | |
|---|---|---|---|---|---|---|---|
| | | | **Excellent** | **Good** | **Fair** | **Poor** | **Heavily polluted** |
| 7. | Manganese (Mn) | mg/L | 0–0.05 | 0.05–0.1 | 0.1–0.3 | 0.3–2 | > 2 |
| 8. | Selenium (Se) | mg/L | 0–0.002 | 0.002–0.005 | 0.005–0.01 | 0.01–0.1 | > 0.1 |
| 9. | Silver (Ag) | mg/L | 0–0.01 | 0.01–0.05 | 0.05–0.1 | 0.1–0.2 | > 0.2 |
| 10. | Zinc (Zn) | mg/L | 0–5 | 5–10 | 10–15 | 15–20 | > 20 |
| 11. | Cadmium (Cd) | mg/L | 0–0.001 | 0.001–0.002 | 0.002–0.003 | 0.003–0.01 | > 0.01 |
| 12. | Lead (Pb) | mg/L | 0–0.002 | 0.002–0.005 | 0.005–0.01 | 0.01–0.1 | > 0.1 |
| 13. | Nickel (Ni) | mg/L | 0–0.005 | 0.005–0.01 | 0.01–0.02 | 0.02–0.5 | > 0.5 |
| 14. | Arsenic (As) | mg/L | 0–0.005 | 0.005–0.01 | 0.01–0.05 | 0.05–0.1 | > 0.1 |
| 15. | Chromium (Cr) | mg/L | 0–0.005 | 0.005–0.01 | 0.01–0.05 | 0.05–0.5 | > 0.5 |

## 3.11 Radon and thoron measurement in mud houses

### 3.11.1 Introduction

Radon is a gas that emanates from $^{238}U$ decay (Appendix 3) whereas thoron is from the decay scheme of $^{232}Th$ (Appendix 4). Radon is found everywhere in the environment and especially in mud dwellings built with soil and rocks with high activity levels. Radon is a gas and can be inhaled through air or ingested by taking contaminated foodstuff or soil. Inhalation of radon and thoron is closely associated with lung cancer because radon and

thoron breaks down fat to their progenies emitting radiations which lodge in the lungs causing damage to the lungs cells thereby resulting to cancer.

The concentration of radon and thoron in mud houses in Ortum, Kenya was measure in this study. A total of 8 houses in Ortum where selected using purposive sampling methods for radon and thoron measurement. The discriminative radon-thoron detectors (RADUET) were hanged in the houses about 2 meters from the ground to prevent the children from interfering with the detector and 0.5 meters away from the wall. The world average exposure to natural radiation is estimated to be 2.4 mSv/y whereby radon and thoron attribute to 1.2 and 0.1 mSv/y respectively. Radon, thoron and their progeny are the major contributors of exposure to natural radiation sources in Ortum because they are airborn and their levels are enhanced in mud house especially those that are not well ventilated, (Tokonami *et, al*., 2015).

### 3.11.2 Radon-thoron measurement using discriminative monitor (RADUET)

The radiation exposure dose received from radon and thoron due to inhalation in mud houses in Ortum was determined using a passive integrating radon-thoron discriminative monitor called the RADUET as shown in Plate 3.22 and figure 3.7. The monitor is small, portable, compact and easy to use. The monitor is cylindrical, made of electroconductive plastic and consists of two different diffusion chambers with an inner volume of approximately 30cm$^3$. The CR-39 (Plate 3.23 and figure 3.8) was used as a detecting material which is placed at the bottom of the chamber using a sticky clay. Radon in air deffuses into the chamber through a small invisible air gap between the lid and bottom of

the detector. Thoron can scarcely enter the chamber due to its small pathway because of its very short half-life of 55.4 seconds compared to radon with a half-life of 3.82 days.

For thoron to be detected, six holes of 6 mm in diameter are opened at the side of the other chamber and covered with an electroconductive sponge in order to prevent the radon and thoron decay products and aerosols from getting inside. The monitors were exposed for about 3 months (103 days) and the CR-39 plates were removed from the chamber and chemically etched using a 6 M NaOH solution at 60 $^0$C for 24 hours. The track reading was done using a microscope to count the alpha tracks to determine the track density as shown in Figure 3.9. The thoron progeny concentration was then obtained as equilibrium equivalent thoron concentration (EETC) using the track density and conversion factor.

The relationship between the track density (DT) and thoron progeny concentration, i.e. equilibrium equivalent thoron concentration is expressed as shown in Equation 3.21 (Tokonami *et al*., 2015)

$$\mathrm{EETC} = \frac{DT}{C \times T} \quad 3.21$$

Where DT is the track density (tracks/mm$^2$), C is the conversion factor experimentally obtained (0.017 tracks/mm$^2$/ (Bq/m$^3$ day)), T is the exposure period (103 day) and EETC the equilibrium equivalent thoron concentration (Bq/m3)


Plate 3.22: RADUET Monitors

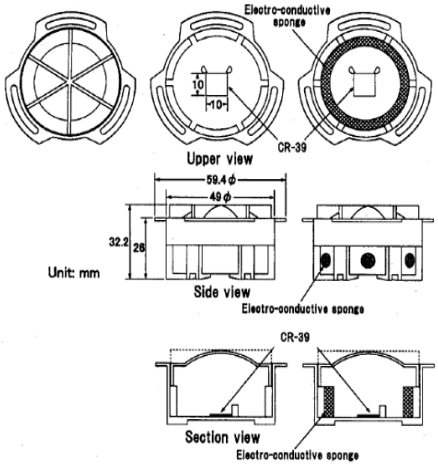


Figure 3.7: RADUET diagram

Plate 3.23: The CR-39 plate

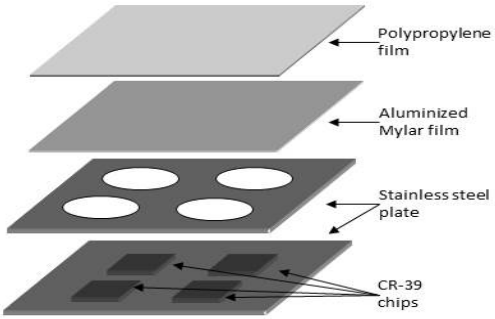


Figure 3.8: CR-39 Schematic diagram

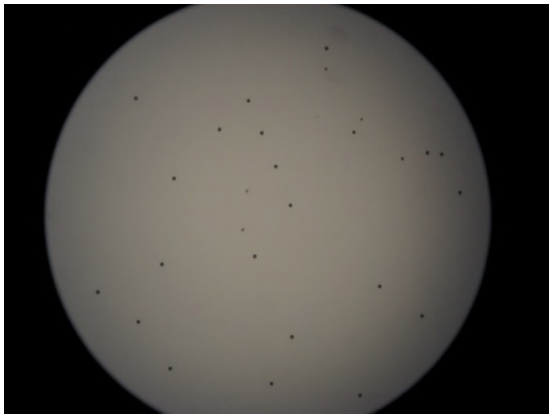

Figure 3.9: Typical image of formed tracks in the CR-39.

Radon and thoron concentrations was obtained using the total track densities replaced into equations 3.22 and 3.23 respectively.

$$C_{Rn} = (d_L - b)\, x\, \frac{f_{Tn2}}{t\, x\, (f_{Rn1}\, x\, f_{Tn2} - f_{Rn2} x\, f_{Tn1})} - (d_H - b)\, x\, \frac{f_{Tn1}}{t\, x\, (f_{Rn1}\, x\, f_{Tn2} - f_{Rn2} x\, f_{Tn1})} \quad 3.22$$

$$C_{Tn} = (d_H - b)\, x\, \frac{f_{Rn1}}{t\, x\, (f_{Rn1}\, x\, f_{Tn2} - f_{Rn2}\, x\, f_{Tn1})} - (d_L - b)\, x\, \frac{f_{Rn2}}{t\, x\, (f_{Rn1}\, x\, f1_{Tn2} - f_{Rn2}\, x\, f_{Tn1})} \quad 3.23$$

$C_{Rn}$ and $C_{Tn}$ are the mean radon and thoron concentrations in Bq/m$^3$, $d_L$ and $d_H$ are the alpha track densities (track/m$^2$) taken from the CR-39 detectors of low and high air-exchange rate chambers, $f_{Rn1}$ and $f_{Tn1}$ are the calibration coefficients for radon and thoron for the low air exchange chamber, $f_{Rn2}$ and $f_{Tn2}$ are the calibration coefficients for radon and thoron for the high air-exchange rate chamber, t is the exposure time in hours and b is the background track density of the CR-39 detector in tracks/m$^2$.

The Annual effective dose exposure (E) due to radon and thoron was evaluated using the Equations 3.24 and 3.25 given by Chen *et al*., 2015.

$E_{Rnp} = C_{Rn}$ x 0.4 x 7000 x ($9x10^{-9}$) 3.24

$E_{Tnp} = C_{Th}$ x 0.02 x7000 x ($40x10^{-9}$) 3.25

Where $C_{Rn}$ and $C_{Th}$ are radon and thoron concentration respectively, 0.4 and 0.02 are the typical equilibrium factors for radon and thoron respectively, 7000 is the time in hours spent in a dwelling in a year and the (9 nSv (Bq h m$^{-3}$))$^{-1}$ and (40 nSv (Bq h m$^{-3}$))$^{-1}$ are dose conversion factors for radon and thoron progeny, respectively (Chen *et al*., 2015). The World Health Organization (WHO, 2009) recommends that the upper levels of radon should not exceed 300 Bq/m$^3$ or 8 pCi/L (1 pCi/L = 37 Bq/m$^3$) which is equivalent to an effective dose of 5 mSv.

### 3.12 RESRAD

The RESRAD computer code developed by Argonne National Laboratory (ANL) for the United States Department of Energy (DOE) was used to simulate effective dose and cancer risk due to natural background radiation exposure due to inhalation, ingestion and external radiation pathwaysin Ortum . The model allows one to set pathways, input data, modify data and view output in terms of a report and an interactive graphics. In this study, RESRAD ONSITE 7.2 family of codes was used to compute radiation dose and risk analysis due to ingestion, inhalation and external radiation from the environment as shown in Figure 3.10.

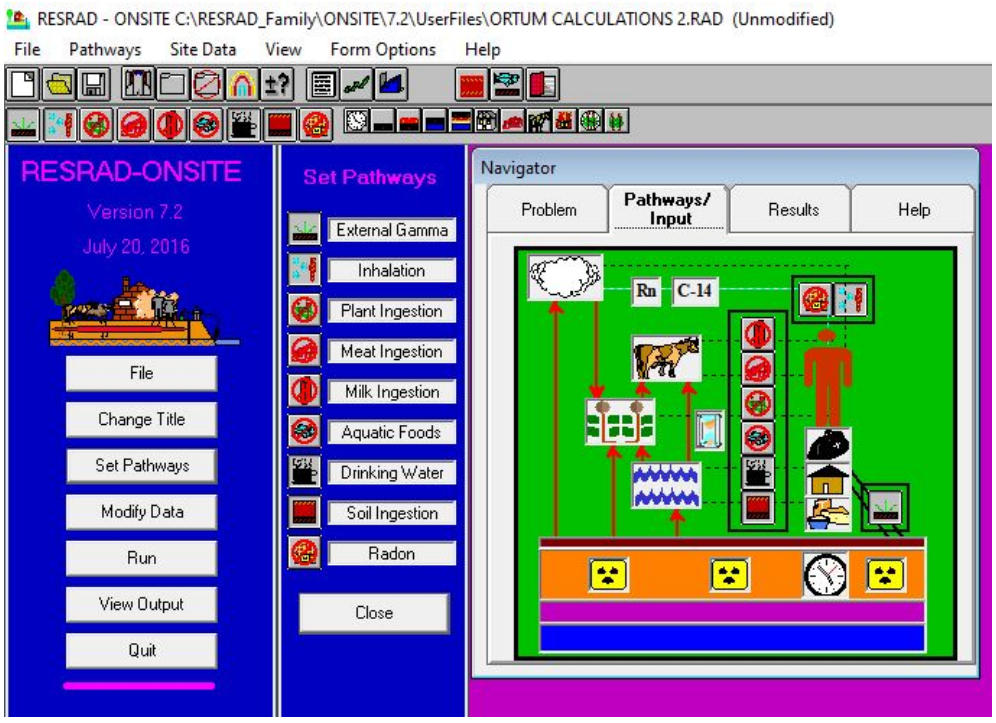


Figure 3.10: RESRAD ONSITE pathways (Yu *et al*., 2001)

In this research, the resident farmer scenario was used to compute exposure levels. RESRAD assumes an average inhalation rate of 0.96 $m^3$/h for the resident farmer and 1.3 m3/h industrial worker (EPA, 1997). It also assumes that soil ingestion rate per year is 36.5 g/y and water intake rate is 1.5 litres per day which is equivalent to 510 l/y.

### 3.12.1 RESRAD dose calculation

The dose received by an individual living in Ortum region was calculated as shown in Equation 3.26 and illustrated in figure 3.11.

$$Dose = Soil\ Concentration\ (Bq/kg) \times TF \times ED \qquad 3.26$$

Where TF is the transport factor and ED the exposure duration.

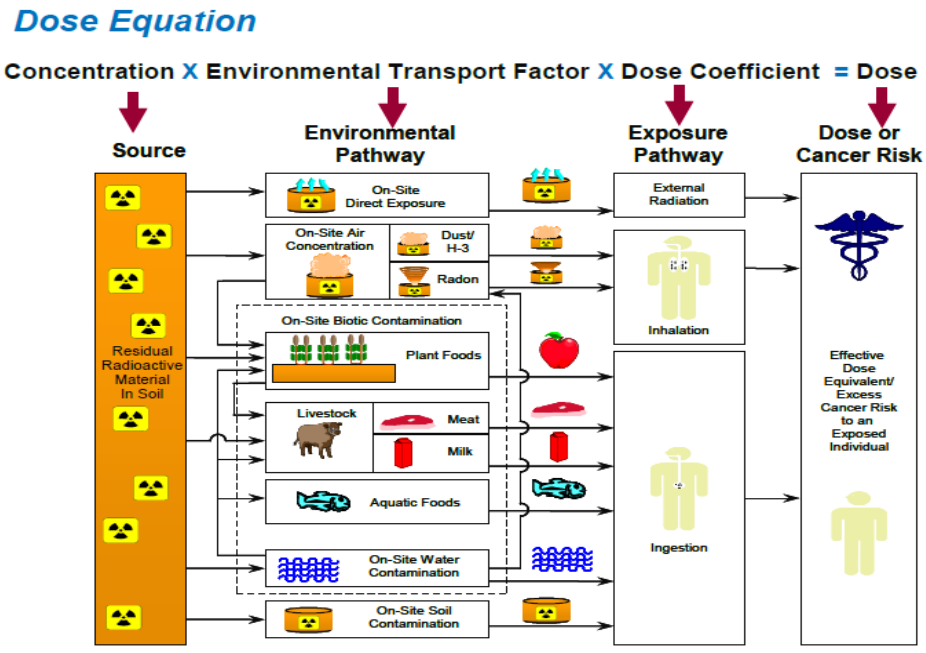


Figure 3.11: Radiation pathways for calculating annual dose (Yu *et al*., 2001)

### 3.12.2 RESRAD cancer risk

The external radiation pathway, exposure time and the risk coefficient were used in the RESRAD code to calculate the cancer risks using the Equation 3.27.

$$CR = \sum_{j=1}^{N} ETF_{j,p}(t) \times SF_{ij}(t) \times S_i\,(o) \times BRF_{i,J} \times RC_{i,l} \times ED \qquad 3.27$$

Where CR is Cancer Risk, $\sum$ is symbol for sum, $ETF_{j,p,}(t)$ is the environmental transport factor, $SF_{ij,}(t)$ is the soil concentration factor, $S_i(0)$ is the soil concentration at time = 0, $BRF_{ij}$ is the branching factor, $RC_{j,1}$ is the risk coefficient and $ED$ is the duration of exposure (Yu *et al.,* 2001).

The total cancer risk was obtained by getting the sum of the cancer risks of $^{238}$U, $^{232}$Th and $^{40}$K radionuclide as shown in the Equation 3.28.

$$(Grand\ total\ cancer\ risk)_p\,(t) = \sum_{J=1}^{N}(CancerRisk)_{jp} \qquad 3.28$$

Where $\sum$ is a symbol for summation, J=1 is the cancer risk due to radionuclide j=1 and N is the cancer risk due to the N$^{th}$ radionuclides.

### 3.13 Data analysis

The RESRAD ONSITE computer programme was used to compute the annual absorbed dose and the associated cancer risk due to exposure to background radiation for a resident farmer scenario in Ortum. Zeta score $|\zeta|$ was performed to compare the measured results and reference values for data quality check to ascertain if the experimental values obtained

fall within the acceptable range. The Origin program was used to analyze data obtained and draw graphs while the R-Studio and Geographic Information System (GIS) software were used to plot the map of the sampling points and assign colour to the different level of radiation at different points in order to generate radiation heat maps.

# CHAPTER FOUR: RESULTS AND DISCUSSION

## 4.1 Introduction

Analysis of background radiation exposure, radon an thoron concentration and elemental concentration in air, soil, rocks and water was done and discussed in this research study. The results of analysis of collected samples and reference materials for EDXRF and HPGe detectors are also presented in this chapter.

## 4.2 Results of background radiation in air

The results of the levels of background radiation in air in Ortum at 1 m above the ground was determined at 61 different sampling points and recorded as shown in Table 4.1. The results show variations in the background radiation levels from one sampling point to another and this might be due to the variation in the mineral content in the rocks and soil in the study area.

Table 4.1: Background radiation in air at 1m above the ground

| S/ No. | Site | Altitude | Longitude (E) | Latitude (N) | Counts Per Second | Dose rate (µSv/h) | nGy/h | mSv/y |
|---|---|---|---|---|---|---|---|---|
| 1 | S1 | 1438 | 35° 21′ 33″ | 01° 26′ 10″ | 14±3 | 0.08 | 80±14 | 0.70 |
| 2 | S2 | 1562 | 35° 21′ 42″ | 01° 26′ 18″ | 10±2 | 0.09 | 90±07 | 0.79 |
| 3 | S3 | 1543 | 35° 21′ 43″ | 01° 26′ 03″ | 12±3 | 0.09 | 90±07 | 0.79 |
| 4 | S4 | 1583 | 35° 21′ 51″ | 01° 26′ 02″ | 12±3 | 0.08 | 80±07 | 0.70 |
| 5 | S5 | 1608 | 35° 22′01″ | 01° 25′ 57″ | 13±3 | 0.09 | 90±14 | 0.79 |
| 6 | S6 | 1601 | 35° 21′ 58″ | 01° 26′ 15″ | 19±4 | 0.08 | 80±7 | 0.70 |
| 7 | S7 | 1633 | 35° 22′ 07″ | 01° 25′ 50″ | 14±3 | 0.08 | 80±14 | 0.70 |
| 8 | S8 | 1645 | 35° 22′ 10″ | 01° 25′ 41″ | 34±5 | 0.13 | 130±28 | 1.14 |
| 9 | S9 | 1659 | 35° 22′ 19″ | 01° 25′ 49″ | 38±4 | 0.15 | 150±00 | 1.32 |
| 10 | S10 | 1648 | 35° 22′ 14″ | 01° 26′ 02″ | 25±3 | 0.14 | 140±28 | 1.23 |
| 11 | S11 | 1477 | 35° 21′ 01″ | 01° 25′ 34″ | 23±3 | 0.16 | 160±14 | 1.40 |
| 12 | S12 | 1480 | 35° 22′10″ | 01° 25′ 25″ | 32±4 | 0.15 | 150±14 | 1.31 |

| S/ No. | Site | Altitude | Longitude (E) | Latitude (N) | Counts Per Second | Dose rate (µSv/h) | nGy/h | mSv/y |
|---|---|---|---|---|---|---|---|---|
| 13 | S13 | 1629 | 35° 21′ 56″ | 01° 25′ 20″ | 36±4 | 0.14 | 140±28 | 1.23 |
| 14 | S14 | 1635 | 35° 22′ 06″ | 01° 25′ 12″ | 30±3 | 0.14 | 140±00 | 1.23 |
| 15 | S15 | 1668 | 35° 22′ 27″ | 01° 25′40″ | 16±3 | 0.13 | 130±14 | 1.14 |
| 16 | S16 | 1472 | 35° 21′ 47″ | 01° 25′ 45″ | 21±3 | 0.09 | 90±14 | 0.79 |
| 17 | S17 | 1501 | 35° 21′30″ | 01° 25′ 52″ | 17±2 | 0.08 | 80±14 | 0.70 |
| 18 | S18 | 1425 | 35° 21′ 21″ | 01° 26′ 05″ | 22±3 | 0.09 | 90±07 | 0.79 |
| 19 | S19 | 1411 | 35° 21′ 14″ | 01° 26′ 19″ | 19±4 | 0.08 | 80±00 | 0.70 |
| 20 | S20 | 1407 | 35° 21′ 25″ | 01° 26′27″ | 14±2 | 0.09 | 90±14 | 0.79 |
| 21 | S21 | 1540 | 35° 21′ 37″ | 01° 25′ 21″ | 17±3 | 0.08 | 80±07 | 0.70 |
| 22 | S22 | 1602 | 35° 21′ 58″ | 01° 25′ 48″ | 19±3 | 0.07 | 70±07 | 0.61 |
| 23 | S23 | 1561 | 35° 21′ 02″ | 01° 25′ 26″ | 27±4 | 0.16 | 160±14 | 1.40 |
| 24 | S24 | 1538 | 35° 21′ 04″ | 01° 25′ 40″ | 35±5 | 0.16 | 160±28 | 1.40 |
| 25 | S25 | 1551 | 35° 20′57″ | 01° 25′42″ | 31±4 | 0.12 | 120±00 | 1.05 |
| 26 | S26 | 1587 | 35° 21′ 04″ | 01° 25′ 34″ | 38±4 | 0.13 | 130±14 | 1.14 |
| 27 | S27 | 1470 | 35° 21′ 09″ | 01° 25′ 56″ | 31±4 | 0.08 | 80±00 | 0.70 |
| 28 | S28 | 1609 | 35° 20′ 58″ | 01° 25′ 28″ | 29±3 | 0.13 | 130±14 | 1.14 |
| 29 | S29 | 1598 | 35° 20′ 55″ | 01° 25′ 30″ | 33±4 | 0.13 | 130±14 | 1.14 |
| 30 | S30 | 1572 | 35° 20′ 57″ | 01° 25′ 32″ | 29±4 | 0.13 | 130±07 | 1.14 |
| 31 | S31 | 1580 | 35° 20′ 53″ | 01° 25′ 34″ | 25±4 | 0.10 | 100±07 | 0.88 |
| 32 | S32 | 1569 | 35° 20′ 56″ | 01° 25′ 36″ | 28±4 | 0.10 | 100±14 | 0.88 |
| 33 | S33 | 1540 | 35° 21′ 04″ | 01° 25′ 36″ | 38±4 | 0.16 | 160±07 | 1.40 |
| 34 | S34 | 1560 | 35° 21′ 00″ | 01° 25′ 35″ | 38±3 | 0.20 | 200±14 | 1.75 |
| 35 | S35 | 1555 | 35° 21′ 03″ | 01° 25′ 33″ | 25±3 | 0.15 | 150±14 | 1.31 |
| 36 | S36 | 1565 | 35° 21′ 03″ | 01° 25′30″ | 18±4 | 0.12 | 120±07 | 1.05 |
| 37 | S37 | 1566 | 35° 21′ 14″ | 01° 25′ 45″ | 18±3 | 0.09 | 90±00 | 0.79 |
| 38 | S38 | 1531 | 35° 21′ 06″ | 01° 25′ 32″ | 27±5 | 0.12 | 120±07 | 1.05 |
| 39 | S39 | 1529 | 35° 21′ 10″ | 01° 25′ 31″ | 28±3 | 0.10 | 100±14 | 0.88 |
| 40 | S40 | 1525 | 35° 21′ 14″ | 01° 25′ 33″ | 23±3 | 0.11 | 110±00 | 0.96 |
| 41 | S41 | 1491 | 35° 21′ 20″ | 01° 25′20″ | 16±4 | 0.09 | 90±14 | 0.79 |
| 42 | S42 | 1528 | 35° 21′ 13″ | 01° 25′ 29″ | 24±4 | 0.12 | 120±07 | 1.05 |
| 43 | S43 | 1530 | 35° 21′ 08″ | 01° 25′ 29″ | 24±3 | 0.15 | 150±07 | 1.31 |
| 44 | S44 | 1530 | 35° 21′ 11″ | 01° 25′ 28″ | 23±3 | 0.13 | 130±14 | 1.14 |
| 45 | S45 | 1524 | 35° 21′ 09″ | 01° 25′ 25″ | 24±4 | 0.12 | 120±07 | 1.05 |
| 46 | S46 | 1628 | 35° 21′ 06″ | 01° 25′ 21″ | 21±2 | 0.14 | 140±07 | 1.23 |
| 47 | S47 | 1650 | 35° 22′ 16″ | 01° 25′ 35″ | 16±2 | 0.80 | 80±14 | 0.70 |
| 48 | S48 | 1583 | 35° 21′ 03″ | 01° 25′ 39″ | 17±3 | 0.09 | 90±14 | 0.79 |

| S/ No. | Site | Altitude | Longitude (E) | Latitude (N) | Counts Per Second | Dose rate (µSv/h) | nGy/h | mSv/y |
|---|---|---|---|---|---|---|---|---|
| 49 | S49 | 1527 | 35° 21′ 11″ | 01° 25′ 36″ | 18±3 | 0.09 | 90±00 | 0.79 |
| 50 | S50 | 1601 | 35° 21′ 43″ | 01° 25′ 36″ | 14±2 | 0.08 | 80±07 | 0.70 |
| 51 | S51 | 1664 | 35° 21′ 11″ | 01° 25′ 15″ | 18±2 | 0.09 | 90±07 | 0.79 |
| 52 | S52 | 1670 | 35° 21′ 46″ | 01° 25′ 15″ | 16±2 | 0.10 | 100±14 | 0.88 |
| 53 | S53 | 1578 | 35° 21′ 50″ | 01° 26′ 8″ | 17±2 | 0.08 | 80±07 | 0.70 |
| 54 | S54 | 1541 | 35° 21′ 02″ | 01° 25′ 42″ | 19±3 | 0.09 | 90±14 | 0.79 |
| 55 | S55 | 1484 | 35° 21′ 03″ | 01° 25′ 51″ | 24±3 | 0.14 | 140±07 | 1.23 |
| 56 | S56 | 1553 | 35° 21′ 01″ | 01° 25′ 37″ | 22±4 | 0.10 | 100±07 | 0.88 |
| 57 | S57 | 1568 | 35° 21′ 00″ | 01° 25′ 30″ | 23±3 | 0.15 | 150±14 | 1.31 |
| 58 | S58 | 1597 | 35° 21′29 " | 01° 25′ 30″ | 24±2 | 0.15 | 150±35 | 1.31 |
| 59 | S59 | 1622 | 35° 21′ 00″ | 01° 25′ 15″ | 24±3 | 0.10 | 100±14 | 0.88 |
| 60 | S60 | 1528 | 35° 21′ 03″ | 01° 26′ 9″ | 20±3 | 0.09 | 90±07 | 0.79 |
| 61 | S61 | 1619 | 35° 21′ 49″ | 01° 25′ 25″ | 19±3 | 0.09 | 90±15 | 0.79 |
| | **Average** | | | | **27±16** | **0.12±0.9** | **112±30** | **0.99 ± 0.26** |

The average dose rate in air was found to be 112 ± 30 nGy/h ranging from 70 ± 07 to 200 ± 14 nGy/h. This is almost double the worldwide average value of 60 nGy/h given by UNSCEAR, 2000. All the 61 survey points recorded high background radiation above the world average value of 60 nGy/h as shown in Figure 4.1.

The sampling points at the quarry site (S24, S26, S34, S39, S40, S46) had the highest levels of radiation at S34 with an average of 200 ± 14 nGy/h followed by the high-altitude areas close to Cheranganyi hills (S9, S10, S12 and S14). The average dose rate was 0.99 ± 0.25 mSv/y which indicates that Ortum is not a High Background Radiation Area (HBRA).

The results of radiation in air shows a slight increase in the outdoor radiation with a correlation of r = 0.22 showing that the height and radiation levels are slightly correlated. This increase in radiation level in air with increase in altitude may be as a result of the geological difference in rocks at different altitudes and changes in equipment sensitivity at different altitudes resulting from pressure and temperature changes. Hashemi *et al*., 2019 also pointed out that exposure to cosmic radiation is also influenced by altitude which contributes to background radiation.

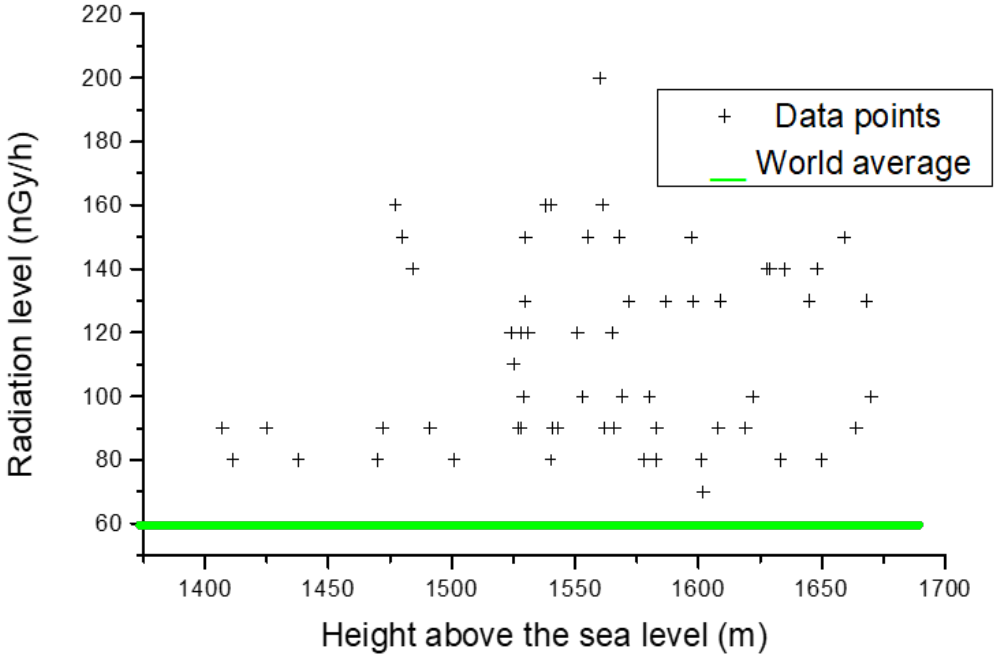


Figure 4.1: Plot of radiation level against height above the sea level

### 4.2.1 Mapping of radiation levels in air

The RStudio 3.6.1 software provided by IAEA was used for statistical computing and graphics in this research for mapping radiation levels in air at different points in Ortum

(Deng *et al*., 2014). The levels of radiation as shown in Table 4.1 and Figure 4.1 shows that the quarry area in Ortum recorded high level of radiation in air than other parts. The heat maps in Figure 4.2, 4.4 and 4.5 also show that the areas around the quarry and high-altitude areas close to the Cheranganyi hills experience high levels of radiation in air than other parts of Ortum.

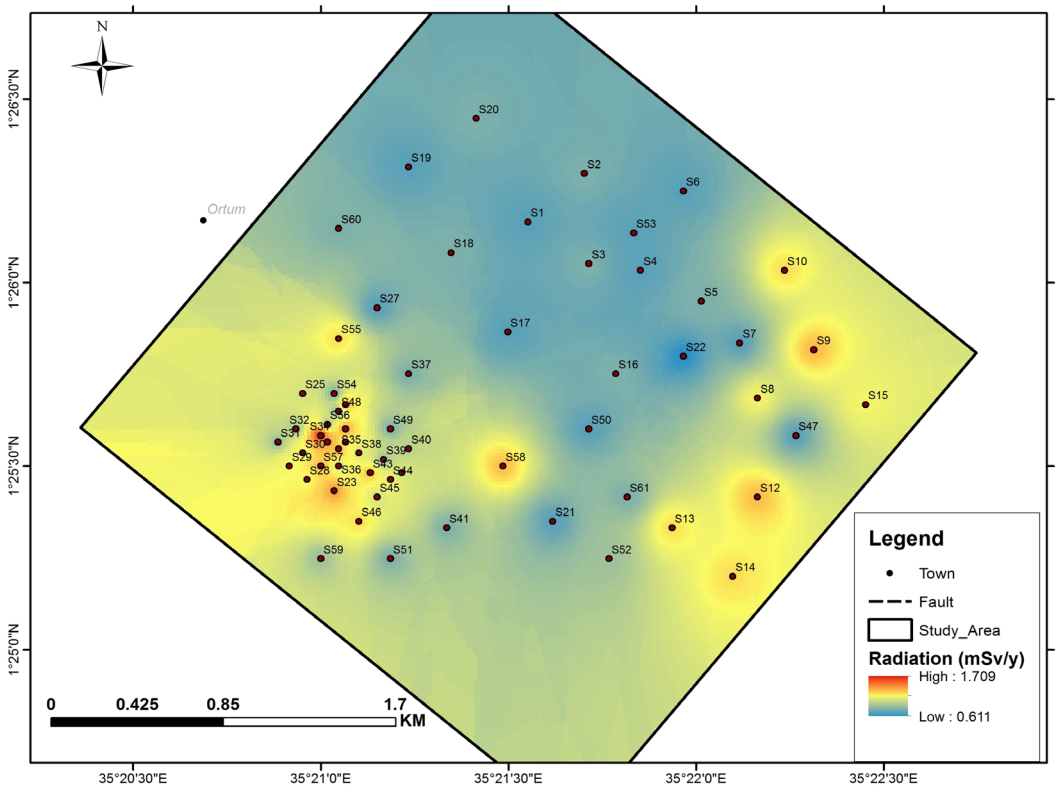


Figure 4.2: Radiation level heat map

The increase in radiation level with altitude might be attributed to increase in comic radiation which varies with hight and weather changes in the atmosphere which affect radiations reaching the earth from the sun. It is important to note that most residents in Ortum live in the low land and away from the quarry where high background radiation is experienced.

The heat maps in Figure 4.2 shows the sampling points and the difference in background radiation being shown by the different colours at the sampling points. Figure 4.3, shows the heat map with the quarry area and along the cheranganyi hills showing high background radiation than other sampling points. Figure 4.4 shows the probability of the levels of background radiation at different sampling points and Figure 4.5 shows the radiation level heat map superimposed on a satellite image. The variation of background radiation in air indicates that some parts of Ortum experience high background radiation compared to others. The quarry area experiences the highest level of background radiation compared to other regions in Ortum. This can be attributed to deposition of soils with high levels of radionuclides at the quarry site resulting to high background radiation.

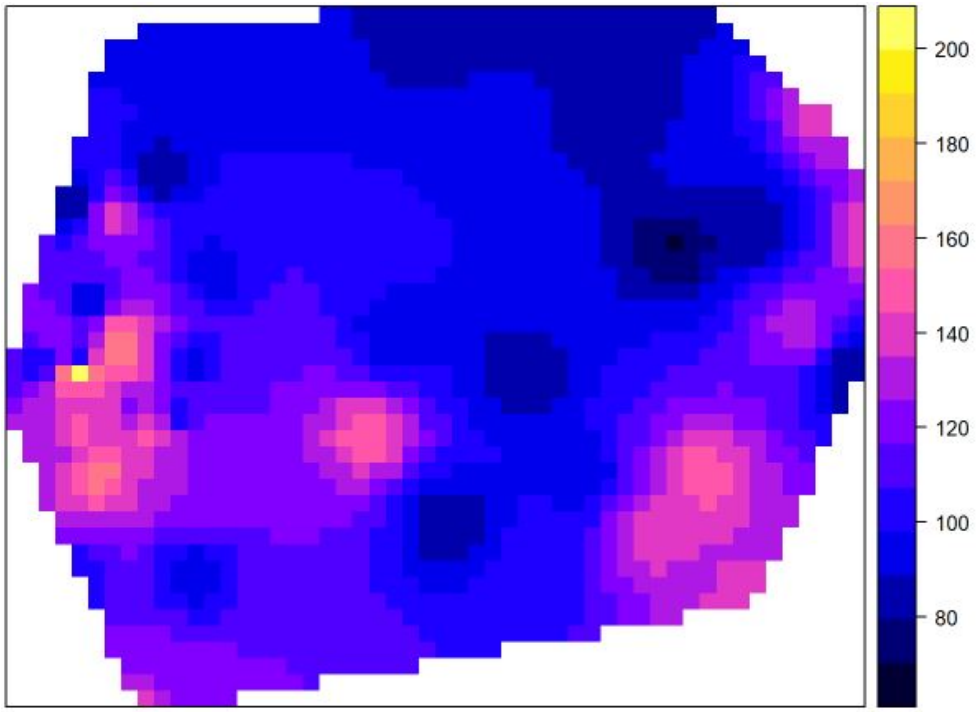


Figure 4.3: Heat map for radiation levels (nGy/h) (Scale 1cm=200m)

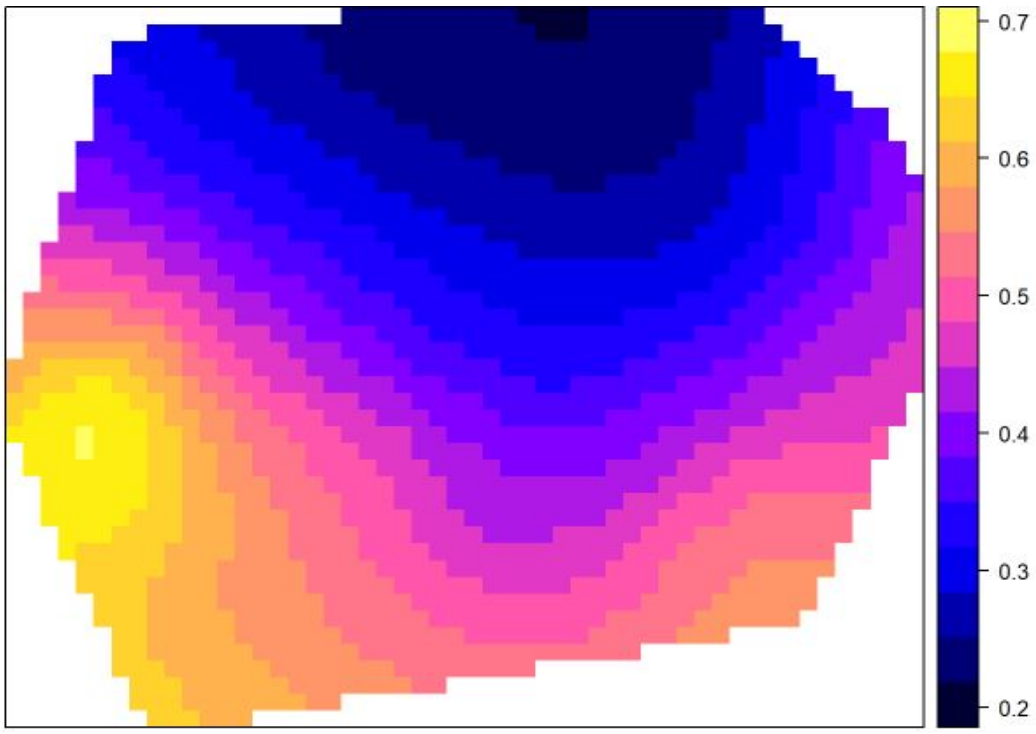


Figure 4.4: Map for probability of dose >200 nGy/h (1 cm =200m)

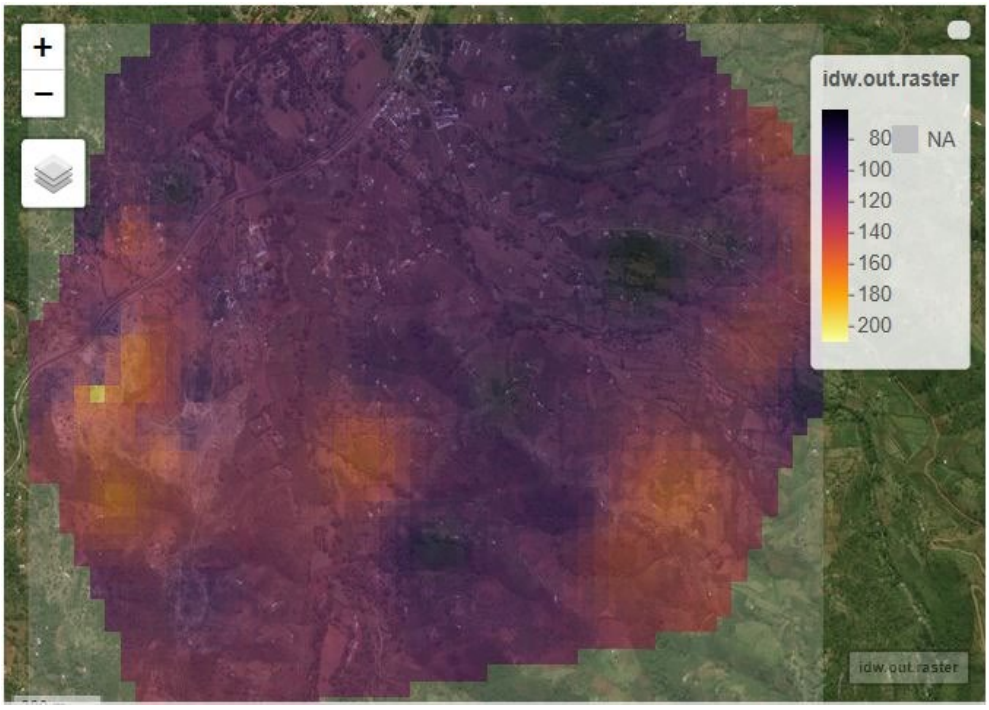


Figure 4.5: Radiation level map superimposed on a satellite image (Scale 1cm =200m)

### 4.3 Results of levels of $^{238}U$, $^{232}Th$ and $^{40}K$ in soil and rocks

The levels of naturally occurring radionuclides $^{238}U$, $^{232}Th$ and $^{40}K$ in soil and rocks in Ortum were determined using the HPGe detector at the Institute of Nuclear Science and Technology, University of Nairobi.

#### 4.3.1 Results of efficiency calibration for HPGe detector

The results of efficiency calibration using IAEA reference materials RGU-1, RGTh-1 and RGK-1 are shown in the table 4.2 and the efficiency calibration curve obtained using equation 3.3 is shown in figure 4.6. The efficiency calibration curve shows that the efficiency of the HPGe detector reduces with increase in energy of the radionuclide.

Table 4.2: Results of efficiency calibration for the HPGe detector

| Reference | Nuclide | Energy (keV) | Intensity | Mass | Probability | Activity | efficiency |
|---|---|---|---|---|---|---|---|
| RGTh-1 | Pb-212 | 238 | 8.09 | 0.2357 | 0.200 | 3250±10 | 0.053±0.018 |
| RGU-1 | Pb-214 | 351 | 6.65 | 0.2353 | 0.180 | 4940±30 | 0.0318±0.012 |
| RGU-1 | Bi-214 | 609 | 5.57 | 0.2353 | 0.452 | 4940±30 | 0.010±0.008 |
| RGTh-1 | Ac-228 | 912 | 1.31 | 0.2357 | 0.258 | 3250±10 | 0.007±0.002 |
| RGK-1 | K-40 | 1461 | 1.44 | 0.2787 | 0.107 | 14000±400 | 0.003±0.001 |

The results of efficiency versus energy were fitted as shown in figure 4.6 using the second order polynomial equation 4.1.

$$Ef = Ef_o + A_1 \times E + A_2 \times E^2 \qquad 4.1$$

Where Ef is the efficiency, $Ef_o$ if the efficiency at E = 0, E is the energy and $A_1$ and $A_2$ are constants.

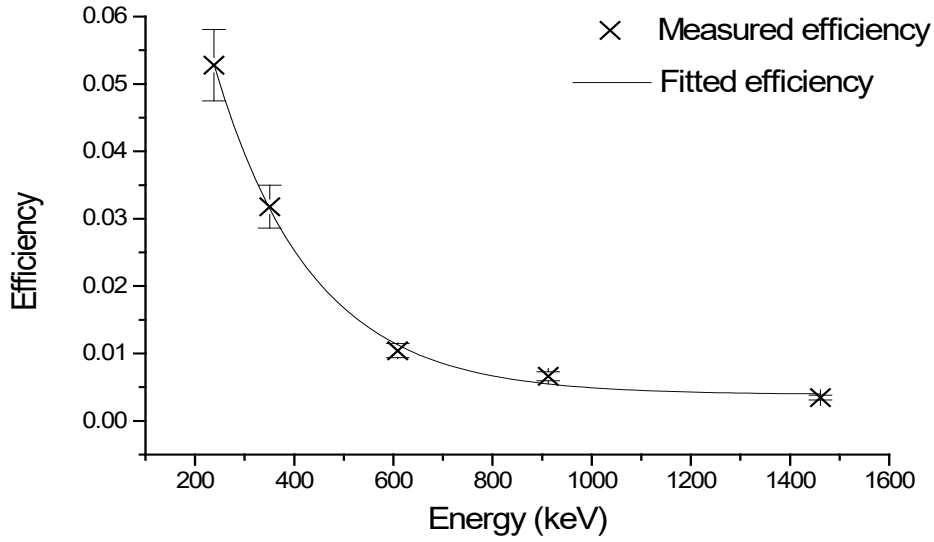


Figure 4.6: HPGe detector efficiency calibration curve

### 4.3.2 Results of energy calibration for HPGe detector

Energy calibration was done using the Equation 3.4 with gamma lines $^{214}$Pb (351 KeV), $^{214}$Bi (609 KeV), $^{228}$Ac (911 KeV), $^{40}$K (1460 KeV) and $^{214}$Bi (1765 KeV) and the results shows that the plot of energy against the channel number gives a straight line which can be expressed as equationas 4.2 as shown in the figure 4.7.

$$E = 4.1912\ x\ Ch\ -\ 65.623 \qquad 4.2$$

Where E is the energy of the gamma radiation and Ch is the channel number.

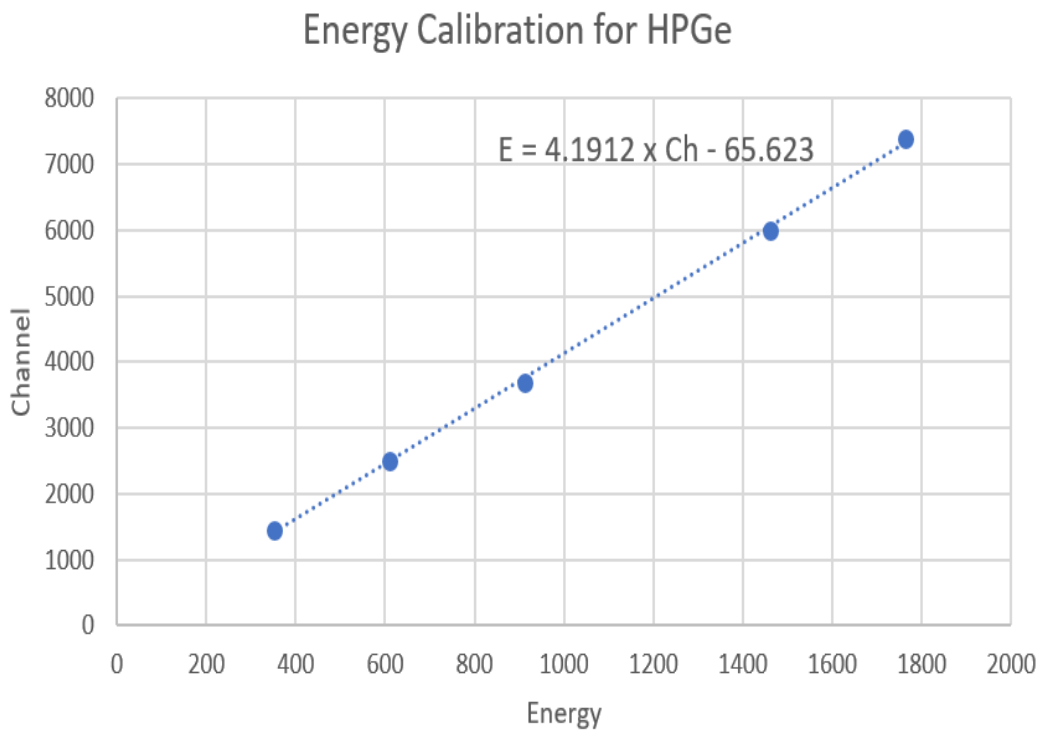


Figure 4.7: Energy calibration curve for HPGe detector obtained in this study

### 4.3.3 Results of analysis of certified reference material using HPGe detector

The IAEA certified reference material IAEA-375 (Soil material) was analyzed for quality control and the results recorded in the Table 4.3 below. The results show good correlation between the measured value and the reference value for all the radionuclides of interest since the Z-score for all values shows that they fall within the acceptable limits whereby Zeta |ζ| <1.96 is OK, |ζ| >1.96 is questionable results and |ζ| >2.576 is not OK.

Table 4.3: Measured and reference values for IAEA soil 375 for HPGe detector

| HPGe | Measured value | | Reference value | | Comparison | | |
|---|---|---|---|---|---|---|---|
| **Nuclide** | **Activity** | | **Activity** | | **%** | | |
| | **Bq/Kg** | **± 1σ** | **Bq/Kg** | **± 1σ** | **Deviation** | **ζ-score** | **OK?** |
| K-40 | 578 | 25 | 608 | 2 | -4.93% | -1.196 | **OK** |
| Cs-137 | 33.4 | 1.3 | 33.2 | 0.23 | 0.60% | 0.151 | **OK** |
| Ra-226 | 22.9 | 1.6 | 22 | 0.2 | 4.09% | 0.558 | **OK** |
| Ra-228 | 32.7 | 2.1 | 31.9 | 0.3 | 2.51% | 0.377 | **OK** |
| Th-232 | 32.7 | 2.1 | 33.4 | 0.28 | -2.10% | -0.330 | **OK** |
| U-238 | 29 | 2.1 | 28.3 | 0.24 | 2.47% | 0.331 | **OK** |

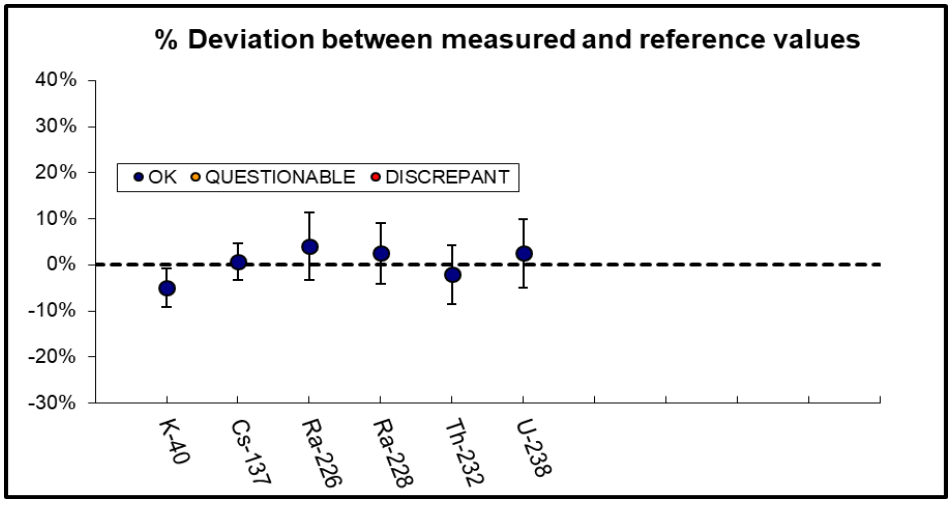


Figure 4.8: IAEA Soil-375 deviation between measured and reference values

The results in Table 4.3 and Figure 4.8 above show a good correlation of r = 0.99 between the measured and the certified values for the HPGe detector system at the Institute of Nuclear Science and Technology. This implies that the results obtained using the HPGe detector are reliable.

### 4.3.4 Activity concentration of $^{238}U$, $^{232}Th$ and $^{40}K$ in soil sample

After one month, the activity concentrations of $^{238}U$, $^{232}Th$ and $^{40}K$ in 35 surface soil samples and 24 soils samples collected at different depth was determined using HPGe spectrometer. Analysis for each soil sample was repeated three time and the average and standard deviation recorded. The equations 3.7, 3.8, 3.9 and 3.10 were use to find Annual effective dose equivalent, Radium equivalent, Extern hazard index and Internal hazard index respectively and the results tabulated in Table 4.4. The activity concentration in soil samples collected from the surface ranged from 20 to 67 Bq/kg, 33 to 85 Bq/kg and 148 to 1019 Bq/kg for $^{238}U$, $^{232}Th$ and $^{40}K$ respectively with an average value of 40 ± 1 Bq/kg, 56±1 Bq/kg and 425± 19 Bq/kg for $^{238}U$, $^{232}Th$ and $^{40}K$ respectively as shown in Table 4.4 and Figures 4.8, 4.9 and 4.10.

Table 4.4: $^{238}U$, $^{232}Th$ and $^{40}K$ activity concentration in soil samples (Bq/kg)

| S.No. | Site | Alti-tude | $^{232}Th$ Bq/kg | $^{238}U$ Bq/kg | $^{40}K$ Bq/kg | $Ra_{eq}$ | $H_{ex}$ | $H_{in}$ | ADRA (nGy/h) | AEDE (mSv/y) |
|---|---|---|---|---|---|---|---|---|---|---|
| 1 | S1 | 1438 | 46±2 | 25±2 | 169±8 | 104 | 0.28 | 0.35 | 47±5 | 0.29 |
| 2 | S2 | 1562 | 55±4 | 43±2 | 340±17 | 148 | 0.40 | 0.52 | 68±6 | 0.42 |
| 3 | S3 | 1543 | 45±2 | 34±2 | 308±15 | 122 | 0.33 | 0.42 | 56±4 | 0.35 |
| 4 | S4 | 1583 | 37±2 | 25±2 | 148±7 | 88 | 0.24 | 0.31 | 40±4 | 0.25 |
| 5 | S5 | 1608 | 33±2 | 20±2 | 271±6 | 87 | 0.24 | 0.29 | 41±3 | 0.25 |
| 6 | S6 | 1601 | 37±2 | 26±2 | 252±11 | 99 | 0.27 | 0.34 | 46±4 | 0.28 |
| 7 | S7 | 1633 | 35±1 | 24±1 | 246±7 | 94 | 0.25 | 0.32 | 43±5 | 0.27 |
| 8 | S8 | 1645 | 51±4 | 35±2 | 316±15 | 133 | 0.36 | 0.45 | 61±5 | 0.38 |
| 9 | S9 | 1659 | 71±3 | 52±3 | 1019±35 | 232 | 0.63 | 0.77 | 110±8 | 0.68 |
| 10 | S10 | 1648 | 71±4 | 54±3 | 1001±50 | 232 | 0.63 | 0.77 | 111±11 | 0.68 |
| 11 | S11 | 1477 | 62±2 | 38±2 | 569±23 | 171 | 0.46 | 0.57 | 80±6 | 0.49 |
| 12 | S12 | 1480 | 46±1 | 31±3 | 311±15 | 122 | 0.33 | 0.41 | 56±4 | 0.35 |
| 13 | S13 | 1629 | 48±2 | 34±2 | 276±11 | 124 | 0.34 | 0.43 | 57±5 | 0.35 |
| 14 | S14 | 1635 | 52±3 | 39±3 | 410±20 | 145 | 0.39 | 0.50 | 67±8 | 0.41 |

| S.No. | Site | Alti-tude | $^{232}$Th Bq/kg | $^{238}$U Bq/kg | $^{40}$K Bq/kg | $Ra_{eq}$ | $H_{ex}$ | $H_{in}$ | ADRA (nGy/h) | AEDE (mSv/y) |
|---|---|---|---|---|---|---|---|---|---|---|
| 15 | S15 | 1668 | 36±2 | 25±3 | 228±6 | 94 | 0.25 | 0.32 | 43±4 | 0.27 |
| 16 | S16 | 1472 | 72±5 | 66±4 | 875±43 | 236 | 0.64 | 0.82 | 112±9 | 0.68 |
| 17 | S17 | 1501 | 39±1 | 27±2 | 287±9 | 105 | 0.28 | 0.36 | 49±4 | 0.30 |
| 18 | S18 | 1425 | 62±2 | 47±2 | 453±22 | 170 | 0.46 | 0.58 | 79±6 | 0.48 |
| 19 | S19 | 1411 | 36±2 | 27±2 | 283±9 | 101 | 0.27 | 0.34 | 47±5 | 0.29 |
| 20 | S20 | 1407 | 44±2 | 30±2 | 288±12 | 115 | 0.31 | 0.39 | 53±5 | 0.33 |
| 21 | S24 | 1538 | 64±4 | 46±1 | 497±24 | 175 | 0.47 | 0.60 | 81±7 | 0.50 |
| 22 | S26 | 1587 | 74±3 | 58±3 | 669±33 | 215 | 0.58 | 0.74 | 100±10 | 0.62 |
| 23 | S34 | 1560 | 41±2 | 29±2 | 300±10 | 110 | 0.30 | 0.38 | 51±7 | 0.31 |
| 24 | S37 | 1566 | 48±3 | 32±2 | 287±10 | 122 | 0.33 | 0.42 | 56±8 | 0.34 |
| 25 | S39 | 1566 | 42±2 | 30±3 | 265±10 | 111 | 0.30 | 0.38 | 51±5 | 0.31 |
| 26 | S40 | 1520 | 72±8 | 52±5 | 414±21 | 187 | 0.50 | 0.64 | 86±7 | 0.53 |
| 27 | S41 | 1491 | 47±3 | 32±3 | 307±13 | 123 | 0.33 | 0.42 | 57±5 | 0.35 |
| 28 | S46 | 1628 | 44±3 | 32±3 | 227±11 | 112 | 0.30 | 0.39 | 52±4 | 0.32 |
| 29 | S48 | 1583 | 83±6 | 61±4 | 727±36 | 236 | 0.64 | 0.80 | 110±13 | 0.68 |
| 30 | S50 | 1601 | 72±5 | 50±4 | 550±27 | 195 | 0.53 | 0.66 | 90±9 | 0.55 |
| 31 | S52 | 1540 | 71±4 | 53±3 | 702±35 | 208 | 0.56 | 0.71 | 98±7 | 0.60 |
| 32 | S58 | 1597 | 43±3 | 31±2 | 285±12 | 113 | 0.31 | 0.39 | 52±5 | 0.32 |
| 33 | S59 | 1622 | 51±4 | 35±3 | 394±14 | 138 | 0.37 | 0.47 | 64±7 | 0.39 |
| 34 | S60 | 1528 | 61±3 | 39±2 | 346±15 | 152 | 0.41 | 0.52 | 70±8 | 0.43 |
| 35 | S61 | 1619 | 85±4 | 67±3 | 682±34 | 242 | 0.65 | 0.83 | 112±8 | 0.69 |
| **Average** | | | **56±4** | **40±3** | **425±19** | **153 ±49** | **0.41 ±0.13** | **0.52± 0.16** | **69±23** | **0.42 ± 0.13** |
| **World average** | | | **45** | **33** | **420** | | | | | |

The results of $^{238}$U, $^{232}$Th and $^{40}$K activity in soil samples show variation of radiation levels from one soil sampling point to another with some sampling points exhibiting higher levels of radiation than other. The average activity levels for $^{232}$Th, $^{238}$U and $^{40}$K in soils were found to be within the world reported range but slightly above the world average levels of 45 Bq/kg for $^{232}$Th, 33 Bq/kg for $^{238}$U and 420 Bq/kg for $^{40}$K (UNSCEAR, 2000).

The $Ra_{eq}$ ranged from 87 to 242 Bq/kg with an average of 153 ± 49 Bq/kg. The External Hazard Indices ($H_{ex}$) was found to range from 0.24 to 0.65 with an average value of 0.41 ± 0.13 while the Internal hazard index ($H_{in}$) was found to range from 0.29 to 0.83 with an average of 0.52 ± 0.16. Both $H_{ex}$ and $H_{in}$ were lower than unity (< 1) which is the permissible limit given by Inoue K. *et al*., 2017 for use of soil and rock materials for building housed. The average measured dose rate in air was found to be 112 ± 30 nGy/h as shown in Table 4.1 while the calculated dose rate in air (ADRA) was found to be 69 ± 23 nGy/h as shown in Table 4.4.

The experimental value of ADRA was found to be 114 ± 34 nGy/h which is almost double the calculated value of 69 ± 23 nGy/h at the 35 sampling points as shown in Table 4.5. This result can be due to the contribution from cosmic rays and the terrain in Ortum which is not flat but quite rough with hills and troughs which can affect the dose conversion factor. The average Annual Effective Dose Equivalent (AEDE) was found to be 0.42 ± 0.13 mSv/y ranging from 0.25 mSv/y to 0.69 mSv/y. The AEDE value is below Schroeyers, 2017 recommended value of 1 mSv/y for use of building materials.

The activity concentration in soil samples from Ortum shows that the radiological risk associated with the use of soils materials from the region may not cause any significant danger and hence the soils may be used for construction of dwellings and for agriculture purposes.

The $^{232}$Th activity concentration vary from one place to another with an average concentration of 56 ± 4 Bq/kg in 35 surface soil samples collected from Ortum as shown in Table 4.4 and Figure 4.9. The range of $^{232}$Th was found to be 33 ± 2 Bq/kg to 85 ± 4 Bq/kg at sampling points S5 and S61 respectively. The average level is higher than the world average activity of 45 Bq/kg as reported by Schroeyers, (2017). This implies that the soil samples from Ortum have high concentration of $^{232}$Th.

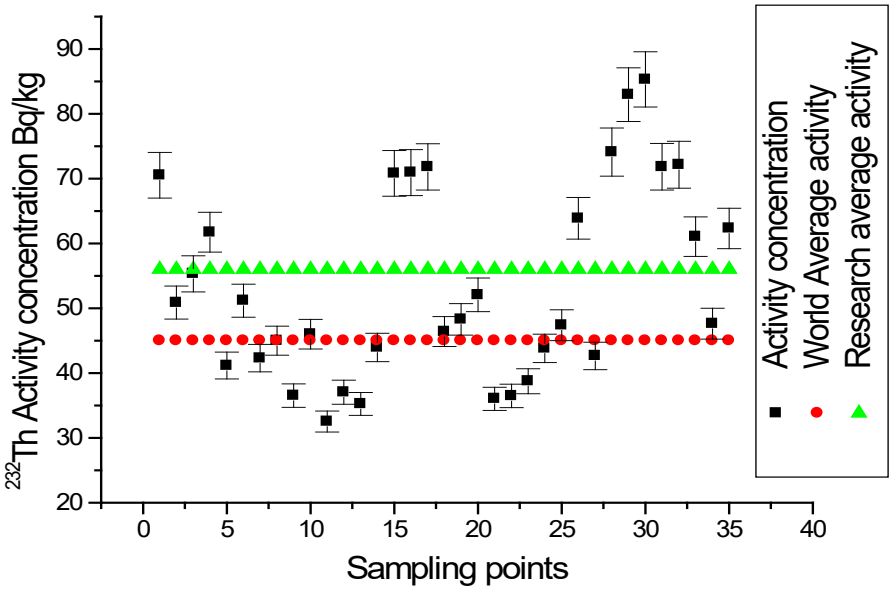


Figure 4.9: Activity concentration levels of $^{232}$Th in soils from different sampling points

The Figure 4.10 show the variation of activity concentration of $^{238}$U from one sampling point to another with an average concentration of 40 ± 3 Bq/kg in 35 surface soil samples analyzed. The range of $^{238}$U in the soil samples collected was from 20 ± 2 Bq/kg to 67 ± 3 Bq/kg at sampling points S5 and S61 respectively. This implies that the average activity concentration of $^{238}$U is higher than the world average activity value of 33 Bq/kg as

reported by Schroeyers, (2017). This implies that the soil samples from Ortum have high concentration of $^{238}U$.

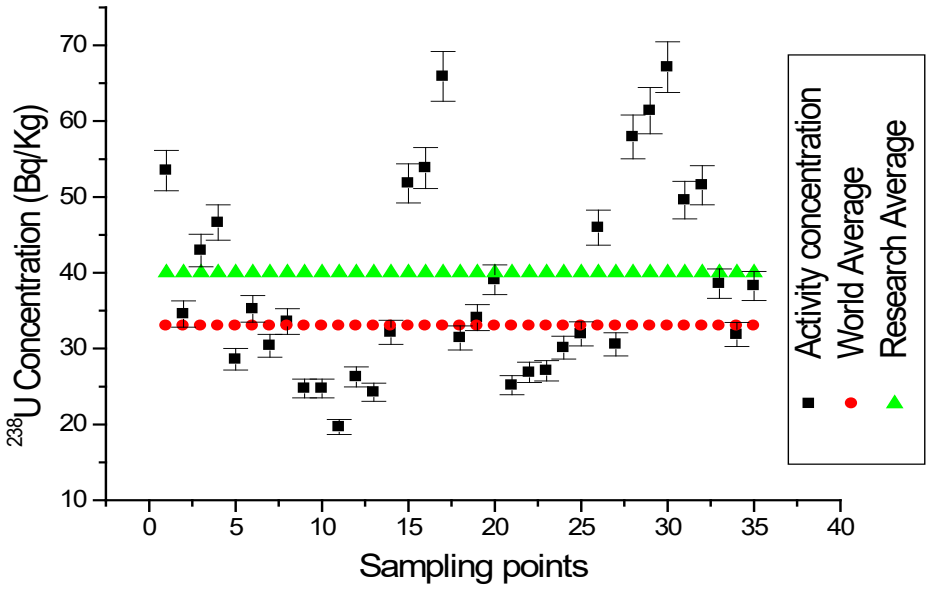


Figure 4.10: $^{238}U$ Activity concentration levels in soil from different sampling points

The Figure 4.11 show the variation of activity concentration of $^{40}K$ from one sampling point to another with an average concentration of 425 ± 19 Bq/kg in 35 surface soil samples analyzed which falls within the world average activity concentration of 420 Bq/kg as reported by Schroeyers, (2017). The range of $^{40}K$ was from 148 ± 7 Bq/kg to 1019 ± 35 Bq/kg collected from sampling points S4 and S9 respectively. This implies that the soil samples in Ortum are within the world average levels for $^{40}K$.

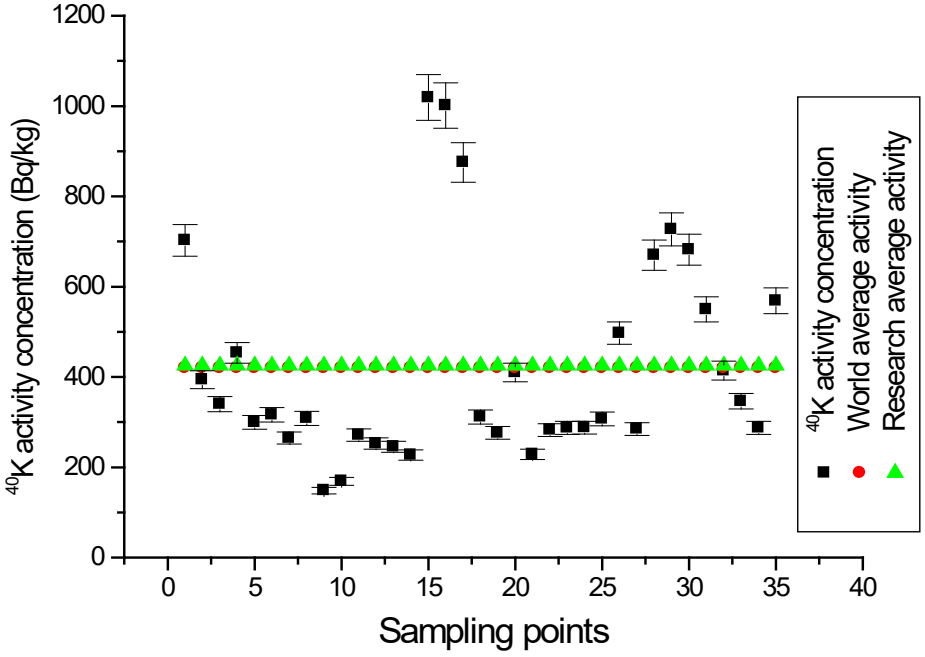


Figure 4.11: $^{40}$K Activity concentration levels in soils from different sampling points

### 4.3.5 Experimental and calculated absorbed dose rate in air

The results of the experimental and calculated dose rate in air is shown in table 4.5 and in Figure 4.11. The results of the dose rate in table 4.5 shows that the experimental or measured dose rate was higher than the calculated dose rate (ADRA) using the equation 3.6 and the concentration of $^{232}$Th, $^{238}$U and $^{40}$K in the soil samples collected.

Table 4.5: Experimental and calculated dose rate in air at the 35 selected sites in this work

| | Site | Calculated Values (C) ADRA (nGy/h) | Experimental Values (E) (nGy/h) | Percent error (\|E-C\|/E) % |
|---|---|---|---|---|
| 1. | S1 | 47±5 | 80±14 | 41 |
| 2. | S2 | 68±6 | 90±07 | 24 |
| 3. | S3 | 56±4 | 90±14 | 37 |
| 4. | S4 | 40±4 | 80±07 | 50 |
| 5. | S5 | 41±3 | 90±14 | 55 |
| 6. | S6 | 46±4 | 80±7 | 43 |
| 7. | S7 | 43±5 | 80±14 | 46 |
| 8. | S8 | 61±5 | 130±28 | 53 |
| 9. | S9 | 110±8 | 150±00 | 26 |
| 10. | S10 | 111±11 | 140±28 | 21 |
| 11. | S11 | 80±6 | 160±14 | 50 |
| 12. | S12 | 56±4 | 150±14 | 62 |
| 13. | S13 | 57±5 | 140±28 | 59 |
| 14. | S14 | 67±8 | 140±0 | 52 |
| 15. | S15 | 43±4 | 130±24 | 67 |
| 16. | S16 | 112±9 | 90±14 | 24 |
| 17. | S17 | 49±4 | 80±14 | 39 |
| 18. | S18 | 79±6 | 90±07 | 12 |
| 19. | S19 | 47±5 | 80±00 | 41 |
| 20. | S20 | 53±5 | 90±14 | 41 |
| 21. | S24 | 81±7 | 160±28 | 49 |
| 22. | S26 | 100±10 | 130±14 | 23 |
| 23. | S34 | 51±7 | 200±14 | 74 |
| 24. | S37 | 56±8 | 190±07 | 70 |
| 25. | S39 | 51±5 | 100±14 | 49 |
| 26. | S40 | 86±7 | 110±00 | 22 |
| 27. | S41 | 57±5 | 90±14 | 37 |
| 28. | S46 | 52±4 | 140±07 | 63 |
| 29. | S48 | 110±13 | 90±14 | 22 |
| 30. | S50 | 90±9 | 80±7 | 13 |
| 31. | S52 | 98±7 | 100±14 | 2 |
| 32. | S58 | 52±5 | 150±28 | 65 |
| 33. | S59 | 64±7 | 100±14 | 36 |
| 34. | S60 | 70±8 | 90±7 | 22 |
| 35. | S61 | 112±8 | 90±15 | 25 |
| **Average** | | **69±23** | **114±34** | |

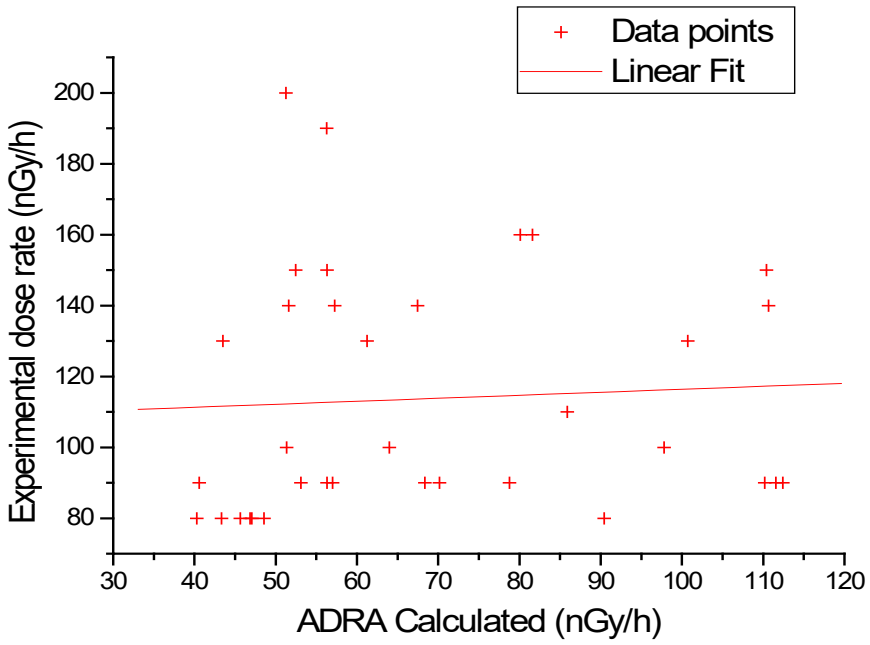


Figure 4.12: Correlation of experimental and calculated dose rate in air

Figure 4.12 shows the plot of the experimental dose rate using the survey meters and the calculated dose rate in air (ADRA). The values are not consistent, and a simple linear fit does not show a clear relationship or directly proportionality. However, the experimental dose rate in air was higher than the calculated dose rate at all sampling points. The average experimental dose rate (114 ± 34 nGy/h) was found to be about twice that of the calculated dose rate in air (69 ± 23 nGy/h) as shown in the Table 4.5. Looking at the percent error values for each of the samples in Table 4.5, there is no simple single conversion factor that can account for the variation between the measured (E) and calculated (C) values. However, the variation in the results can be reduced by modifying the the conversion factor used in equation 3.6 to calculate ADRA.

### 4.3.6 Activity concentration in soils samples from the quarry site

The activity concentration of radionuclides in soils samples collected around the quarry site were found to be slightly higher than those collected from other areas. The levels of radionuclides were also higher than the average values for $^{238}U$ (41 ± 12 Bq/kg) and $^{232}Th$ (56 ± 15 Bq/kg) but the levels of $^{40}K$ (395 ± 16 Bq/kg) were lower than the average values in the 35 soil samples collected as shown in Table 4.1 and 4.6. This can be as a result of soils with high concentration of radionuclides being transported by wind to the quarry site and anthropogenic activities which may lead to high levels of radionuclides $^{238}U$ and $^{232}Th$ and $^{40}K$ in soil as shown in Table 4.7.

Table 4.6: Activity concentration in soil samples from the quarry site

| **No** | **Site** | **Height** | **$^{232}Th$** | **$^{238}U$** | **$^{40}K$** | **Raeq** | **$H_{ex}$** | **$H_{in}$** | **ADRA** | **AEDE** |
|---|---|---|---|---|---|---|---|---|---|---|
| 1 | S24 | 1538 | 64±4 | 46±01 | 497±24 | 175 | 0.47 | 0.60 | 81.62 | 0.50 |
| 2 | S26 | 1587 | 74±3 | 58±3 | 669±33 | 215 | 0.58 | 0.74 | 100.70 | 0.62 |
| 3 | S34 | 1560 | 41±2 | 29±2 | 300±10 | 110 | 0.30 | 0.38 | 51.25 | 0.31 |
| 4 | S39 | 1566 | 42±2 | 30±3 | 265±10 | 111 | 0.30 | 0.38 | 51.33 | 0.31 |
| 5 | S40 | 1520 | 72±8 | 52±5 | 414±21 | 186.60 | 0.50 | 0.64 | 85.88 | 0.53 |
| 6 | S46 | 1628 | 44±3 | 32±3 | 227±11 | 112.48 | 0.30 | 0.39 | 51.62 | 0.32 |
| **Average** | | **1566 m** | **56±15 Bq/kg** | **41±12 Bq/kg** | **395±16 Bq/kg** | **151±46 Bq/kg** | **0.41± 0.12** | **0.52± 0.15** | **70±21 (nGy/h)** | **0.43± 0.14 (mSv/y)** |

### 4.3.7 Activity concentration of $^{238}U$, $^{232}Th$ and $^{40}K$ in rock samples

The average activity concentration of $^{238}U$, $^{232}Th$, and $^{40}K$ in rock samples was 24 ± 2 Bq/kg, 35 ± 3 Bq/kg and 176 ± 6 Bq/kg respectively as shown in Table 4.7. The average activity concentration of $^{238}U$, $^{232}Th$, and $^{40}K$ in soil samples was found to be higher than that in the rock samples by 40%, 37.5% and 58.5% respectively implying that the soils originate from other regions.

Table 4.7: $^{238}U$, $^{232}Th$ and $^{40}K$ activity concentration in rock samples

| Rock sample | $^{238}U$ (Bq/Kg) | $^{232}Th$ (Bq/Kg) | $^{40}K$ (Bq/Kg) | $Ra_{eq}$ (Bq/Kg) | $H_{ex}$ |
|---|---|---|---|---|---|
| **Rock-01** | 26±1 | 39 ±3 | 192±5 | 96.62 | 0.26 |
| **Rock-02** | 25±2 | 37±2 | 188±4 | 93.08 | 0.25 |
| **Rock-03** | 25±1 | 31±1 | 173±3 | 83.34 | 0.23 |
| **Rock-04** | 25±1 | 32±1 | 170±4 | 83.86 | 0.23 |
| **Rock-05** | 20±2 | 37±2 | 178±4 | 86.82 | 0.23 |
| **Rock-06** | 24±1 | 35±1 | 169±4 | 87.55 | 0.24 |
| **Rock-07** | 27±1 | 37±2 | 181±3 | 93.87 | 0.25 |
| **Rock-08** | 26±2 | 35±1 | 177±4 | 89.93 | 0.24 |
| **Rock-09** | 24±1 | 35±2 | 176±4 | 87.39 | 0.24 |
| **Rock-10** | 21±2 | 34±1 | 186±4 | 83.69 | 0.23 |
| **Average** | **24 ± 2** | **35 ± 3** | **176** ± 6 | **87.06** | **0.24** |
| **World Av.** | **33 Bq/Kg** | **45 Bq/Kg** | **420 Bq/Kg** | | |
| **Range** | **20 to 27** | **31 to 39** | **163 to 192** | | |

### 4.3.8 Radiation levels of $^{238}U$, $^{232}Th$ and $^{40}K$ in soil with depth

The activity levels of $^{238}U$, $^{232}Th$ and $^{40}K$ in soil samples collected at different depths 0-5 cm (surface soil) 10 - 20 cm and 30 - 40 cm was analyzed. The activity concentration of $^{238}U$ and $^{232}Th$ reduced with increase in depth as shown in Table 4.8 and Figure 4.13 and 4.14. This implies that soil with high levels of $^{238}U$ and $^{232}Th$ might have been transported

through natural and/or artificial ways to Ortum from the surrounding regions with elevated levels of radionuclides. Likewise, the difference might be due to the use of fertilizers with high levels of radionuclides and anthropogenic activities. The concentration of $^{40}K$ increased with increase in depth as shown in the Figure 4.15 and this could be due to leaching leading to $^{40}K$ concentrating in sub surface soils.

Table 4.8: $^{238}U$, $^{232}Th$ and $^{40}K$ radiation level in soil samples with depth

| Soil | Depth | $^{238}U$ (Bq/Kg) | $^{232}Th$ (Bq/Kg) | $^{40}K$ (Bq/Kg) |
|---|---|---|---|---|
| **S1** | **0-5 cm** | 24.75±1.36 | 46.00±1.77 | 168.77±08.44 |
| | **10-20 cm** | 25.54±1.19 | 42.45±1.63 | 289.33±13.83 |
| | **30-40cm** | 20.36±1.30 | 43.83±2.74 | 462.55±18.55 |
| **S13** | **0-5 cm** | 45.95±1.02 | 63.88±2.23 | 496.91±24.85 |
| | **10-20 cm** | 47.30±2.37 | 52.46±2.57 | 589.34±29.51 |
| | **30-40cm** | 40.72±1.18 | 45.77±1.42 | 592.56±32.18 |
| **S15** | **0-5 cm** | 65.90±4.19 | 71.81±3.57 | 875.35±43.77 |
| | **10-20 cm** | 50.28±2.34 | 52.63±2.27 | 857.74±39.08 |
| | **30-40cm** | 40.62±1.92 | 49.45±2.23 | 927.02±43.23 |
| **S22** | **0-5 cm** | 26.84±1.70 | 36.48±2.26 | 282.52±09.13 |
| | **10-20 cm** | 24.83±1.22 | 38.37±1.08 | 411.25±24.67 |
| | **30-40cm** | 24.02±1.08 | 37.77±1.92 | 602.33±32.87 |
| **S23** | **0-5 cm** | 31.84±2.02 | 47.61±1.84 | 287.33±09.37 |
| | **10-20 cm** | 32.26±2.22 | 52.38±1.98 | 433.54±24.65 |
| | **30-40cm** | 26.25±2.88 | 46.82±2.77 | 518.69±28.69 |
| **S37** | **0-5 cm** | 28.58±2.70 | 41.16±1.82 | 299.52±09.98 |
| | **10-20 cm** | 26.28±2.53 | 38.24±1.45 | 354.23±12.45 |
| | **30-40cm** | 22.63±1.98 | 35.81±1.42 | 582.66±15.29 |
| **S46** | **0-5 cm** | 32.14±2.30 | 43.95±1.85 | 227.27±11.36 |
| | **10-20 cm** | 25.60±1.89 | 38.72±2.23 | 463.73±22.30 |
| | **30-40cm** | 26.50±2.13 | 36.83±2.11 | 452.78±21.40 |
| **S50** | **0-5 cm** | 49.56±2.34 | 71.82±3.35 | 549.69±27.48 |
| | **10-20 cm** | 42.38±2.83 | 58.45±2.32 | 555.34±26.78 |
| | **30-40cm** | 40.78±2.55 | 52.48±1.83 | 765.43±33.85 |
| **Average** | **0-5 cm** | **38.19±3.84** | **52.84±2.71** | **398.42±18.05** |
| | **10-20 cm** | **34.31±2.45** | **46.71±2.57** | **494.31±24.16** |
| | **30-40cm** | **30.24±2.19** | **43.60±2.43** | **613.00±28.26** |

The figure 4.13 shows a general trend of $^{238}U$ reducing with increasing depth with the highest activity level of 65.90 ± 4.19 Bq/kg recorded for surface soil at site S15 and the lowest activity found in the soil sampling S1 at a depth of 30 cm to 40 cm. The average trend of $^{238}U$ activity concentration reducing with depth may be due to deposition of soil by wind and water from regions of high activity concentration.

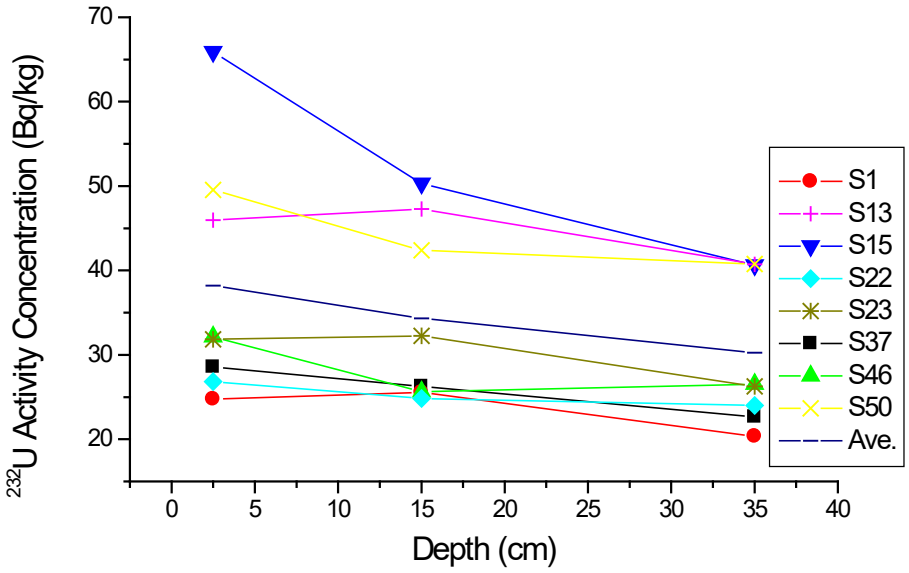


Figure 4.13: Uranium-238 concentration in soil with depth

Figure 4.14 shows $^{232}Th$ activity variation for soil samples with depth. The general trend shows that the activity concentration reduced with increase in depth. This can be as a result of anthropogenic activities and transportation of soils rich in $^{232}Th$ to the region from other places.

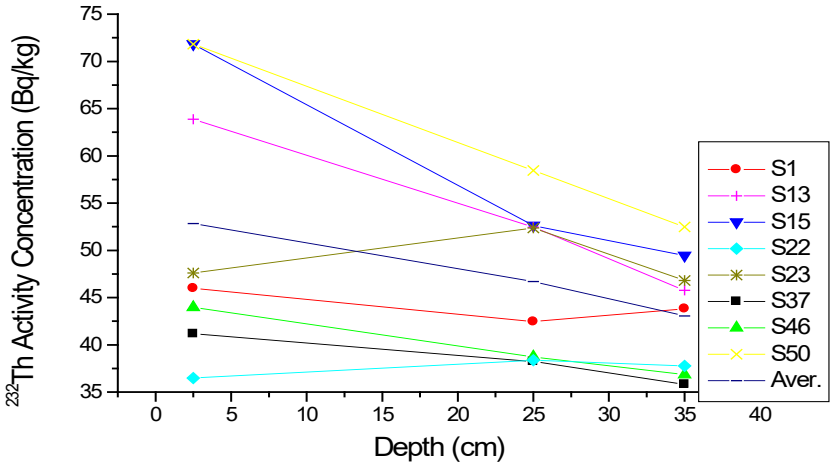


Figure 4.14: Thorium-232 activity concentration in soil with depth

The figure 4.15 shows a general trend of $^{40}$K increasing with increasing depth with the highest activity level of 927.02 ± 43.23 Bq/kg recorded for soil at a depth of 30 cm to 40 cm at site S15 and the lowest activity was 168.77 ± 08.44 Bq/kg found in the soil from the sampling point S1 at a depth of 0 cm to 5 cm. The average trend of activity concentration increased with depth can be attributed to leaching.

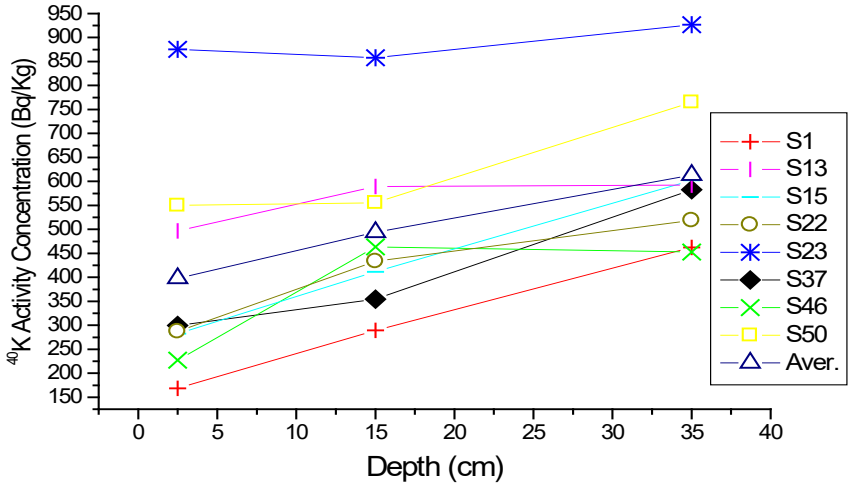


Figure 4.15: Potassium-40 activity concentration in soil with depth

Figure 4.16 shows the average trend of $^{238}U$, $^{232}Th$ and $^{40}K$. The Figure shows that $^{238}U$ and $^{232}Th$ activity decreases with increasing depth while $^{40}K$ increases with increasing depth.

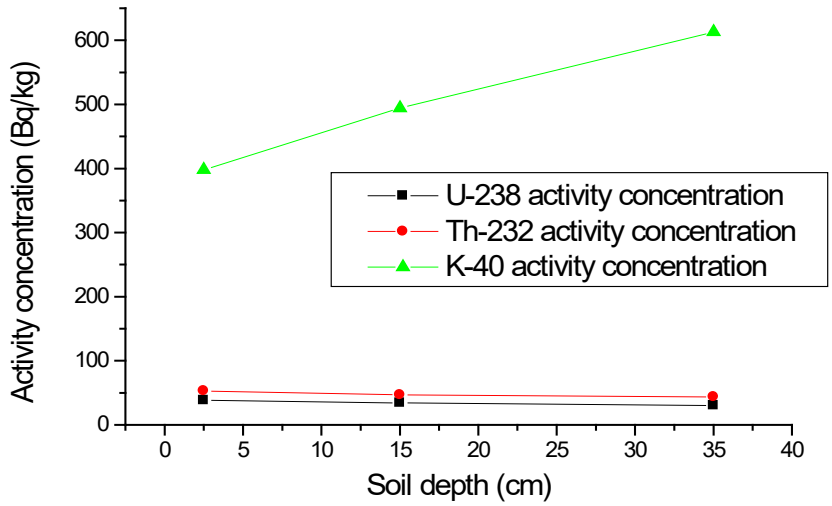


Figure 4.16: Average activity concentration in soils with depth

### 4.3.9 Relationship of $^{238}U$ and $^{232}Th$ activity concentration in soil samples

The uranium-thorium activity concentration was plotted as shown in Figure 4.17. The figure shows a very consistent relationship between $^{238}U$ and $^{232}Th$ activity with a correlation coefficient of r = 0.964. This means that if the concentration of uranium or thorium is known, it is possible to estimate the concentrations of the other radionuclide using the linear Equation 4.1

$$U = A + B \times Th \qquad 4.1$$

Where A and B are constants and U is the $^{238}U$ concentration and Th is the $^{232}Th$ concentration. In this case, we can use the straignt line Equation 4.2 to determine the concentration of either $^{238}U$ or $^{232}Th$ if one is known.

$$U = -(6.12 \pm 0.21) + (0.83 \pm 0.006) \times Th \quad 4.2$$

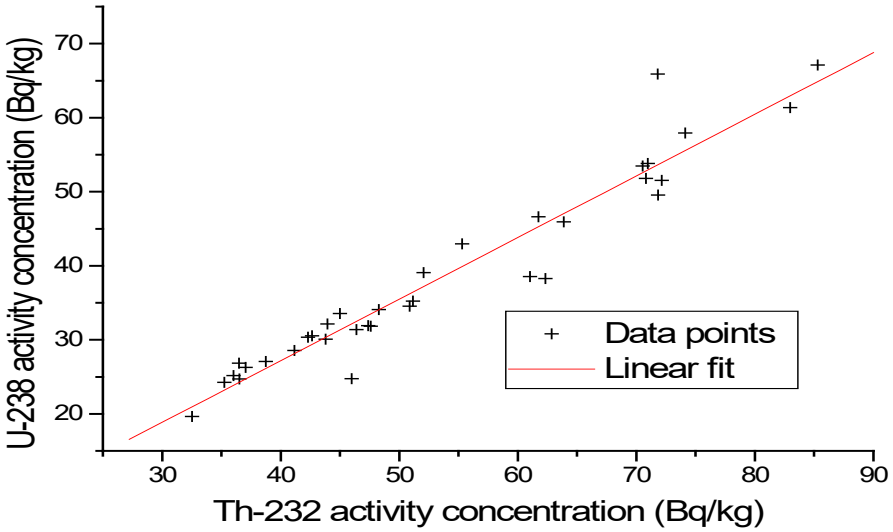


Figure 4.17: Comparison uranium and thorium activity concentration

The uranium-thorium relationship in figure 4.17 show that the source or origin of the soil samples from Ortum is the same since uranium and thorium ratio is almost the same and it may be concluded that soils from Ortum originate from the same geological formation.

### 4.3.10 Results of dose to risk conversion

The radiation risk leading to death in Ortum was estimated using equation 3.10. Using the US Department of energy recommended AEDE-to-fatal cancer risk factors of 5 x $10^{-3}$ $mSv^{-1}$ (D) (Lawrence, 2002) for the public, the population of Ortum 3,372 (P) according to Kenya Bureau of Statistics Census, 2019 and the Annual effective dose of 0.42 mSv/y we have from equation 3.10;

$NP = D \times E \times P = 5 \times 10^{-3} \times 0.42 \times 3{,}372 = 7.081$.

The results implies that about 7 people or 0.2% of the people in Ortum are likely to die due to exposure to background radiation. This is insignificant and hence the lifetime risk of someone dying due to radiation related illness is low.

### 4.3.11 Results of lifetime cancer risk ($LTCR_{BR}$)

The Lifetime cancer risk ($LTCR_{BR}$) due to external exposure was calculated using equation 3.11 and found to be $1.47 \times 10^{-3}$ using the average annual effective dose rate of $4.2 \times 10^{-4}$ Sv/y (Table 4.3), average lifetime of 70 years and the risk factor 0.05.

The $LTCR_{BR}$ results of $1.47 \times 10^{-3}$ is less than the world average of $2.99 \times 10^{-3}$ (Ahmad *et al*., 2019). This implies that the radiological risk due to background radiation in Ortum is low and insignificant since about 1.5 people out of 1000 are likely to die due to exposue to background radiation in their lifetime.

## 4.4 Results of elemental analysis in soil samples using EDXRF

The results of elemental analysis of the 35 surface soil samples and 24 soil samples collected at different depths using the EDXRF spectrometer are presented in table 4.11.

### 4.4.1 Results of analysis of reference material using the EDXRF

The Reference Material (RM) IAEA-375 (soil) and Proficiency Test for X Ray Fluorescence Laboratories (PTXRF-09) provided by the International Atomic Energy Agency (IAEA) (IAEA, 2018) were prepared into pellets and analyzed using the EDXRF

Spectrometer with the same procedure used to analyze soil samples to verify if the results obtained are accurate and comparable. The results obtained from the analysis were correlated with the certified values as shown in Table 4.9. Zeta score test was done whereby Zeta $|\zeta|$ <1.96 is OK, $|\zeta|$ >1.96 is questionable results and $|\zeta|$ >2.576 is not OK. The results of the measured and reference values were plotted as shown in Figure 4.18. The Z-score results shows that the all the measured and reference values are in good agreement and that they fall within the acceptable limits (OK) and none of the results were questionable or not OK.

Table 4.9: Measured and reference values for IAEA-375 Reference Material

| | **Measured value** | | **Reference value** | | **Comparison** | | |
|---|---|---|---|---|---|---|---|
| **Nuclide** | **Conc. (ug/kg)** | **± 1σ** | **Conc. (ug/kg)** | **± 1σ** | **Deviation (%)** | **ζ-score** | **OK?** |
| Zn | 78.8 | 4.3 | 75 | 0.4 | 5.07% | 0.880 | **OK** |
| Cu | 18.8 | 0.7 | 20 | 0.5 | -6.00% | -1.395 | **OK** |
| Ni | 64.5 | 2.7 | 60 | 3.6 | 7.50% | 1.000 | **OK** |
| Pb | 20.4 | 1.2 | 20 | 0.4 | 2.00% | 0.316 | **OK** |

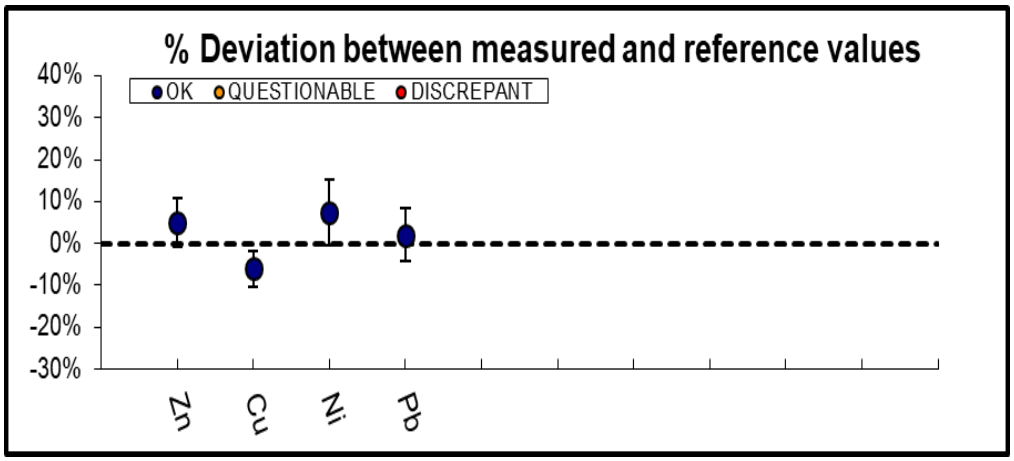


Figure 4.18: Zeta score graph for IAEA-375 reference material

The results of analysis of certified reference material PTXRF-09 are shown in Table 4.10 and Figure 4.19. The results show that the Zeta |ζ| score test values were less than 1.96 (<1.96) which falls under OK showing that the measure and the certified values were in good agreement. The correlation coefficient between certified values and the measured values for CRM PTXRF-09 was found to be equal to r = 0.99 hence the values obtained from the experiment are credible and in agreement with the certified values.

Table 4.10: Measure and certified values for EDXRF for CRM PTXRF-09

| | **Measured value** | | **Reference value** | | **Comparison** | | |
|---|---|---|---|---|---|---|---|
| | **Activity** | | **Activity** | | **%** | | |
| **Nuclide** | **Bq/Kg** | **± 1σ** | **Bq/Kg** | **± 1σ** | **Deviation** | **ζ-score** | **OK?** |
| K | 1.875 | 0.2 | 1.95 | 0.07 | -3.85% | -0.354 | **OK** |
| Ni | 38.6 | 3.95 | 39.95 | 3.51 | -3.38% | -0.255 | **OK** |
| Cu | 23.5 | 1.95 | 20.1 | 2.05 | 16.92% | 1.202 | **OK** |
| Zn | 101.48 | 12.73 | 96.1 | 7.73 | 5.60% | 0.361 | **OK** |
| Pb | 39.53 | 7.95 | 36.93 | 3.43 | 7.04% | 0.300 | **OK** |
| Mn | 1042.37 | 72.62 | 1000 | 60.00 | 4.24% | 0.450 | **OK** |
| Fe | 3.01 | 0.2 | 2.97 | 0.1 | 1.35% | 0.212 | **OK** |
| Ca | 1.29 | 0.08 | 1.38 | 0.05 | -6.52% | -0.954 | **OK** |
| Ti | 4326.19 | 378.1 | 4300 | 200 | 0.61% | 0.061 | **OK** |

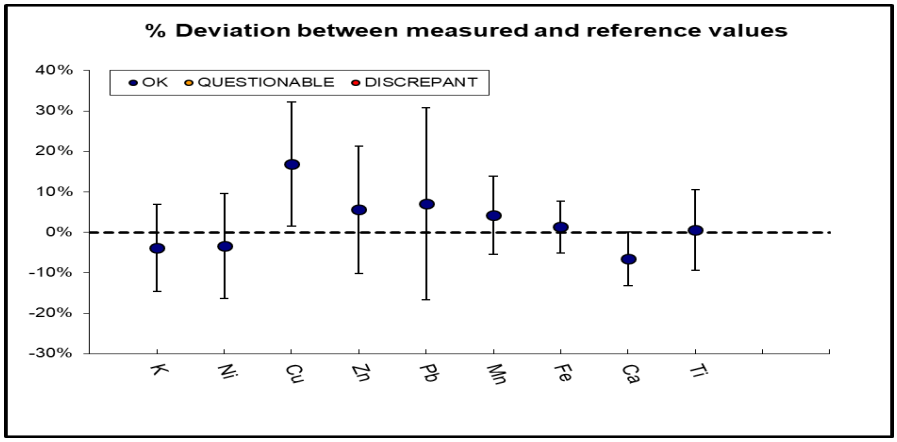


Figure 4.19: Zeta score for CRM PTXRF-09

The results of analysis of the reference materials IAEA-375 (soil material) and Proficiency Test for X Ray Fluorescence Laboratories (PTXRF-09) show good results and correlation between the experimental and the certified values. This implies that the results of elemental concentration of soil samples analyzed using EDXRF spectrometer are credible.

### 4.4.2 Results of energy calibration

The results of energy calibration for EDXRF system using Cr (5.41 keV), Fe (6.4 keV), Ni (7.42 keV) and Mo (17.44 keV) using equation 3.4 is as shown in the energy calibration curve in figure 4.20. The relationship between the counts and energy is a straight line (E = 0.2021 Ch + 49.86) which means that Energy and the Counts are directly proportional.

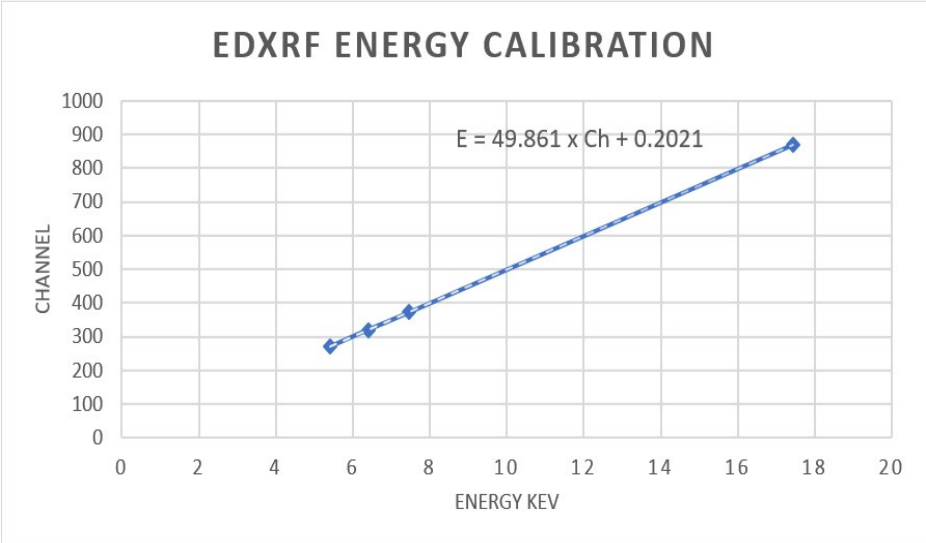


Figure 4.20: Energy calibration curve for EDXRF

### 4.4.3 Results of elemental concentration in soil samples

Assessment of metal pollutants was done for 13 elements in the 35 soil samples collected from Ortum. The results of the mean elemental composition of 13 elements in the soil

samples was 58 ± 8 ppm (Ni), 47 ± 5 ppm (Cu), 73 ± 14 ppm (Zn), 22 ± 6 ppm (Pb), 3.8 ± 0.6 %w (K), 24.4 ± 5.2 %w (Ca), 1.7 ± 0.5 %w (Fe), 7.7 ± 2.3 %w (Ti), 1530 ± 137 ppm (Mn), 61 ± 11 ppm (Rb), 442 ± 23 ppm (Sr), 411 ± 164 ppm (Zr) and 29 ± 5 ppm (Nb) as shown in the Table 4.11 (One percent of weight (%w) is equal to 10000ppm). The concentration of all the 13 elements in the soil was within the world average range. The concentration of the heavy metals of interest due to their adverse health effects in this study Ni, Cu, Zn and Pb were in the order Pb < Cu < Ni <Zn as shown in Figure 4.22. The average concentration of Ni (58 ± 8 ppm), Zn (73 ± 14 ppm) and Pb (22 ± 6 ppm) where above the world average of 20 ppm, 70 ppm and 14 ppm respectively as reported by Towett *et al*, 2015.

The results show that the soil in Ortum contains high levels of heavy metals Ni, Zn and Pb relative to the world average. This can be attributed to anthropogenic activities in the region, the geology of Ortum having high levels of Ni, Zn and Pb in rocks and soil, agricultural activities in the region associated with application of fertilizers with high levels of Pb, Ni and Zn and dumping of wastes with high levels of heavy metals Pb, Zn and Ni. Further research needs to be conducted to find out the sources of high levels of heavy metals Pb, Zn, Ni, Fe, Mn and Sr above the world average in soil samples from Ortum. Proper dumping of domestic and industrial waste containing heavy metals need to be done to avoid possible soil contamination with heavy metals. .

Table 4.11: Elemental concentration in 35 surface soil samples in Ortum

| Site | Ni (ppm) | Cu (ppm) | Zn (ppm) | Pb (ppm) | K (%w) | Ca (%w) | Fe (%w) | Ti (%w) | Mn (ppm) | Rb (ppm) | Sr (ppm) | Zr (ppm) | Nb (ppm) |
|---|---|---|---|---|---|---|---|---|---|---|---|---|---|
| **S1** | 55±3 | 50±3 | 80±15 | 24±8 | 4.7±1.4 | 27.9±2.7 | 5.5±0.5 | 1.2±0.2 | 1038±86 | 68±6 | 722±16 | 740±15 | 24±4 |
| **S2** | 50±3 | 44±2 | 88±12 | 17+6 | 5.1±0.5 | 17.4±1.2 | 6.2±0.4 | 2.1±0.4 | 2319±163 | 78±6 | 469±11 | 406±10 | 34.±4 |
| **S3** | 67±8 | 46±3 | 88±16 | 17±9 | 4.4±0.4 | 32.6±1.8 | 5.3±0.4 | 1.3±0.1 | 851±86.73 | 64±5 | 757±17 | 657±15 | 17±4 |
| **S4** | 76±4 | 51±2 | 90±13 | 19±9 | 3.5±0.3 | 28.9±1.7 | 4.2±0.1 | 2.6±0.2 | 683±75.97 | 71±5 | 726±14 | 641±13 | 20±5 |
| **S5** | 76±5 | 53±3 | 99±14 | 24±6 | 2.6±0.4 | 57.4±3.1 | 3.8±0.1 | 1.4±0.1 | 793±85.30 | 56±4 | 232±7 | 352±9 | 26±4 |
| **S6** | 61±4 | 51±3 | 67±15 | 14±7 | 1.3±0.3 | 39.5±1.1 | 2.9±0.2 | 1.3±0.1 | 618±75.67 | 55±3 | 253±9 | 266±8 | 27±4 |
| **S7** | 66±4 | 50±3 | 85±12 | 21±7 | 3.5±0.3 | 13.4±1.2 | 8.9±0.3 | 1.7±0.1 | 1534±129 | 73±6 | 741±17 | 609±15 | 39±5 |
| **S8** | 62±5 | 44±3 | 73±16 | 14±5 | 2.6±0.3 | 32.8±1.8 | 6.4±0.2 | 1.2±0.1 | 858±86.83 | 54±4 | 423±11 | 391±10 | 33±4 |
| **S9** | 56.±3 | 40±2 | 64±14 | 26±5 | 1.9±0.3 | 43.5±3.9 | 6.0±0.2 | 1.1±0.1 | 903±92.07 | 51±3 | 401±10 | 229±9 | 32±4 |
| **S10** | 63±4 | 47±2 | 63±16 | 27±7 | 2.4±0.5 | 23.8±1.7 | 10.0±0.3 | 1.2±0.2 | 1206±128 | 84±9 | 281±9 | 584±16 | 22±4 |
| **S11** | 49±3 | 39±2 | 38±13 | 26±5 | 1.8±0.3 | 33.6±3.1 | 2.9±0.2 | 1.4±0.2 | 466±86 | 66±5 | 286±15 | 245±14 | 45±6 |
| **S12** | 59±4 | 49±3 | 81±13 | 18±8 | 3.2±0.6 | 11.4±1.5 | 11.0±2.3 | 2.1±0.5 | 2889±152 | 64±4 | 315±7 | 274±8 | 29±4 |
| **S13** | 54±4 | 47±2 | 70±15 | 29±7 | 5.8±0.6 | 15.3±2.2 | 12.5±1.2 | 2.4±0.4 | 2854±134 | 69±6 | 559±11 | 486±8 | 33±5 |
| **S14** | 42±5 | 38±3 | 88±16 | 22±4 | 5.0±0.3 | 18.7±1.2 | 9.7±1.2 | 1.8±0.1 | 2213±135 | 79±6 | 441±13 | 569±13 | 41±5 |
| **S15** | 48±4 | 48±3 | 70±15 | 32±8 | 3.3±0.3 | 19.4±1.2 | 11.3±1.3 | 2.4±0.1 | 2284±124 | 55±4 | 271±8 | 262±8 | 30±4 |
| **S16** | 48±5 | 44±3 | 46±11 | 27±9 | 4.4±0.3 | 22.8±2.3 | 11.7±1.3 | 2.1±0.3 | 1885±127 | 66±5 | 380±10 | 271±9 | 33±5 |
| **S17** | 54±5 | 45±3 | 80±19 | 21±8 | 3.2±0.3 | 18.6±0.5 | 14.0±2.3 | 2.6±0.1 | 1733±125 | 54±4 | 215±7 | 268±8 | 32±4 |
| **S18** | 52±5 | 43+3 | 59±13 | 29±8 | 1.6±0.2 | 14.6±0.2 | 7.7±2.3 | 1.9±0.2 | 2489±215 | 56±4 | 220±5 | 228±8 | 30±4 |
| **S19** | 67±5 | 46±3 | 98±18 | 18±9 | 12±2.6 | 17.6±0.3 | 13.1±2.4 | 2.0±0.4 | 1820±166 | 69±4 | 275±6 | 175±7 | 30±4 |
| **S20** | 72±6 | 48±3 | 96±16 | 16±6 | 1.7±0.2 | 18.3±1.3 | 12.6±2.2 | 2.2±0.3 | 2099±142 | 52±3 | 277±6 | 171±7 | 29±4 |
| **S22** | 73±6 | 47±3 | 94±19 | 20±7 | 2.3±0.3 | 15.2±1.2 | 16.5±1.3 | 2.6±0.2 | 3462±171 | 56±4 | 268±7 | 275±9 | 28±4 |
| **S23** | 52±3 | 44±3 | 57±18 | 37±6 | 5.8±0.5 | 30.1±3.6 | 8.9±1.1 | 1.4±0.5 | 1544±135 | 64±5 | 803±18 | 783±18 | 26±4 |

| Site | Ni (ppm) | Cu (ppm) | Zn (ppm) | Pb (ppm) | K (%w) | Ca (%w) | Fe (%w) | Ti (%w) | Mn (ppm) | Rb (ppm) | Sr (ppm) | Zr (ppm) | Nb (ppm) |
|---|---|---|---|---|---|---|---|---|---|---|---|---|---|
| **S24** | 56±4 | 47±4 | 69±15 | 26±8 | 3.2±0.6 | 12.2±1.3 | 9.0±1.6 | 1.9±0.4 | 1631±113 | 69±4 | 814±17 | 658±16 | 28±4 |
| **S26** | 52±4 | 40±3 | 70±12 | 20±5 | 3.9±0.4 | 27.6±1.6 | 5.7±1.1 | 0.8±0.1 | 859±79 | 64±5 | 497±10 | 576±12 | 29±4 |
| **S34** | 50±5 | 42±2 | 81±12 | 36±8 | 2.9±0.4 | 34.6±1.2 | 7.0±1.0 | 1.3±0.3 | 929±115 | 34±4 | 298±8 | 306±9 | 28±5 |
| **S37** | 53±5 | 59±5 | 88±16 | 30±9 | 1.8±0.3 | 28.3±1.3 | 9.6±1.2 | 2.1±0.1 | 1662±119 | 28±3 | 518±12 | 368±10 | 30±4 |
| **S39** | 60±4 | 52±3 | 85±15 | 17±8 | 5.2±3.0 | 17.8±1.6 | 8.6±2.6 | 2.5±0.6 | 2145±201 | 61±3 | 283±16 | 205±7 | 29±4 |
| **S40** | 65±5 | 57±4 | 97±14 | 16±6 | 7.4±2.1 | 19.3±1.9 | 10.2±2.7 | 1.9±0.5 | 1997±126 | 73±5 | 295±9 | 315±12 | 21±4 |
| **S41** | 58±4 | 50±4 | 71±13 | 21±6 | 3.7±1.0 | 15.4±1.2 | 8.0±0.6 | 1.5±0.2 | 1556±129 | 63±6 | 347±25 | 511±18 | 39±4 |
| **S46** | 57±4 | 47±3 | 55±13 | 12±9 | 2.8±0.7 | 19.8±1.9 | 7.5±0.8 | 1.6±0.3 | 1373±82 | 66±6 | 456±18 | 399±15 | 33±5 |
| **S48** | 58±5 | 55±4 | 75±14 | 27±9 | 4.3±0.9 | 29.5±2.8 | 5.8±1.2 | 1.2±0.1 | 829±89 | 50±4 | 323±9 | 405±13 | 29±4 |
| **S50** | 62±6 | 44±2 | 76±17 | 15±5 | 3.8±0.7 | 35.1±1.9 | 6.9±1.1 | 1.1±0.2 | 1003±97 | 51±4 | 414±13 | 268±9 | 31±2 |
| **S52** | 53±3 | 49±3 | 77±16 | 18±8 | 3.6±0.6 | 16.1±1.9 | 9.3±0.6 | 1.5±0.3 | 1217±98 | 60±4 | 554±15 | 450±13 | 29±4 |
| **S59** | 58±3 | 49±3 | 61±17 | 19±9 | 5.2±0.6 | 12.5±2.0 | 7.7±1.0 | 1.4±0.2 | 898±82 | 54±5 | 398±10 | 523±12 | 26±4 |
| **S60** | 53±3 | 42±3 | 69±12 | 22±5 | 4.3±0.4 | 32.3±1.9 | 8.3±0.4 | 1.3±0.5 | 901±103 | 54±5 | 478±13 | 306±9 | 28±5 |
| **Mean** | **58±8** | **47±5** | **73±14** | **22±6** | **3.8±0.6** | **24.4±5.2** | **7.7±2.3** | **1.7±0.5** | **1530±137** | **61±11** | **442±23** | **411±164** | **29±5** |
| **Max** | **76±5** | **57±4** | **98±18** | **37±6** | **5.8±0.6** | **43.5±3.9** | **16.5±1.3** | **2.6±0.2** | **3462±171** | **84±9** | **814±17** | **783±18** | **45±6** |
| **Min** | **42±5** | **38±3** | **38±13** | **12±5** | **1.3±0.3** | **12.2±1.3** | **2.9±0.2** | **0.8±0.1** | **466±86** | **28±3** | **215±15** | **205±7** | **17±4** |
| **[a]World Average** | **20** | **55** | **70** | **14** | **-** | **-** | **2.8** | **4.4** | **900** | **-** | **375** | **-** | **-** |
| **[a]Range** | **0.2 - 500** | **1.0 - 250** | **10 - 602** | **2.0 - 16,338** | **-** | **-** | **1-550** | **2-240** | **7-9000** | **-** | **32-1000** | **-** | **-** |

[a] Means values compiled by Towett *et al*, 2015

percent of weight (1%w = 10000ppm)

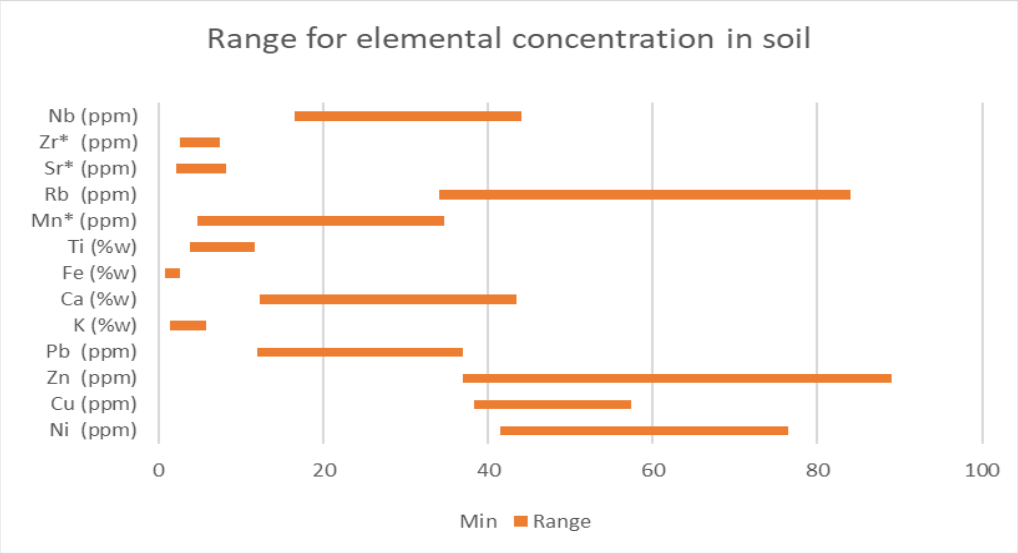


Figure 4.21: The rage of the elemental concentration in soils (* means x $10^2$)

Figure 4.21 shows the range of different elements with Zinc and Rubidium having the highest range while iron having the least range. Figure 4.22 shows the variation of concentration of heavy metal of interest (Ni, Zn, Cu and Pb) from different sampling points due to their toxicity. The figure shows that the concentration of heavy metals was in the order of Zn > Ni > Cu > Pb.

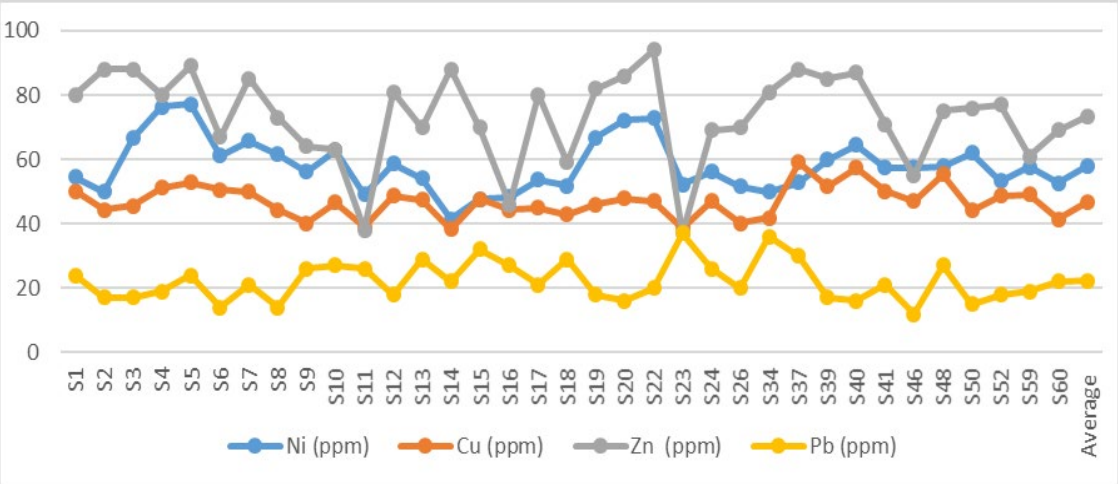


Figure 4.22: Elemental Concentration in surface soils for Ni, Cu, Zn and Pb

### 4.4.4 Elemental concentration of Ni, Cu, Zn and Pb with depth

A total of 24 soils samples from 8 different sampling points and depths were collected and the elemental concentration analyzed using EDXRF spectrometer. Four elements Pb, Ni, Cu and Zn were closely analyzed due to the adverse health effect when they accumulate in the body beyond certain limits. The results obtained are as shown in the Table 4.12.

Table 4.12: Elemental concentration of Ni, Zn, Cu and Pb (mg/Kg) in soil samples with depth

| Sampling point | Depth | Nickel (Ni) | Copper (Cu) | Zinc (Zn) | Lead (Pb) |
|---|---|---|---|---|---|
| **S1** | 0-5 cm | 54±12 | 50±13 | 80±15 | 24±08 |
| | 10-20 cm | 55±15 | 50±12 | 77±14 | 19±02 |
| | 30-40cm | 61±18 | 48±13 | 78±16 | 16±02 |
| **S13** | 0-5 cm | 54±15 | 47±12 | 71±14 | 30±07 |
| | 10-20 cm | 60±21 | 47±12 | 74±14 | 24±10 |
| | 30-40cm | 55±15 | 43±14 | 63±14 | 23±07 |
| **S15** | 0-5 cm | 48±15 | 48±13 | 50±16 | 32±08 |
| | 10-20 cm | 48±17 | 45±10 | 45±11 | 27±12 |
| | 30-40cm | 49±13 | 40±11 | 25±09 | 22±09 |
| **S22** | 0-5 cm | 73±16 | 47±12 | 94±18 | 21±07 |
| | 10-20 cm | 67±23 | 48±08 | 73±19 | 24±07 |
| | 30-40cm | 77±20 | 49±13 | 71±11 | 13±07 |
| **S23** | 0-5 cm | 52±12 | 44±13 | 57±12 | 38±06 |
| | 10-20 cm | 48±14 | 40±12 | 35±11 | 34±05 |
| | 30-40cm | 47±20 | 42±10 | 42±08 | 33±05 |
| **S37** | 0-5 cm | 53±22 | 59±15 | 88±16 | 31±09 |
| | 10-20 cm | 59±19 | 54±13 | 77±15 | 21±09 |
| | 30-40cm | 61±19 | 54±14 | 61±10 | 13±05 |
| **S46** | 0-5 cm | 57±14 | 47±13 | 55±13 | 12±07 |
| | 10-20 cm | 56±14 | 47±12 | 82±17 | 12±07 |
| | 30-40cm | 54±19 | 46±12 | 76±14 | 13±06 |
| **S50** | 0-5 cm | 62±23 | 44±14 | 77±17 | 15±05 |
| | 10-20 cm | 62±14 | 45±14 | 83±16 | 22±06 |
| | 30-40cm | 61±16 | 43±16 | 63±11 | 13±05 |
| **Average** | **0-5 cm** | **57±16** | **48±15** | **72±15** | **25±07** |
| | **10-20 cm** | **57±18** | **46±15** | **68±14** | **23±07** |
| | **30-40 cm** | **58±19** | **45±15** | **60±12** | **18±06** |

The results show a general trend of Cu, Zn and Pb in soil samples reducing with increasing depth while Ni increased with increasing depth. The variation of elemental concentration with depth at different soil sampling points is as shown in Figures 4.13, 4.14, 4.15 and 4.16. Nickel (Ni) concentration with depth at different sites is as shown in figure 4.23.

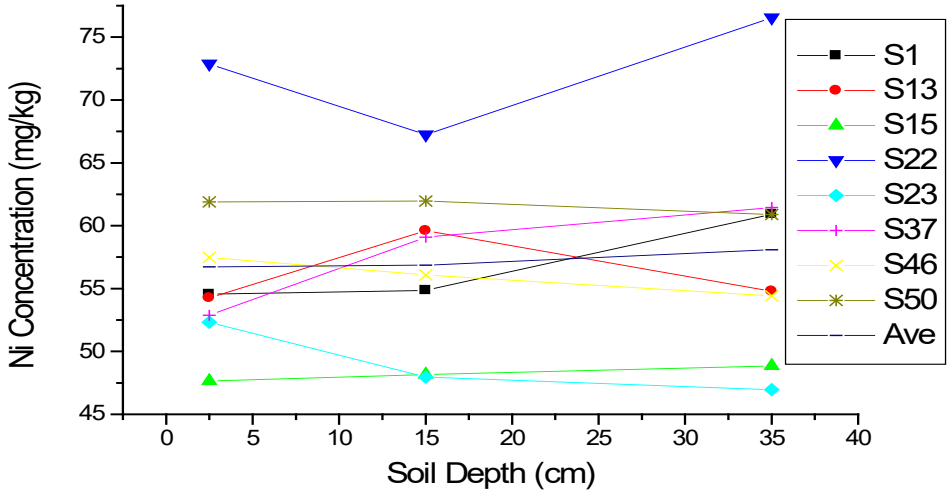


Figure 4.23: Ni concentration in soil samples with depth

Ni concentration with depth from one sampling point to another was seen to be inconsistent. The highest concentration of Ni was 77 ± 20 mg/Kg at site S13 and a depth of 30 to 40 cm and the lowest concentration was 47 ± 20 mg/Kg at site S23 and a depth of 30 cm to 40 cm. Some sites showed Ni concentration reducing with depth while others increasing with depth. The average concentration at different depths increased slightly with increasing depth from 57 ± 16, 57 ± 18 and 58 ± 19 at 0 - 5 cm, 10 - 20 cm and 30 - 40 cm respectively. The increase in Ni concentration with depth can be attributed to leaching of Ni from surface soils hence accumulating in sub-surface soil.

Copper (Cu) concentration in most of the sampling sites reduced with increase in depth for the soil samples collected in Ortum as shown in figure 4.24.

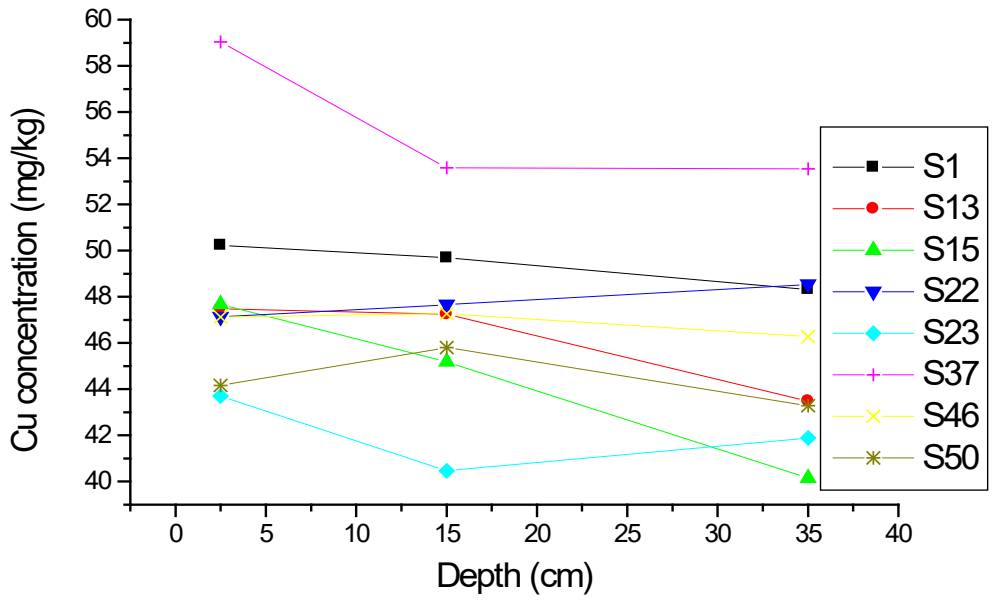


Figure 4.24: Cu concentration in soil samples with depth

The highest concentration of Cu was at site S37 with 59 ± 19 mg/kg from the surface soil and the lowest concentration was recorded at S23 with 35 ± 11 mg/kg at a depth 10 – 20 cm. The average concentration with depth shows a general trend of Cu reducing with increasing depth. This implies that copper concentration is high on the surface soil due to accumulation of Cu from various sources in the environment including industrial sources, pesticides, vehicle fluids leaks and dumping of wastes with high levels of Cu.

Zinc (Zn) concentration varies with depth from one sampling site to another as shown in figure 4.25. The highest concentration of zinc was from the surface soil recorded at site S22 with a concentration of 94 ± 18 mg/kg and the lowest was recorded at a depth of 30 cm to 40 cm at site S15 with a concentration of 25 ± 09 mg/kg. The general trend shows that Zn

concentration decreased with increasing depth which implies that Zn on surface soil originates mostly from anthropogenic sources which include mining, agricultural activities, and dumping of metal-contaminated wastes from domestic sources.

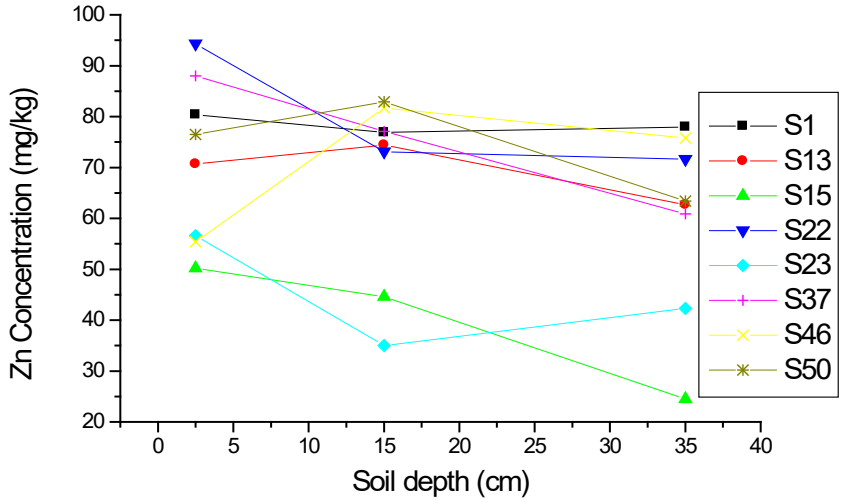


Figure 4.25: Zn concentration in soil samples with depth

The results of lead (Pb) concentration varied with depth from one sampling point to another as shown in figure 4.26.

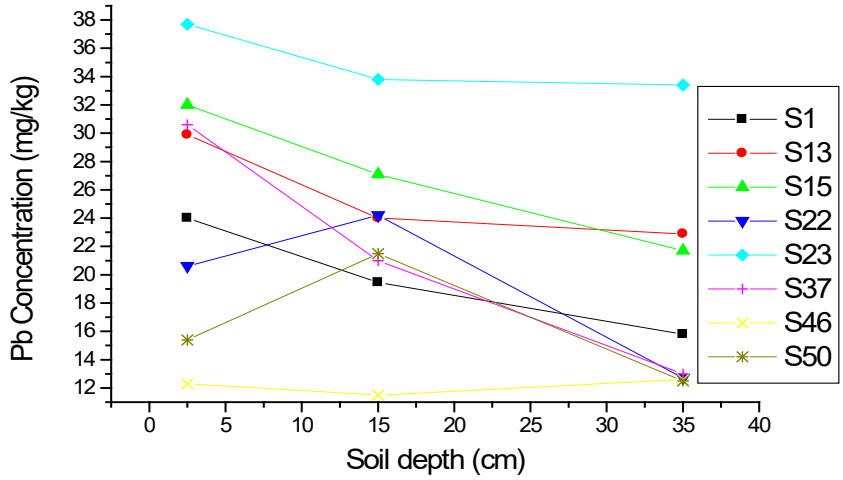


Figure 4.26: Pb concentration in soil samples with depth

The highest concentration of Pb was from the surface soil recorded at site S23 with a concentration of 38 ± 06 mg/kg and the lowest was recorded at a depth of 0 cm to 5 cm and 10 cm to 20 cm at site S46 with a concentration of 12 ± 07 mg/kg. The general trend shows a decrease in Pb concentration with increasing depth which implies that the high level of Pb were found on the surface soil and this might be as a result of human activities like use of fertilizers containing high levels of Pb, deposition of soils with high levels of Pb from other regions and dumping of wastes with high levels of Pb.

The results of the average elemental concentration with depth in the soil samples collected in Ortum show that heavy metals Cu, Zn and Pb generally reduce with increasing depth while that of Ni increases slightly with increasing depth as shown in Figure 4.27.

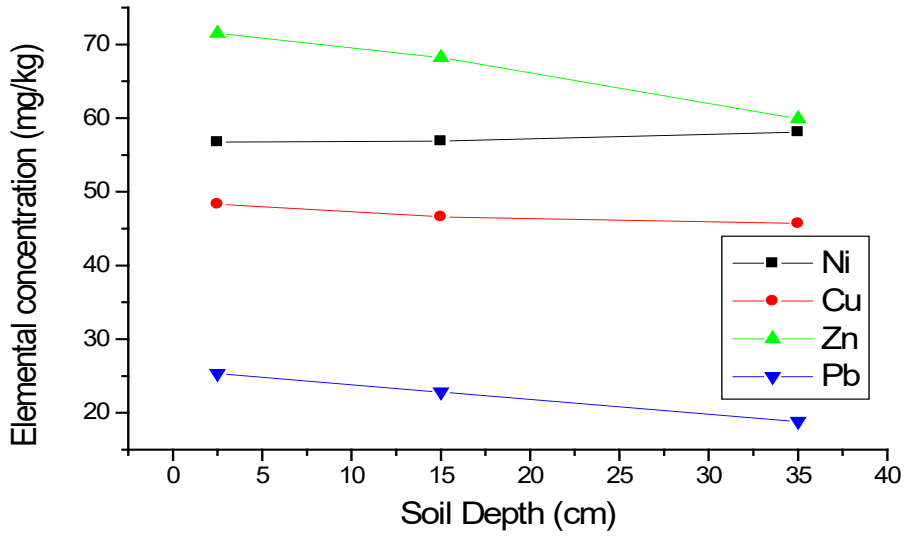


Figure 4.27: Average elemental concentration of Ni, Zn, Cu and Pb in soil with depth

### 4.4.5 Metal pollution indices $I_{geo}$, $E_i$ and $E_r$

The Geoaccumulation index ($I_{geo}$), potential ecological risk ($E_i$) and Synthesized potential ecological risk ($E_r$) were evaluated for heavy metals Ni, Cu, Zn and Pb pollution in soil samples using Equations 3.14, 3.15 and 3.16 respetively. The results abtained are shown in Table 4.13 and the classification was done using Table 3.2 and Table 3.3.

Table 4.13: Metal pollution indices $I_{geo}$, $E_i$ and $E_r$ (Ojenkunle *et al*., 2016)

| **Metal** | **($C_i$)** | **($B_i$)** | **($T_i$)** | **$I_{geo}$** | **pollution classification ($I_{geo}$)** | **$E_i$** | **Risk Index level (Ei)** |
|---|---|---|---|---|---|---|---|
| **Ni** | 58.11 | 56.97 | 5 | -0.56 | Unpolluted | 5.10 | Low risk |
| **Cu** | 46.91 | 22.20 | 5 | 0.49 | unpolluted to moderately polluted | 10.57 | Low risk |
| **Zn** | 73.49 | 47.42 | 1 | 0.047 | unpolluted to moderately polluted | 1.55 | Low risk |
| **Pb** | 22.2 | 44.87 | 5 | -1.60 | Unpolluted | 2.47 | Low risk |
| | | **Average** | | **-0.40** | **unpolluted to moderately polluted** | $Er = \sum_{i=1}^{n} Ei$ **=19.69** | **Low risk** |

The average $I_{geo}$, $E_i$ and $E_r$ were -0.40, 4.92 and 19.69 respectively. This show that the soil in Ortum is between unpolluted and moderately polluted with heavy metals Ni, Cu, Zn and Pb according to the metal pollution classification by Ojenkunle *et al.,* (2016) and the risk associated with the measured elemental concentration of Ni, Zn, Cu and Pb in soils is low as shown in the Table 4.13. The $I_{geo}$ revealed that metal contamination for the selected metals Ni, Cu, Zn and Pb was in the order of Cu > Zn > Ni > Pb.

## 4.5 Results of water sample analysis

### 4.5.1 Water pH analysis

The average Hydrogen Ion Concentration (pH) of the sampled river water was found to be 7.07 ± 0.41 which is neutral while that for borehole water was found to be 6.56 ± 0.16 which is slightly acidic. The results show that the pH of all water sources (rivers and boreholes) in Ortum range from pH 6.50 ± 0.21 to pH 7.71 ± 0.07 which is within the acceptable range of pH 6.5 to 8.5 given by WHO, (2011) for drinking water. The results imply that water pH from the rivers and boreholes in Ortum is at safe levels. The results of the water sampling point location, altitude and the pH were recorded as shown in Table 4.14.

Table 4.14: Water sampling point location, altitude and pH

| **Water Samples** | **Altitude** | **Longitude (E)** | **Latitude (N)** | **pH** |
|---|---|---|---|---|
| WS1 | 1438 | 35° 21′ 18.44″ | 1° 25′ 55.2″ | 6.95 |
| WS2 | 1423 | 35° 21′ 18.1″ | 1° 25′ 55.8″ | 6.81 |
| WS3 | 1418 | 35° 21′ 23.1″ | 1° 25′ 56.7″ | 6.80 |
| WS4 | 1408 | 35° 21′ 22.9″ | 1° 26′ 14.1″ | 7.73 |
| WS5 | 1414 | 35° 21′ 14.1″ | 1° 26′ 8.6″ | 7.71 |
| WS6 | 1419 | 35° 21′ 32.6″ | 1° 26′ 7.9″ | 7.05 |
| WS7 | 1421 | 35° 21′ 32.23″ | 1° 26′ 3.4″ | 7.15 |
| WS8 | 1416 | 35° 21′ 29.6″ | 1° 26′ 17.9″ | 7.25 |
| WS9 | 1403 | 35° 21′ 17.8″ | 1° 26′ 22.8″ | 6.72 |
| **WS10** | 1401 | 35° 21′ 21.2″ | 1° 26′ 25.2″ | 6.50 |
| **Average** | | | | **7.067** |

### 4.5.2 Analysis of ICP-OES reference materials

The results of analyzing standard solutions, (ICP Multi-Element Standard Solution) with known concentrations were recorded as shown in Table 4.15. The statistical correlation comparison results show that the instrument is accurate and gives good and reliable data with a correlation of r = 99.90% between the measured and the standard values.

Table 4.15: Results of measured elemental levels for standard solutions

| | **Standards (ppm)** | | | | | | | **Reference** |
|---|---|---|---|---|---|---|---|---|
| **Element** | **Blank** | **Std 1** | **Std 2** | **Std 3** | **Std 4** | **Std 5** | **Measured** | **Spk7.0/0.7** |
| Ag | 0 | 0.2 | 0.4 | 0.6 | 0.8 | 1.0 | 0.71 | 0.7 |
| Al | 0 | 0.2 | 0.4 | 0.6 | 0.8 | 1.0 | 0.70 | 0.7 |
| As | 0 | 0.2 | 0.4 | 0.6 | 0.8 | 1.0 | 0.68 | 0.7 |
| Ba | 0 | 0.2 | 0.4 | 0.6 | 0.8 | 1.0 | 0.70 | 0.7 |
| Ca | 0 | 2.0 | 4.0 | 6.0 | 8.0 | 10 | 6.93 | 0.7 |
| Cd | 0 | 0.2 | 0.4 | 0.6 | 0.8 | 1.0 | 0.70 | 0.7 |
| Co | 0 | 0.2 | 0.4 | 0.6 | 0.8 | 1.0 | 0.70 | 0.7 |
| Cr | 0 | 0.2 | 0.4 | 0.6 | 0.8 | 1.0 | 0.70 | 0.7 |
| Cu | 0 | 0.2 | 0.4 | 0.6 | 0.8 | 1.0 | 0.68 | 0.7 |
| Fe | 0 | 0.2 | 0.4 | 0.6 | 0.8 | 1.0 | 0.70 | 0.7 |
| K | 0 | 2.0 | 4.0 | 6.0 | 8.0 | 10 | 7.05 | 0.7 |
| Mg | 0 | 2.0 | 4.0 | 6.0 | 8.0 | 10 | 7.01 | 0.7 |
| Mn | 0 | 0.2 | 0.4 | 0.6 | 0.8 | 1.0 | 0.70 | 0.7 |
| Mo | 0 | 0.2 | 0.4 | 0.6 | 0.8 | 1.0 | 0.71 | 0.7 |
| Na | 0 | 2.0 | 4.0 | 6.0 | 8.0 | 10 | 6.83 | 0.7 |
| Ni | 0 | 0.2 | 0.4 | 0.6 | 0.8 | 1.0 | 0.71 | 0.7 |
| Pb | 0 | 0.2 | 0.4 | 0.6 | 0.8 | 1.00 | 0.70 | 0.7 |
| Se | 0 | 0.2 | 0.4 | 0.6 | 0.8 | 1.0 | 0.72 | 0.7 |
| Zn | 0 | 0.2 | 0.4 | 0.6 | 0.8 | 1.0 | 0.70 | 0.7 |

### 4.5.3 Elemental concentration in water samples

The elemental concentration in 10 water samples obtained from rivers and boreholes in Ortum was done using Agilent 5100 ICP-OES and the results obtained were recorded as shown in Table 4.16. The abundance of elements in the water samples was in the order Ca > Na > Mg > K > Ba > Ni > Al > As > Pb > Fe > Co > Mo > Ag > Cr > Se > Cu > Zn > Cd > Mn. The average elemental concentration for all 18 elements analyzed in water samples collected from the rivers and boreholes in Ortum were below the WHO threshold levels except for Ca as shown in Table 4.16.

Table 4.16: Results of mean elemental concentration in water samples (mg/L)

| Element (ppm) | WS1 | WS2 | WS3 | WS4 | WS5 | WS6 | WS7 | WS8 | WS9 | WS10 | Mean | Mean. River | Mean Borehole | WHO mg/L) |
|---|---|---|---|---|---|---|---|---|---|---|---|---|---|---|
| **Nickel (Ni)** | 0.0517 | 0.0371 | 0.0504 | 0.0435 | 0.0533 | 0.0443 | 0.0479 | 0.0393 | 0.0026 | 0.0014 | **0.0372±0.0192** | **0.046±0.006** | **0.002±0.0008** | **0.2** |
| **Copper (Cu)** | 0.0007 | 0.0018 | 0.0003 | 0.0029 | 0.0023 | 0.0015 | 0.0012 | 0.0019 | 0.0008 | 0.0005 | **0.0014±0.0001** | **0.0016±0.0001** | **0.0007±0.0002** | **2.00** |
| **Zinc (Zn)** | 0.0004 | 0.0004 | 0.0008 | 0.0004 | 0.0006 | 0.0007 | 0.0006 | 0.0008 | 0.0002 | 0.0001 | **0.0005±0.001** | **0.0006±0.0002** | **0.0002±0.0000** | **3.00** |
| **Lead (Pb)** | 0.0017 | 0.0025 | 0.0072 | 0.0081 | 0.0032 | 0.0042 | 0.0056 | 0.0082 | 0.0008 | 0.0007 | **0.004±0.002** | **0.005±0.002** | **0.0008±0.0000** | **0.01** |
| **Silver (Ag)** | 0.0018 | 0.0056 | 0.0016 | 0.0021 | 0.0074 | 0.0022 | 0.0051 | 0.0024 | 0.0012 | 0.0007 | **0.003±0.002** | **0.004±0.002** | **0.0010±0.0004** | **0.10** |
| **Aluminum (Al)** | 0.0230 | 0.0194 | 0.0261 | 0.0219 | 0.0347 | 0.0242 | 0.0204 | 0.0161 | 0.0091 | 0.0122 | **0.021±0.007** | **0.023±0.005** | **0.0107±0.0022** | **0.20** |
| **Arsenic (As)** | 0.0045 | 0.0101 | 0.0093 | 0.0098 | 0.0115 | 0.0095 | 0.0112 | 0.0089 | 0.0028 | 0.0021 | **0.008±0.003** | **0.009±0.002** | **0.0025±0.0005** | **0.01** |
| **Barium (Ba)** | 0.1521 | 0.1241 | 0.1409 | 0.1401 | 0.0727 | 0.1322 | 0.1274 | 0.1299 | 0.1115 | 0.1027 | **0.123±0.023** | **0.127±0.282** | **0.1071±0.0062** | **2.00** |
| **Calcium (Ca)** | 70.34 | 45.05 | 78.16 | 73.40 | 72.64 | 62.27 | 75.92 | 78.58 | 83.53 | 98.20 | **73.81±13.78** | **70±12** | **91±10** | **75.00** |
| **Cadmium (Cd)** | 0.0005 | 0.0001 | 0.0001 | 0.0002 | 0.0007 | 0.0004 | 0.0001 | 0.0001 | 0.0000 | 0.0001 | **0.0002±0.0001** | **0.0003±0.002** | **0.0001±0.0000** | **0.003** |
| **Cobalt (Co)** | 0.0053 | 0.0021 | 0.0052 | 0.0036 | 0.0018 | 0.0043 | 0.0029 | 0.0032 | 0.0035 | 0.0038 | **0.0038±0.0011** | **0.0036±0.0015** | **0.0037±0.0002** | **0.04** |
| **Chromium (Cr)** | 0.0018 | 0.0039 | 0.0028 | 0.0025 | 0.0011 | 0.0032 | 0.0039 | 0.0038 | 0.0025 | 0.0021 | **0.0027±0.0011** | **0.0029±0.0010** | **0.0023±0.0002** | **0.05** |
| **Iron (Fe)** | 0.0034 | 0.0042 | 0.0036 | 0.0019 | 0.0024 | 0.0032 | 0.0041 | 0.0045 | 0.0079 | 0.0048 | **0.0040±0.0016** | **0.0034±0.0008** | **0.0064±0.0021** | **0.30** |
| **Potassium (K)** | 3.964 | 4.391 | 4.242 | 5.175 | 9.227 | 6.847 | 5.334 | 4. 562 | 7.469 | 8.342 | **6.11±1.92** | **5.59±2.04** | **7.906±0.6173** | **10.00** |
| **Magnesium (Mg)** | 47.62 | 18.54 | 47.05 | 46.56 | 22.88 | 37.51 | 36.43 | 41.98 | 43.44 | 39.82 | **38.18±10.03** | **37.32±13.00** | **41.63±2.5597** | **60.00** |
| **Manganese (Mn)** | 0.0003 | 0.0001 | 0.0002 | 0.0003 | 0.0001 | 0.0003 | 0.0002 | 0.0002 | 0.0003 | 0.0003 | **0.0002+0.0008** | **0.0002±0.000** | **0.0003±0.0000** | **0.50** |
| **Molybdenum (Mo)** | 0.0036 | 0.0029 | 0.0042 | 0.0041 | 0.0048 | 0.0034 | 0.0037 | 0.004 | 0.0004 | 0.0008 | **0.0032±0.0015** | **0.0038±0.0007** | **0.0006±0.0002** | **0.004** |
| **Sodium (Na)** | 50.90 | 27.90 | 51.92 | 52.68 | 31.26 | 47.24 | 47.90 | 50.01 | 53.68 | 55.26 | **46.87±9.47** | **44.97±11.11** | **54.47±1.1172** | **60.00** |
| **Selenium (Se)** | 0.0018 | 0.0028 | 0.0055 | 0.0018 | 0.0021 | 0.0022 | 0.0031 | 0.0019 | 0.0023 | 0.0027 | **0.0026±0.0011** | **0.0027±0.0014** | **0.0025±0.0003** | **0.01** |

The elemental concentration in water samples collected show that Ca, Co, Fe, K, Mn and Na was higher in borehole water than in the water collected from the river. Ni, Cu, Zn, Pb, Ag, Al, As, Ba, Cd, Cr, Mg, Mo and Se concentration was higher in water collected from the river than the borehole water. The average concentration of all elements was within the permissible levels by WHO, 2004 except for Ca in borehole water which was 91 ± 10 mg/l above the recommended 75 mg/l.

The results of elemental concentration in water samples collected show that heavy metal Ni, Cu, Zn and Ni were higher in river water than in borehole water and this might be as a result of dumping of wastes containing heaving metals in rivers and also agricultural activities close to the river which might lead to heavy metal contamination of the river water. The results show that the water from the rivers in Ortum is fit for domestic and industrial uses because they are not contaminated with heavy metals beyond the WHO (2014) threshold limits. It is recommended that water from the boreholes in Ortum is distilled to remove excess Ca before consumption.

To reduce water pollution from anthropogenic sources, it is recommended that the residents of Ortum should ensure that wastes containing heavy metals should not be dumped into the rivers to maintain the water quality in the rivers. Likewise washing and cleaning of household items and vehicles should not be done in the rivers to avoid possible contamination.

The variation of elemental concentration in water for the selected heavy metals of concern Pb, Zn, Cu and Ni, is shown in Figure 4.28. From the results, the levels of nickel concentration in river water is higher than in borehole water suggesting that there is a possible source of Ni contamination in river water in Ortum and this can be due to the geology of Ortum having high Ni concentration and also dumping of wastes in the rivers.

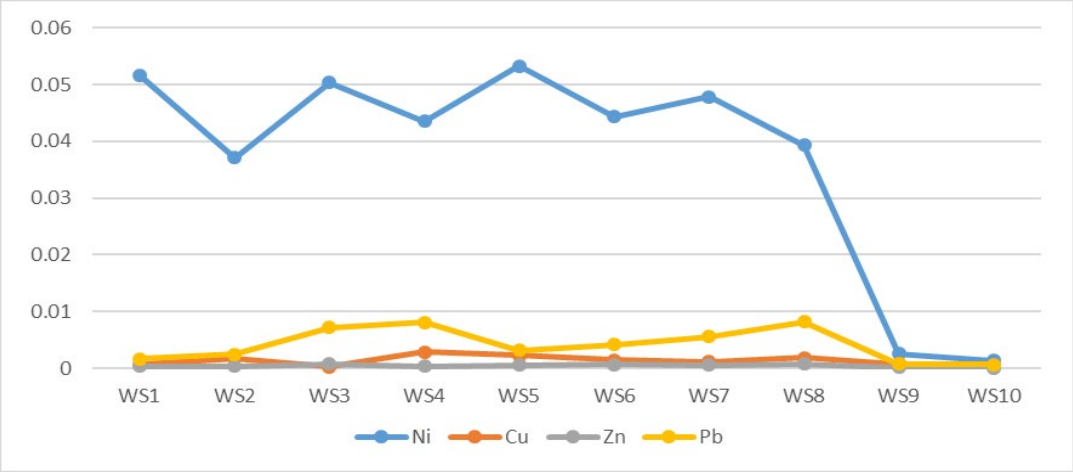


Figure 4.28: Elemental concentration of Ni, Cu, Zn and Pb in water samples

### 4.5.4 Water quality indices

The water quality indices Heavy Metal Pollution Index (MPI) and Metal Index (MI) were evaluated for Ortum water sources from the results of the elemental levels shown in Table.4.16. Water quality classification for the pH and concentration of each metal was done according to the Table 3.5 given by Singh *et al.,* 2016.

The Average MPI for heavy metals Ni, Cu, Zn, Pb, Cr and As was calculated using Equation 3.18 using the average values of heavy metals in water obtained from Table 4.16.

The MPI calculated was found to be 0.0036 which falls under "very lightly polluted water" according to the classification of Table 3.5. The heavy metal index (MI) was calculated using Equation 3.19 and the results recorded in Table 4.17. The average MI was found to be 0.3109 which falls within the classification of pure water category. The results from the water quality indices show that the water in Ortum is not polluted by heavy metals and therefore it is good for domestic, agricultural and industrial use.

Table 4.17: Ortum water quality classification according to Ojekunle *et al*., 2016

| **Element (ppm)** | **Average (mg/L)** | **WHO limits (mg/l)** | **MI** | **Classification** |
|---|---|---|---|---|
| **pH** | 7.07 | 6.5-8.8 | | Excellent |
| **Nickel (Ni)** | 0.03715 | 0.2 | 0.18575 | Good |
| **Copper (Cu)** | 0.00139 | 2 | 0.000695 | Excellent |
| **Zinc (Zn)** | 0.0005 | 3 | 0.000167 | Excellent |
| **Lead (Pb)** | 0.00422 | 0.01 | 0.422 | Good |
| **Silver (Ag)** | 0.00301 | 0.1 | 0.0301 | Good |
| **Aluminum (Al)** | 0.02071 | 0.2 | 0.10355 | Good |
| **Arsenic (As)** | 0.00797 | 0.01 | 0.797 | Good |
| **Barium (Ba)** | 0.12336 | 2 | 0.06168 | Good |
| **Calcium (Ca)** | 73.81 | 75 | 0.984133 | Poor |
| **Cadmium (Cd)** | 0.00023 | 0.003 | 0.076667 | Excellent |
| **Cobalt (Co)** | 0.00357 | 0.04 | 0.08925 | Good |
| **Chromium (Cr)** | 0.00276 | 0.05 | 0.0552 | Excellent |
| **Iron (Fe)** | 0.004 | 0.3 | 0.013333 | Excellent |
| **Potassium (K)** | 6.11 | 10 | 0.611 | Good |
| **Magnesium (Mg)** | 38.18 | 60 | 0.636333 | Good |
| **Manganese (Mn)** | 0.00023 | 0.5 | 0.00046 | Excellent |
| **Molybdenum** | 0.00319 | 0.004 | 0.7975 | Good |
| **Sodium (Na)** | 46.87 | 60 | 0.781167 | Good |
| **Selenium (Se)** | 0.00262 | 0.01 | 0.262 | Good |
| **Average MI** | | | **0.3109** | **Good** |

### 4.5.5 Cancer risk due to heavy metal intake in water

The cancer risk due to heavy metal Ni, Cd, Pb, Cr and As intake in water from Ortum was calculate using equation 3.20 a and 3.20 b. The average concentration of heavy metals in water for Ni, Cd, Pb, Cr and As was taken from Table 4.16 and the Cancer slope factor CSF was given by Markovic, 2020 (Pb = 0.85. Cr = 41, Cd = 6.1, Ni = 0.84, and As = 1.5) were used to calculate the cancer risk as shown in the Table 4.18.

Table 4.18: Results of cancer risk due selected heavy metals in water

| **Metal** | **Average Concentration (mg/L)** | **CSF (mg/kg/day)$^{-1}$** | **CDI Adult (mg/kg/day)** | **Cancer Risk** |
|---|---|---|---|---|
| Ni | 0.0372 | $8.4 \times 10^{-4}$ | $7.97 \times 10^{-4}$ | $6.70 \times 10^{-7}$ |
| Pb | 0.0042 | $8.5 \times 10^{-3}$ | $9.00 \times 10^{-5}$ | $7.65 \times 10^{-7}$ |
| Cd | 0.0002 | $6.1 \times 10^{-3}$ | $4.28 \times 10^{-6}$ | $2.61 \times 10^{-8}$ |
| Cr | 0.0027 | $4.1 \times 10^{-2}$ | $5.79 \times 10^{-5}$ | $2.37 \times 10^{-6}$ |
| As | 0.008 | $1.5 \times 10^{-3}$ | $1.71 \times 10^{-4}$ | $2.57 \times 10^{-6}$ |
| **$LTCR_{WP}$** | | | | **$1.92 \times 10^{-6}$** |

The lifetime cancer risk due to intake of heavy metals Ni, Cd, Pb, Cr and As in water from Ortum falls within the acceptable range of $1 \times 10^{-6}$ and $1 \times 10^{-4}$ given by Markovic *et al*., 2020. The sum of the cancer risk ($LTCR_{WP}$) from heavy metals Ni, Cd, Pb, Cr and As was found to be equal to $1.92 \times 10^{-6}$ which is within the acceptable range. This indicates that about 2 out of 1 million or 0.00019% of the people in Ortum are likely to die of cancer due to intake of water from Ortum.

### 4.6 Exposure due to radon and thoron

The results of the track densities from CR-39 plates from mud houses varied from one house to another and was recorded as shown in Table 4.19. The equilibrium equivalent thoron concentration (EETC) was calculated using equation 3.21 and the radon and thoron concentration was calculated using equation 3.22 and 3.23 respectively and the results shown in Table 4.20.

Table 4.19: Results of average track density and EETC

| | **House geographic position** | | **CR-39 ID Plate** | **Track density** | **EETC (Bq/m3)** |
|---|---|---|---|---|---|
| **House 1** | 1° 26'17.4" N | 35°21' 26.8" E | G151 -154 | 8.1 ± 0.5 | 4.7 ±1.1 |
| **House 2** | 1° 25'53.4" N | 35° 21' 22.5" E | G222-226 | 14.5 ± 2.6 | 18.8 ± 1.5 |
| **House 3** | 1° 26'04.5" N | 35° 21' 57.1" E | G055-058 | 1.5 ± 0.2 | 0.9 ± 0.6 |
| **House 4** | 1° 25'46.2" N | 35° 21' 48.5" E | G051-054 | 10.2 ± 0.5 | 6.0 ± 1.2 |
| **House 5** | 1° 25'28.6" N | 35° 21' 38.8" E | G043-046 | 18.4 ± 0.7 | 10.7 ± 1.0 |
| **House 6** | 1° 25'47.2" N | 35° 22' 17.4" E | G063-066 | 12.3 ± 0.6 | 7.2 ± 1.1 |
| **House 7** | 1° 25'30.1" N | 35° 22' 6.85" E | G087-090 | 2.5 ± 0.2 | 1.4 ± 0.3 |
| | | | **Average** | **9.64 ± 0.76** | **5.67 ± 0.97** |

Table 4.20: Results of radon and thoron concentration (Bq/$m^3$)

| **Radon** | **$C_{Rn}$ (Bq/m3)** | **$E_{Rn}$ mSv/y** | **Thoron** | **$C_{Tn}$ (Bq/$m^3$)** | **$E_{Th}$ mSv/y** |
|---|---|---|---|---|---|
| **G025** | 16± 6 | 0.4032 | G026 | 47 ±14 | 0.2632 |
| **G013** | 46± 7 | 1.1592 | G014 | 110 ±30 | 0.6160 |
| **G029** | 72 ±13 | 1.8144 | G030 | 35 ±16 | 0.1960 |
| **G021** | 49 ±7 | 1.2348 | G022 | 73 ±26 | 0.4088 |
| **G019** | 38 ±5 | 0.9576 | G020 | 55 ±20 | 0.3080 |
| **G023** | 46 ±7 | 1.1592 | G024 | 42 ±20 | 0.2352 |
| **G015** | 18 ±7 | 0.4536 | G016 | 18 ±11 | 0.1008 |
| **Average** | **40 ±19** | **1.03** | | **54 ±30** | **0.304** |

The results show that radon and thoron concentration ranged from 16 ± 6 to 72 ± 13 Bq/$m^3$ with an average of 40 ± 19 Bq/$m^3$ and 18 ± 11 to 110 ± 30 Bq/$m^3$ with an average of 54 ± 30 Bq/$m^3$ respectively. The average radon concentration falls within the world average value of 40 Bq/$m^3$ as reported by Chen *et al*., 2015 while thoron concentration is 5 times higher than the world average concentration of 10 Bq/$m^3$ given by UNSCEAR, (2000). The radon and thoron concentration is mud house in Ortum were lower than the lower limit of 100 Bq/$m^3$ and a higher limit of 300 Bq/$m^3$ except for G013 which had thoron value slightly above the WHO, 2009 lower limit.

This implies that residents of Ortum are exposed to low levels of thoron and radon and hence low risk of respiratory infections including lung cancer. It is recommended that houses in Ortum should be constructed with good ventilation to allow radon and thoron to escape from the houses hence reducing exposure to radon and thoron gas. Similar study was conducted in mud house in Mrima Hills in Kenya (Chege *et al*., 2015) where the average radon and thoron concentration were found to be 34 Bq/$m^3$ and 652 Bq/$m^3$ respectively which indicates that thoron concentration is above the WHO, 2009 recommended limit of 300 Bq/$m^3$. Studies in Canada by Chen *et al*., 2015 found that the average concentrations of radon and thoron was 96 Bq/$m^3$ and 9 Bq/m3 respectively which is below the recommended lower limit.

### 4.7 Results of dose and cancer risk evaluation using RESRAD

The RESRAD ONSITE computer code was used to calculate the dose and the lifetime cancer risk for residents in Ortum using the resident farmer exposure scenario model (Yu *et al*., 2001). RESRAD considers the external gamma dose, dust inhalation dose and soil ingestion dose pathways as shown in Figure 4.29. The parameters in Table 4.21 were used in the RESRAD program to simulate the dose and cancer risk as shown in Figure 4.30. The results from the simulation in terms of graphs and reports can be accessed as shown in Figure 4.31.

Table 4.21: The parameters used for RESRAD computation

| | **Parameter** | **Value** |
|---|---|---|
| 1. | Soil activity concentration | $^{40}$K – 11486.4 pCi/g (425 Bq/kg) |
| | | $^{232}$Th -1513.5 pCi/g (56 Bq/kg) |
| | | $^{238}$U - 1081 pCi/g (40 Bq/kg) |
| 2. | Times for Calculation | 1, 30, 70 and 100 years |
| 3. | Exposure duration | 100 years |
| 4. | Study area | 5 km$^2$ |
| 5. | Inhalation rate | 8400 m$^3$/year (Yu *et al*., 2001) |
| 6. | Soil ingestion | 36.5 g/year (Yu *et al*., 2001) |
| 7. | Drinking water intake | 510 l/kg (Yu *et al*., 2001) |
| 8. | Storage times before use | 1 day (Yu *et al*., 2001) |

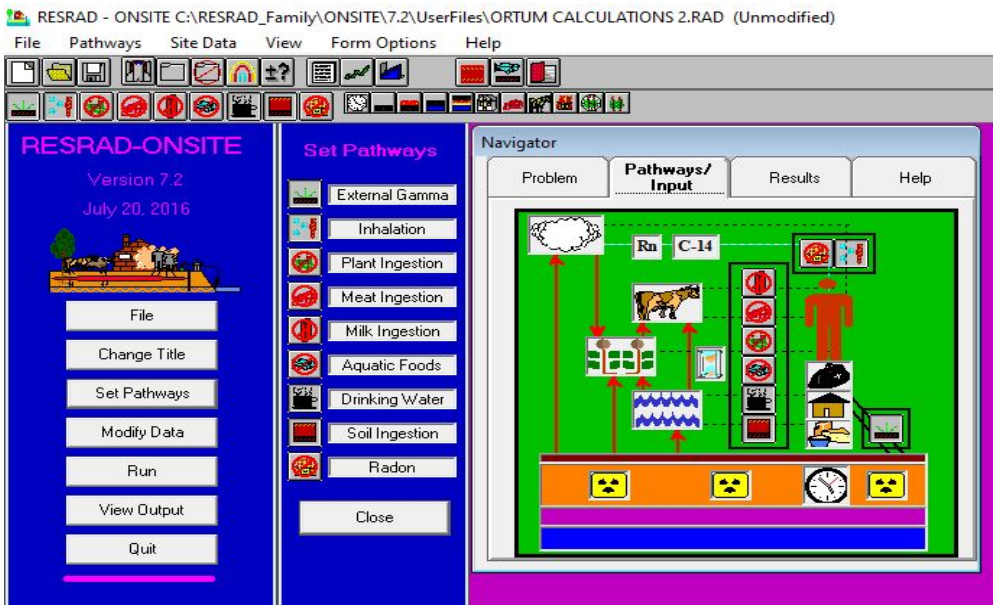


Figure 4.29: RESRAD pathway navigation display

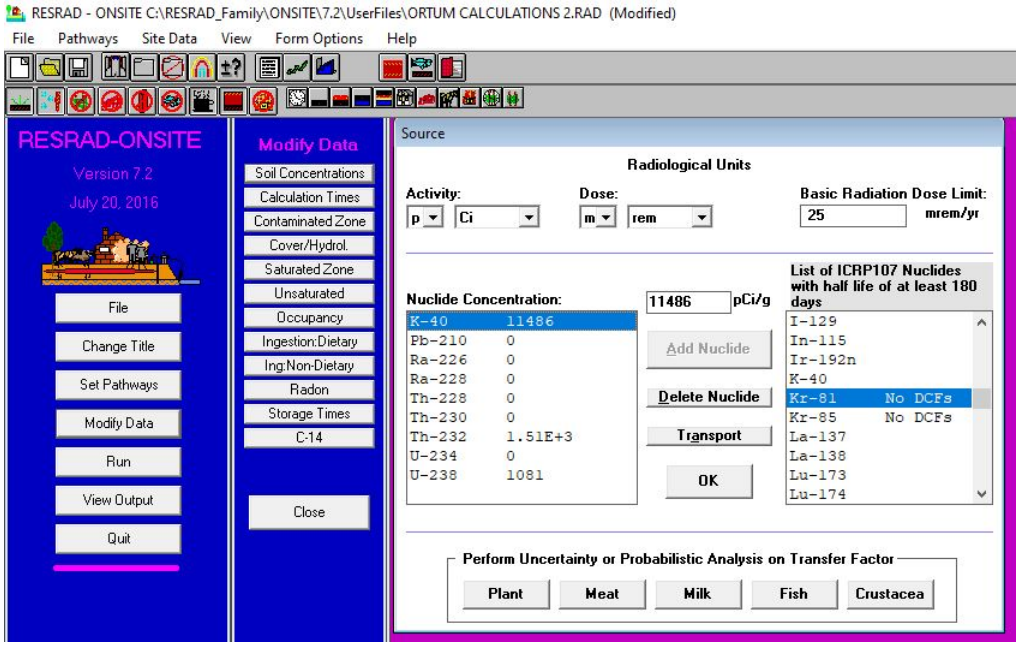


Figure 4.30: RESRAD soil concentration data input display

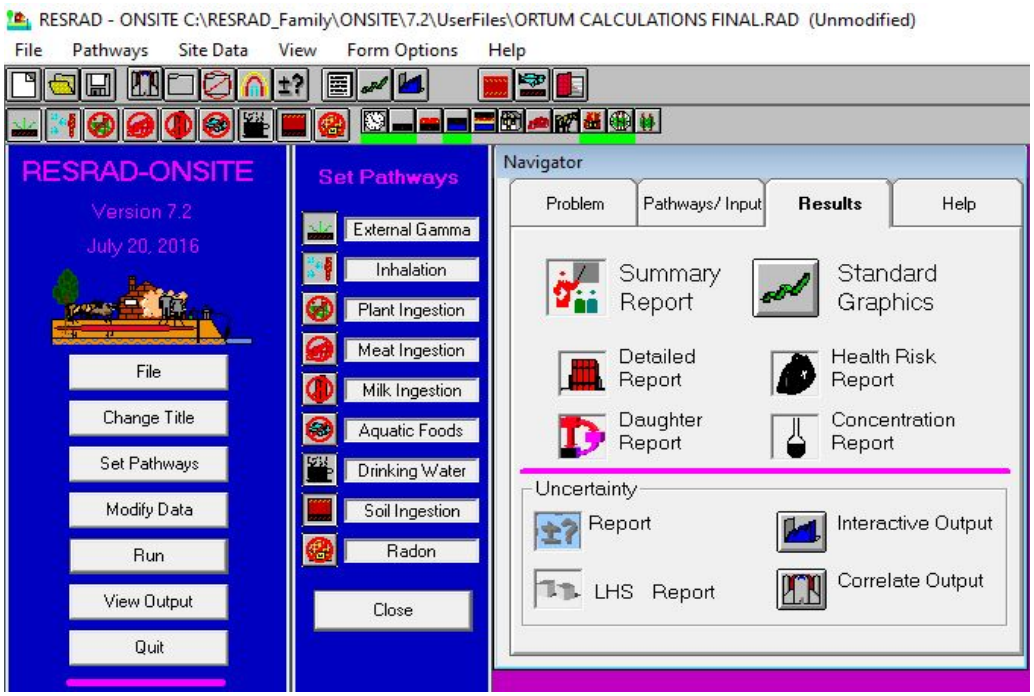


Figure 4.31: RESRAD results navigation display

The RESRAD ONSITE programme assumes that the risk and dose have a linear relationship which means that increase in the dose received increases the risk of getting cancer. The average activity concentration for $^{232}$Th, $^{238}$U and $^{40}$K in Bq/kg was converted to pCi/g using the conversion 1 Bq/kg = 27.03 pCi/g and used in the RESRAD program.

### 4.7.1 Dose received from background radiation using RESRAD program

The results of annual dose received by an individual from background radiation calculated using the RESRAD ONSITE code program by inputing the average concentration of $^{238}$U, $^{232}$Th and $^{40}$K in the soil were recorded in Table 4.22 and shown in Figure below.

Table 4.22: The dose contribution from $^{232}$Th, $^{238}$U and $^{40}$K for all pathways

| Time (years) | $^{40}$K (mrem/year) | $^{232}$Th (mrem/year) | $^{238}$U (mrem/year) | Total Dose (mrem/year) |
|---|---|---|---|---|
| **T = 0** | 2.70 E +01 | 1.13 E+00 | 1.18 E-02 | 2.82 E +01 |
| **T = 1** | 2.43 E +01 | 4.73 E+00 | 1.39 E-02 | 2.92 E +01 |
| **T = 10** | 9.41 E +00 | 5.56 E +01 | 3.07 E-03 | 6.53 E +01 |
| **T =30** | 1.14 E+00 | 8.91 E+01 | 5.53 E-03 | 9.18 E+02 |
| **T = 70** | 1.04 E+00 | 1.37 E+02 | 7.13 E-03 | 1.39 E+02 |
| **T = 100** | 1.01 E+00 | 1.69 E+02 | 6.86 E-03 | 1.72 E+02 |

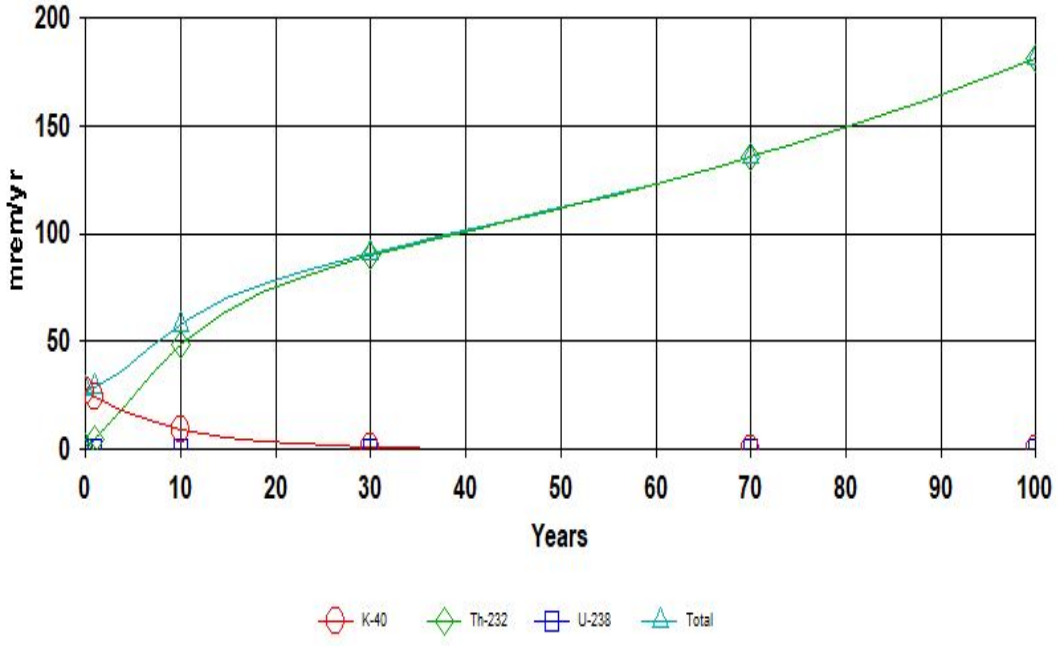


Figure 4.32: Dose for all pathways summed for 232Th, 238U and 40K

Figures 4.32 shows annual dose received due to $^{232}$Th, $^{238}$U and $^{40}$K radionuclides by the resident farmer through external, inhalation and soil ingestion pathways. The Figure 4.31

shows that a significant amount of dose is received from $^{232}Th$ because the dose rate due to gamma radiation from the thorium decay chain is greater than that from the uranium decay chain. Dose increases with time increases from about 30 mrem/y to about 180 mrem/y after 100 years. The figure show a general increase in the dose with time. Thorium ($^{232}Th$) is the highest contributor to the total dose followed by potassium ($^{40}K$) and lastly uranium ($^{238}U$).

The dose due to potassium reduces with time due to the decrease in the concentration of potassium in the soil as a result of leaching. Accumulated dose from all pathways and all nuclides increases with time from about 30 mrem/y (0.3 mSv/y) to 139 mrem/y (1.39 mSv/y) after 70 years which is below the recommended dose limit 2.4 mSv/y (240 mrem/y), and not exceeding 50 mSv/y in any single year (ICRP, 2007). This shows that exposure to radiation in Ortum is low and does not cause any significant health concerns to the people.

### 4.7.2 Results of RESRAD lifetime cancer risk

The results of cancer risk calculation from RESRAD programme was obtained from equation 3.27 and 3.28 and results tabulated as shown in figures 4.33.

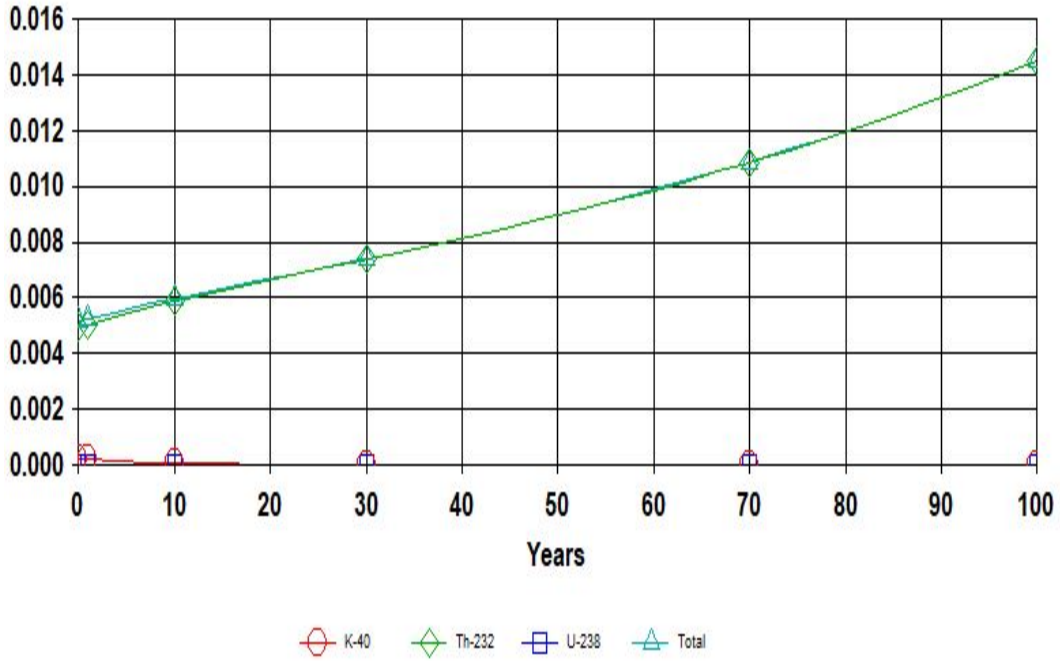


Figure 4.33: All pathway cancer risk summed for $^{232}Th$, $^{238}U$ and $^{40}K$

The Figures 4.33 show the cancer risk due to exposure received from $^{232}Th$, $^{238}U$ and $^{40}K$ by Ortum resident farmer scenario from external, inhalation and soil ingestion pathways. The highest contributor to cancer risk is $^{232}Th$ followed by $^{238}U$ and lastly $^{40}K$.

The data obtained show a general increase in cancer risk with time from 0.005 at time = 0 to about 0.145 after 100 year. This implies that a resident farmer who has lived in Ortum for 70 years has 0.011 or 1.1% chance of getting cancer due to background radiation in Ortum. This implies that 1 out of 100 people who have lived in Ortum have a chance of getting cancer.

The risk due to inhalation of radon and thoron was not inputted directly into the RESRAD program for dose and cancer risk evaluation because the risk due to radon and thoron is

based on the uranium concentration in soil (Ziajahromi *et al.,* 2015). Comparing the calculated lifetime cancer risk due to background radiation ($LTCR_{BR}$) (0.00147) and RESRAD lifetime cancer risk (0.011) due to background radiation, it is noted that the value for $LTCR_{BR}$ is less than the RESRAD value. because the RESRAD program takes into account all sources of radiation including contribution from radon and thoron, radiation in food and radiation in drinking water which leads to a higher cancer risk and sometime may lead to overestimation of the final dose or cancer risk.

The results show that the lifetime cancer risk in Ortum is low compared to other regions with high levels of $^{232}Th$, $^{238}U$ and $^{40}K$ and hence the risk of getting cancer in Ortum due to exposure to background radiation is low.

# CHAPTER FIVE: CONCLUSIONS AND RECOMMENDATIONS

## 5.1 Conclusions

The study provides important baseline data on background radiation in air, soil and rocks and the elemental concentration in soil, rocks and water from Ortum which is located in West-Pokot county in Kenya. The results from the study shows that the average outdoor absorbed dose rate in air at a height of 1 m above the ground at 61 different sampling points was 112 ± 30 nGy/h which is nearly twice the world average value of 60 nGy/h, (UNSCEAR, 2000).

The average activity concentration of radionuclides $^{238}U$, $^{232}Th$, and $^{40}K$ in soil samples collected from Ortum were slightly above the world average levels. The activity concentration of $^{238}U$ and $^{232}Th$ in the soils samples slightly reduce with increase in depth while the activity concentration of $^{40}K$ increased with increase in depth. The average radiation indices External Radiation Index ($H_{ex}$) and Internal Radiation Index ($H_{in}$) were found to be 0.41 and 0.52 respectively which is lower than unity (<1) recommended by UNSCEAR, 2000. This implies that the radiological risk associated with the use of soils from the region is insignificant and hence the soil and rock from the region may be used for construction of dwellings, agriculture and other industrial purposes.

The results of the average radon ($^{222}Rn$) and thoron ($^{220}Rn$) concentration in mud houses in Ortum were found to be 10 $Bq/m^3$ and 54 $Bq/m^3$ respectively. This is within the world average value and lower than the threshold lower and upper limits of 100 $Bq/m^3$ and 300 $Bq/m^3$ recommended by WHO, 2009. This implies that there is low risk of residents of

Ortum getting cancer due to exposure to radon and thoron in the mud dwellings. It should be noted that chronic exposure to even small amounts of radon and thoron can still lead to lung cancer. Hence residents in Ortum should ensure that their houses are well ventilated to reduce the concentration of radon and thoron gas in the houses.

The result of the lifetime cancer risk ($LTCR_{BR}$) due to background radiation exposue was found to be $1.47 \times 10^{-3}$ (0.147%). The cancer risk simulation using the RESRAD ONSITE programme for a resident farmer who has lived in Ortum for 70 years was found to be $1.1 \times 10^{-2}$ which implies that there is a 1.1% chance of the resident farmer getting cancer. The risk calculated using the RESRAD program is higher because RESRAD takes into account all sources of radiation including radon and thoron. The results show that the radiological risk due to exposure to background radiation in Ortum is low.

The elemental concentration of the 13 elements analysed in the soil samples from Ortum fall within the world average range. The elemental concentration of Pb, Zn, Ni, K, Ca, Ti, Mn, Rb, Sr, Y and Zr were found to exceed the world average values while those of Cu and Fe were lower than the world average values given by Towett *et al*., 2015. The Geoaccumulation Index ($I_{geo}$), Potential Ecological Risk Index ($E_i$) and Synthesized Potential Ecological Risk Index ($E_r$) metal pollution indices in soils were found to be -0.40, 4.92 and 19.69 respectively. This according to the classification index by Wu *et al*., 2018 implies that the soil is moderately polluted and the risk associated to heavy metal concentration in soils is low.

The results of elemental concentration in soils with depth for the metals of interest Pb, Zn, Cu and Ni show that Pb, Zn and Cu concentration in soils samples reduced slightly with increase in depth implying that the top soils containing high levels of heavy metals may have originated from anthropogenic sources or other places in the surrounding environment since the concentration of heavy metals in rocks is less than that of the soil samples. The concentration of Ni increased with increasing depth indicating that there is high downward mobility of Ni which may be due to leaching effect. The result of the the elemental concentration in soil and rock samples indicate that they are lower than the threshold levels and hence they do not pose any significant health risk to the residents of Ortum.

The elemental concentration in water samples was within the WHO, 2011 permissible limits except for Nickel (Ni) and calcium (Ca) which were slightly higher in river water and borehole water respectively. The presence of heavy metals Zn, Ni, Cu, Cd and Pb in water is attributed to geological and anthropogenic origin which include agricultural activities, mining and damping of hospital and domestic wastes in rivers. The low population in Ortum may have resulted to low levels of water pollution from industrial and domestic sources.

The results of pH analysis show that the pH of all water samples from different sources and sampling points in Ortum fall within the permissible limits set by WHO for safe drinking water with an average pH of $7.07 \pm 0.41$ which is neutral. The Average MPI was found to be equal to 0.0034 which falls under very lightly polluted water while the average

heavy metal index (MI) was found to be 0.399 which falls within pure water classification. The pH and the heavy metal indices show that all water sources in Ortum are safe for domestic, agricultural and industrial use.

The lifetime cancer risk ($LTCR_{WP}$) due to of heavy metals Ni, Cd, Pb, Cr and As intake in water was found to be $1.92 \times 10^{-6}$ which falls within the acceptable range of $1 \times 10^{-6}$ and $1 \times 10^{-4}$ given by Markovic *et al*., 2020. This implies that about 2 out of 1 million people in Ortum are likely to die of cancer due to intake of heavy metals in water from Ortum. Hence the risk of getting cancer for a resident of Ortum due to exposure to heavy metals in water in negligible.

This study provides the baseline data on exposure to background radiation and elemental concentration in soil and water in Ortum. The results show that exposure to background radiation and heavy metals in Ortum is within the acceptable limits and that people in Ortum should effectively manage and use soil and water resources resources to avoid contamination.

## 5.2 Recommendations

i. The results of this study show that the background radiation in air and levels of radionuclides $^{238}U$, $^{232}Th$, and $^{40}K$ are within the acceptable limits. However, further studies need to be conducted to identify sources of high levels of radiation in air and in soils around the quarry and Cheranganyi hills in Ortum.

ii. The average experimental dose rate in air (112 ± 30 nGy/h) was found to be about twice the calculated dose rate in air (ADRA) (69 ± 23 nGy/h). Further studies need to be conducted to find out why we have the big difference and identify the possible sources of high outdoor absorbed dose rate in air.

iii. Based on the results of the $^{238}U$, $^{232}Th$, and $^{40}K$ in soil and rock samples, further studies should be carried out to find out find out why soil samples have higher levels of radionuclides than the rock samples and also identify sources of high levels of radionuclides in soil samples in Ortum.

iv. Radon and thoron concentration was within the WHO limits but above the world average levels. The data found can be used in setting up reference levels for national radon policy to minimize exposure. Residents in Ortum are encouraged to build well ventilated houses to reduce exposure to radon and thoron gas.

v. The elemental concentration in soil and water samples are within the permissible levels for domestic and industrial applications. However, proper methods of waste disposal should be put in place to avoid possible contamination of soil and water resources in the region. Further research is recommended to investigate reasons for

some heavy metal reducing with depth including migration of heavy metals into the groundwater and plants.

vi. This research study on background radiation and elemental concentration levels in Ortum may be used as baseline data for public information and for policy development.

vii. This study can be extended to cover other regions of West Pokot and Kenya.

## REFERENCES

Abelard, (2004). Ionising radiation and health - risk analysis (https://www.abelard.org/briefings/ionising-radiation.php).

Ahmad, A. Y., Al-Ghouti, M. A., AlSadig, I., and Abu-Dieyeh, M. (2019). Vertical distribution and radiological risk assessment of 137 Cs and natural radionuclides in soil samples. Scientific reports, 9(1), 1-14.

Al-Zahrani, 2017. Estimation of natural radioactivity in local and imported polished granite used as building materials in Saudi Arabia. *Journal of Radiation Research and Applied Sciences,* 10 (2017) 241-245.

Ali A., Hussain H., Mohammed H. and Suha H., (2015). Radon Concentration in selected samples of tap water in Baghdad Government/Iraq. Research Journal of Applied Sciences, Engineering and Technology 11(12): 1358-1364, 2015 ISSN: 2040-7459; e-ISSN: 2040-7467

Balakrishnan, A., and Ramu, A. (2016). Evaluation of heavy metal pollution index (HPI) of ground water in and around the coastal area of Gulf of Mannar biosphere and Palk Strait. Journal of Advanced Chemical Sciences, 331-333.

Beretka, J. and Mathew P. J. (1985). Natural radioactivity of Australian building materials, industrial wastes and by-products. *Health Physics* 48: 87-95.

Bray, F., Ferlay, J., Soerjomataram, I., Siegel, R. L., Torre, L. A., and Jemal, A. (2020). Global cancer statistics 2018: GLOBOCAN estimates of incidence and mortality worldwide for 36 cancers in 185 countries. CA: a cancer journal for clinicians, 68(6), 394-424.

Brimhal, W.H. and Adams J.A.S., (1982). Concentration changes of thorium, uranium and metals in hydrothermally altered Conway Granite. New Hampshire. *Geochimica and Cosmochimica Acta* 33**:** 130-131.

Campbell, G. S., and Norman, J. M. (1998). Radiation basics. In An introduction to environmental biophysics (pp. 147-165). Springer, New York, NY.

Cetnar, J. (2006). General solution of Bateman equations for nuclear transmutations. Annals of Nuclear Energy, 33(7), 640-645.

Chege, M. W., Hashim, N. O., Merenga, A. S., Meisenberg, O., and Tschiersch, J. (2015). Estimation of annual effective dose due to radon and thoron concentrations in mud

dwellings of Mrima Hill, Kenya. Radiation protection dosimetry, 167(1-3), 139-142.

Chen, J., Bergman, L., Falcomer, R., and Whyte, J. (2015). Results of simultaneous radon and thoron measurements in 33 metropolitan areas of Canada. Radiation protection dosimetry, 163(2), 210-216.

Deng, W., Wang, Y., Liu, Z., Cheng, H., and Xue, Y. (2014). HemI: a toolkit for illustrating heatmaps. PloS one, 9(11), e111988.

Elliott, H. A. L., Wall, F., Chakhmouradian, A. R., Siegfried, P. R., Dahlgren, S., Weatherley, S., and Deady, E. (2018). Fenites associated with carbonatite complexes: A review. Ore Geology Reviews, 93, 38-59.

Environmental Protection Agency (EPA) (1997). Exposure factors handbook. Washington, DC, EPA/600/P-95/002F a-c.

Environmental Protection Agency (EPA, 2017). Radiation Protection: Health Effects. https://19january2017snapshot.epa.gov/radiation/radiation-health-effects_.html.

Ehleringer, J. R., Barnette, J. E., Jameel, Y., Tipple, B. J., and Bowen, G. J. (2016). Urban water–a new frontier in isotope hydrology. Isotopes in environmental and health studies, 52(4-5), 477-486.

Fakhri, Y., Kargosha, M., Langarizadeh, G., Zandsalimi, Y., Amirhajeloo, L. R., Moradi, M., and Mirzaei, M. (2016). Effective dose radon 222 of the tap water in children and adults people; Minab city, Iran. Global journal of health science, 8(4), 234.

Farai, I. P., Obed R. I. and Jibri N. N. (2006). Soil radioactivity and incidence of cancer in Nigeria. *Journal of Environmental Radioactivity* 90: 29-36.

Fereira, A. D. O., and Pecequilo, B. R. (2019). Dose rates evaluation of some granitic rocks from the Paraná state.

Finestone, E. M., Braun, D. R., Plummer, T. W., Bartilol, S., and Kiprono, N. (2020). Building ED-XRF datasets for sourcing rhyolite and quartzite artifacts: A case study on the Homa Peninsula, Kenya. Journal of Archaeological Science: Reports, 33, 102510.

Ford, C. A. (2007). Debating disarmament: Interpreting article VI of the treaty on the non-proliferation of nuclear weapons. Nonproliferation Review, 14(3), 401-428.

Hashim, N. O. (2001) the levels of radionuclides and elements in selected Kenyan coastal ecosystem. M.Sc. Thesis, Kenyatta University, Nairobi, Kenya.

Hashemi, M., Akhoondi, L., Saghi, M. H., and Eslami, A. (2019). Assessment of indoor gamma radiation and determination of excess lifetime cancer risk in Tehran in winter and spring 2017. Radiation protection dosimetry, 184(2), 148-154.

Health Physics Society, (2010). *Environmental Radiation Fact sheet*. https://hps.org/documents/environmental_radiation_fact_sheet.pdf

Hendrichs, J., Vreysen, M. J. B., Enkerlin, W. R., and Cayol, J. P. (2005). Strategic options in using sterile insects for area-wide integrated pest management. In Sterile insect technique (pp. 563-600). Springer, Dordrecht.

Hain, M., Bartl, J., and Jacko, V. (2005). The use of infrared radiation in measurement and non-destructive testing. Measurement science review, 5(3), 10-14.

Holmes-Siedle, A., and Adams, L. (1993). Handbook of radiation effects.

Hughes, C. E., Airey, P. L., Duran, E. B., Miller, B. M., and Sombrito, E. (2004). Using radiotracer techniques for coastal hydrodynamic model evaluation. Journal of environmental radioactivity, 76(1-2), 195-206.

IAEA, (1987). IAEA -Soil-7, Report IAEA/RL/l12

IAEA, (1997). Sampling, storage and sample preparation procedures for X ray fluorescence analysis of environmental materials. Technical Reports Series No. 486 Pp 10-11.

IAEA, (2003). Guidelines for radioelement mapping using gamma ray spectrometry data. IAEA, Vienna Austria. Pp 13.

IAEA, (2018). Worldwide Interlaboratory Comparison on the Determination of Trace Elements and Methyl Mercury in Sediment Sample. IAEA-MESL-ILC-TE-SEDIMENT-2018.

IAEA, (2019). Guidelines on soil and vegetation sampling for radiological monitoring.

ICRP (2007). ICRP recommendations by Streffer, C. Radiation protection dosimetry, 127(1-4), 2-7.

Johri, N., Jacquillet, G., and Unwin, R. (2010). Heavy metal poisoning: the effects of cadmium on the kidney. Biometals, 23(5), 783-792.

Kebwaro, J, I. V. S Rathore, N. O. Hashim and A.O. Mustapha (2011). Radiometric Assessment of natural radioactivity levels around Mrima Hill, Kenya. *International Journal of Physical Sciences*. 6, 3105-3110.

Kinyua, A. (1982). Multi-element analysis of solid and liquid samples by X-ray Fluorescence. M.Sc. Thesis, University of Nairobi. Pp 15-25.

Koki, I. B., Bayero, A. S., Umar, A., and Yusuf, S. (2015). Health risk assessment of heavy metals in water, air, soil and fish. African journal of pure and applied chemistry, 9(11), 204-210.

Kolb, D. K., Hill, J. W., and McCreary, T. W. (2012). Chemistry for changing times. Pearson Higher Ed.

Krieger, R. (1981). Radioactivity of construction materials. *Betonwerk fertigteil-technik* 47**:** 468-473.

Kumar, A., Usha, N., Sawant, P. D., Tripathi, R. M., Raj, S. S., Mishra, M., and Kushwaha, H. S. (2011). Risk assessment for natural uranium in subsurface water of Punjab State, India. Human and Ecological Risk Assessment, 17(2), 381-393.

Kumar, R., Sengupta, D., and Prasad, R. (2003). Natural radioactivity and radon exhalation studies of rock samples from Surda Copper deposits in Singhbhum shear zone. Radiation Measurements, 36(1-6), 551-553.

Lawrence, A. (2002). United States Government Department of Energy.

Marković, S., Vučković, B., Nikolić-Bujanović, L., Kurilić, S. M., Todorović, N., Nikolov, J., and Đokić, B. (2020). Heavy metals and radon content in spring water of Kosovo. Scientific reports, 10(1), 1-12.

McClellan, T., Deenik, J., and Singleton, P. (2013). Soil nutrient management for Maui county. College of Tropical Agriculture and Human Resources (CTAHR). University of Hawaii at Manoa. Retrieved on, 26.

Mohammadi, A. A., Zarei, A., Majidi, S., Ghaderpoury, A., Hashempour, Y., Saghi, M. H., and Ghaderpoori, M. (2019). Carcinogenic and non-carcinogenic health risk assessment of heavy metals in drinking water of Khorramabad, Iran. MethodsX, 6, 1642-1651.

Mohanty, A. K., Sengupta, D., Das S. K., Saha, S. K. and Van K. V. (2004). Natural radioactivity and radiation exposure in the high background area at chhatrapur beach placer deposit of Orissa,India. *Journal of environmental Radioactivity* **75:** 15-33.

Moussa, B. and Mounia, T. (2015). X-Ray Fluorescence Analytical Techniques. Centre National des Sciences et Technologies Nucléaires (CNSTN). Pp 25-38.

Molins, R. A. (Ed.). (2001). Food irradiation: principles and applications. John Wiley & Sons.

Mustapha, A. O., Patel J. p. and Rathore, I. V. S (1999). Assessment of human exposures to natural sources of radiation. *Journal of Radiation Protection Dosimetry* **82:** 285-292.

National Cancer Institute (2015). Cancer causing substances in the environment. USA.

Njuguna, S. M., Yan, X., Gituru, R. W., Wang, Q., and Wang, J. (2017). Assessment of macrophyte, heavy metal, and nutrient concentrations in the water of the Nairobi River, Kenya. Environmental monitoring and assessment, 189(9), 1-14.

Ntengwe, F. W. (2005). An overview of industrial wastewater treatment and analysis as means of preventing pollution of surface and underground water bodies—the case of Nkana Mine in Zambia. Physics and Chemistry of the Earth, Parts A/B/C, 30(11-16), 726-734.

Nwankwo, C. U, Ogundare F. O. and Folley D. E. (2015). Radioactivity concentration variation with depth and assessment of workers' doses in selected mining sites. *Journal of Radiation Research and Applied Sciences.* University of Ibadan, Nigeria 8: 216-220.

Ojekunle, O. Z., Ojekunle, O. V., Adeyemi, A. A., Taiwo, A. G., Sangowusi, O. R., Taiwo, A. M., and Adekitan, A. A. (2016). Evaluation of surface water quality indices and ecological risk assessment for heavy metals in scrap yard neighbourhood. SpringerPlus, 5(1), 1-16.

Organization for Economic Cooperation and Development (OECD) (1979). Exposure to radiation from the natural radioactivity in building materials. Report by a group of experts of the OECD Nuclear Energy Agency, Paris, France.

Otwoma D., Patel, J., Bartilol, S. and Mustapha A. (2013). Estimation of annual effective dose and radiation hazard due to natural radionuclides in mount Homa, southwestern Kenya. *Radiation protection Dosimetry Advances Access*. Oxford University Press. Pp 1-8.

Ozasa, K., Cullings, H. M., Ohishi, W., Hida, A., and Grant, E. J. (2019). Epidemiological studies of atomic bomb radiation at the Radiation Effects Research Foundation. International journal of radiation biology, 95(7), 879-891.

Patel J. P. (1991). Environmental Radiation survey of the area of high natural radioactivity of Mrima hill of Kenya. *Discovery and Innovation* 3: 31-35.

Poshtegal, M. K., and Mirbagheri, S. A. (2019). The heavy metals pollution index and water quality monitoring of the Zarrineh river, Iran. Environmental & Engineering Geoscience, 25(2), 179-188.

Ramli A. T., Wahab A. M. and Wood, A. K. (2004). Environmental $^{238}U$ and $^{232}Th$ concentration measurements in an area of high level natural background radiation at Palong, Johor, Malaysia. *Journal of Environmental Radioactivity* 80: 287-304.

Republic of Kenya (2011). Ministry of Public Health and sanitation and Ministry of Medical Services (2011). National Cancer Control Strategy 2011-2016. Pp 6-7.

Ribeiro, B. T., Nascimento, D. C., Curi, N., Guilherme, L. R. G., Costa, E. T. D. S., Lopes, G., and Carneiro, J. P. (2019). Assessment of Trace Element Contents in Soils and Water from Cerrado Wetlands, Triângulo Mineiro Region. Revista Brasileira de Ciência do Solo, 43.

Schroeyers, W. (Ed.). (2017). Naturally Occurring Radioactive Materials in Construction: Integrating Radiation Protection in Reuse (COST Action Tu1301 NORM4BUILDING). Woodhead Publishing.

Shaltout, A. A., Dabi, M. M., Ibrahim, M. M., Al-Ghamdi, A. S., and Elnagar, E. (2020). Applicability of low-cost binders for the quantitative elemental analysis of urinary stones using EDXRF based on fundamental parameter approach. Biological trace element research, 195(2), 417-426.

Singh, A. P., Dhadse, K., and Ahalawat, J. (2019). Managing water quality of a river using an integrated geographically weighted regression technique with fuzzy decision-making model. Environmental monitoring and assessment, 191(6), 1-17.

Stochioiu, A., Mihai, F., and Stochioiu, C. (2004). Environmental radioactivity assessment studies on placement area of the new extreme light infrastructure nuclear physics facility. Rom. J. Physics, 59, 808-816.

Tokonami S., H. Kudo, Y. Omori, T. Ishikawa, K. Iwaoka, S. K. Sahoo, N. Akata, m. Hosoda, P. Wanabongse, C. Pornnumpa, Q.Sun, X. Li and S. Akiba (2015). Comparative Dosimetry for Radon and Thoron in High Background Radiation Areas in China. Radiation Protection Dosimetry Pp 1-5.

Tokonami, S. (2010). Why is 220Rn (thoron) measurement important?. Radiation protection dosimetry, 141(4), 335-339.

Tzortzis, M., Tsertos, H., Christofides, S., and Christodoulides, G. (2003). Gamma-ray measurements of naturally occurring radioactive samples from Cyprus characteristic geological *rocks. Radiation Measurements* 37**:** 221–229.

UNSCEAR, (2000). Sources and effects of ionizing radiation. United Nations Scientific Committee on the Effects of Atomic Radiation. Report on the General Assembly on the effects of Atomic Radiation. United Nations, New York.

UNSCEAR, (2000) (United Nation Scientific Committee on the Effects of Atomic Radiation Report) Sources and effects of ionizing radiation. In Annex B: Exposure due to Natural Radiation Sources. Vol. 1 New York (NY): United Nation; 2000.

UNSCEAR, (2008). Sources and effects of ionizing radiation. United Nations Scientific Committee on the Effects of Atomic Radiation. Report to the General Assembly Volume 1, United Nations, New York Pp 233

UNSCEAR, (2012). Sources, effects and risks of ionizing radiation. United Nations Scientific Committee on the Effects of Atomic Radiation. Report to the General Assembly. United Nations, New York.

United Nations Scientific Committee on the Effects of Atomic Radiation. (2017). Sources, Effects and Risks of Ionizing Radiation, United Nations Scientific Committee on the Effects of Atomic Radiation (UNSCEAR) 2016 Report: Report to the General Assembly, with Scientific Annexes. United Nations.

US Energy Information Administration (2019). Electricity explained. Independent Statistics & Analysis.

Wanjala, F.O., Hashim, N.O., Otwoma, D. Nyambura, C., Kebwaro, J., Ndege, M. and Bartilol, S. (2020). Environmental assessment of heavy metal pollutants in soils and water from Ortum, Kenya. Environ Monit Assess 192, 118 doi:10.1007/s10661-020-8070-3

Wanjala, F. O., N O Hashim, D Otwoma, C Nyambura, J Kebwaro, A Mauring, J Bartilol, and M Chege (2019). Human exposure to background radiation in Ortum, Kenya, Radiation Protection Dosimetry. ncz264, https://doi.org/10.1093/rpd/ncz264

Wanjala, O. F., I. V. S. Rathore, and J. Murungi. "Assessment of heavy metals concentration in soils at selected Points on roads and sites around Nairobi using EDXRF Spectrometer." (2016).

Waterstram-Rich, K. M., and Gilmore, D. (2016). LIC-Nuclear Medicine and PET/CT: Technology and Techniques. Elsevier Health Sciences.

Wheal, M. S., Fowles, T. O., and Palmer, L. T. (2011). A cost-effective acid digestion method using closed polypropylene tubes for inductively coupled plasma optical emission spectrometry (ICP-OES) analysis of plant essential elements. Analytical Methods, 3(12), 2854-2863.

White, P. J., and Brown, P. H. (2010). Plant nutrition for sustainable development and global health. Annals of botany, 105(7), 1073-1080.

World Health Organization (WHO), (2004). Guidelines for drinking water quality. 3rd edition, Vol.1. Geneva: World Health Organization. Pp 315-324.

World Health Organization. (2009). WHO handbook on indoor radon: a public health perspective. World Health Organization.

World Health Organization (2011). Guidelines for drinking-water quality. WHO chronicle by Edition, F 38(4), 104-108.

World Health Organization (WHO), (2016). Ionizing radiation, health effects and protective measures. (https://www.who.int/news-room/fact-sheets/detail/ionizing-radiation-health-effects-and-protective-measures).

World Nuclear Association (WNA), (2012). Radiation, N. Health Effects.

Wu, W., Wu, P., Yang, F., Sun, D. L., Zhang, D. X., and Zhou, Y. K. (2018). Assessment of heavy metal pollution and human health risks in urban soils around an electronics manufacturing facility. Science of the Total Environment, 630, 53-61.

Wu, Z., Wang, X., Chen, Y., Cai, Y., and Deng, J. (2018). Assessing river water quality using water quality index in Lake Taihu Basin, China. Science of the Total Environment, 612, 914-922.

Yu, C., Zielen A. J., Cheng J.J., LePoire D.J., Gnanapragasam E., Kamboj S., Arnish J., Wallo III A., Williams W.A., and Peterson H. (2001). User's Manual for RESRAD Version 6. Environmental Assessment Division, Argonne National Laboratory.

Zanzonico, P., and Stabin, M. (2009). Benefits of medical radiation exposures. Health Physics Society. Available from: http://hps. org/hpspublications/articles/Benefitsofmedradexposures. html [Last accessed on].

Ziajahromi, S., Khanizadeh, M., and Nejadkoorki, F. (2015). Using the RESRAD code to assess human exposure risk to 226Ra, 232Th, and 40K in soil. Human and Ecological Risk Assessment: An International Journal, 21(1), 250-264.

# APPENDICES

## Appendix 1: Published papers

1. F O Wanjala, N O Hashim, D Otwoma, C Nyambura, J Kebwaro, A Mauring, J Bartilol, and M Chege (2019). HUMAN EXPOSURE TO BACKGROUND RADIATION IN ORTUM, KENYA, *Radiation Protection Dosimetry*, , ncz264, https://doi.org/10.1093/rpd/ncz264

2. Wanjala, F. O., Hashim, N. O., Otwoma, D., Nyambura, C., Kebwaro, J., Ndege, M., and Bartilol, S. (2020). Environmental assessment of heavy metal pollutants in soils and water from Ortum, Kenya. Environmental Monitoring and Assessment, 192(2), 118.

3. Wanjala, F.O., Otwoma, D., Kitao, T.F., and Hashim, N.O. (2015). Assessment of Natural Radioactivity and its Radiological Impact in Ortum Region in Kenya. *Radiation Safety for Sustainable Development,*(p. 176). Kenya (INIS)

4. Catherine Nyambura, Nadir Omar Hashim, Margaret Wairimu Chege, Shinji Tokonami and Felix Wanjala Omonya (2019) Cancer and non-cancer health risks from carcinogenic heavy metal exposures in underground water from Kilimambogo, Kenya. *Groundwater for Sustainable Development. Elsevier*. https://doi.org/10.1016/j.gsd.2019.100315

## Appendix 2: Conferences attended

1. F. W. Omonya, Dr. N. O. Hashim, Dr. D. Otwoma, C. Nyambura (2018). Human exposure to natural radioactivity in Ortum, Kenya Presented at the.5$^{th}$ African Regional IRPA Congress, 6 to 9 September 2018, Tunis, Tunisia.

2. F.O. Wanjala, N.O. Hashim, D. Otwoma, and Dr. Stephanie Handley-Sidhu (2017). Assessment of natural radioactivity in air in Ortum, Kenya. Presented at the 9th Hope meeting held at Tokyo International Forum Tokyo, Japan, from 27 February to 2 March 2017.

3. F.O. Wanjala, N.O. Hashim and D. Otwoma (2019) Peaceful Uses of Nuclear Science and Technology in Kenya. Presented at Kenyatta University Biennial Research and Innovation Conference held at Kenyatta University from 22 to 25 October 2019.

## Appendix 3: Uranium decay scheme

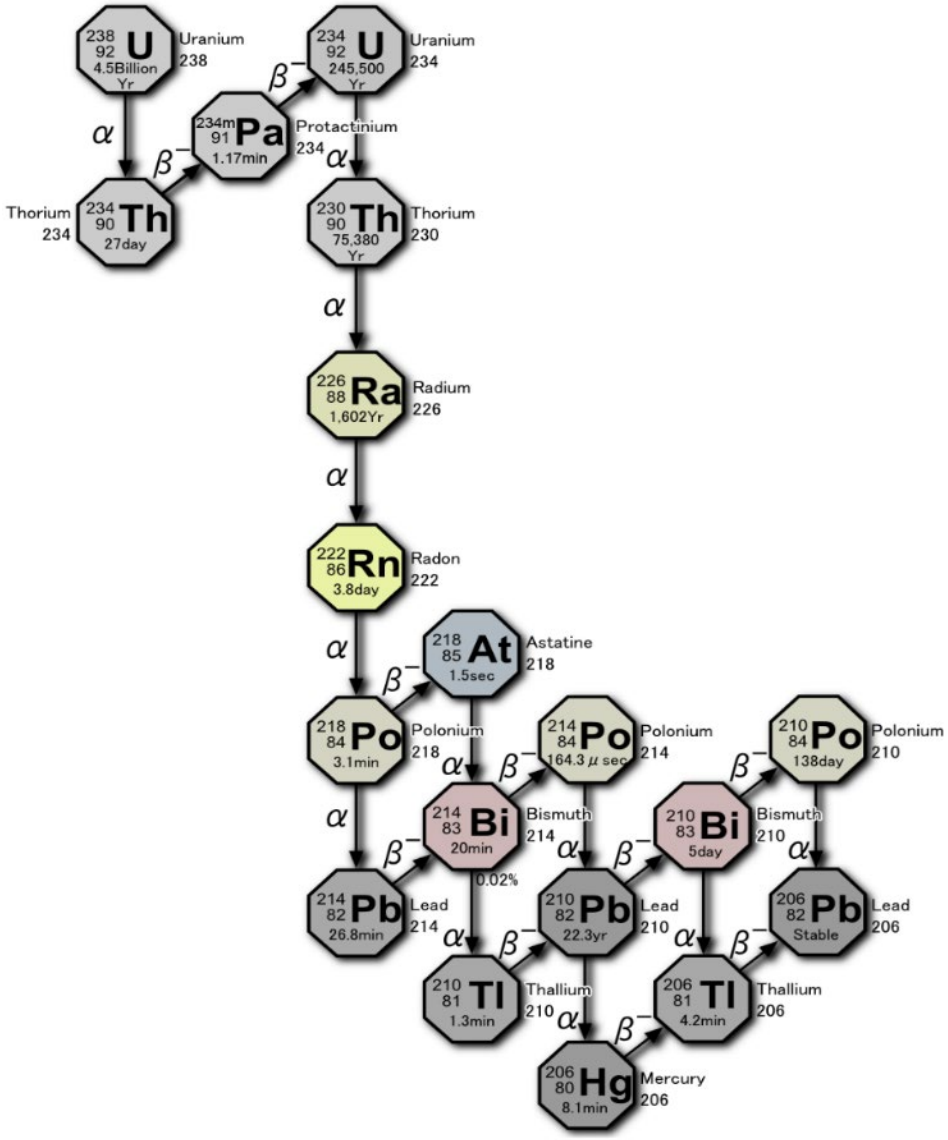

**Appendix 4: Thorium decay scheme**

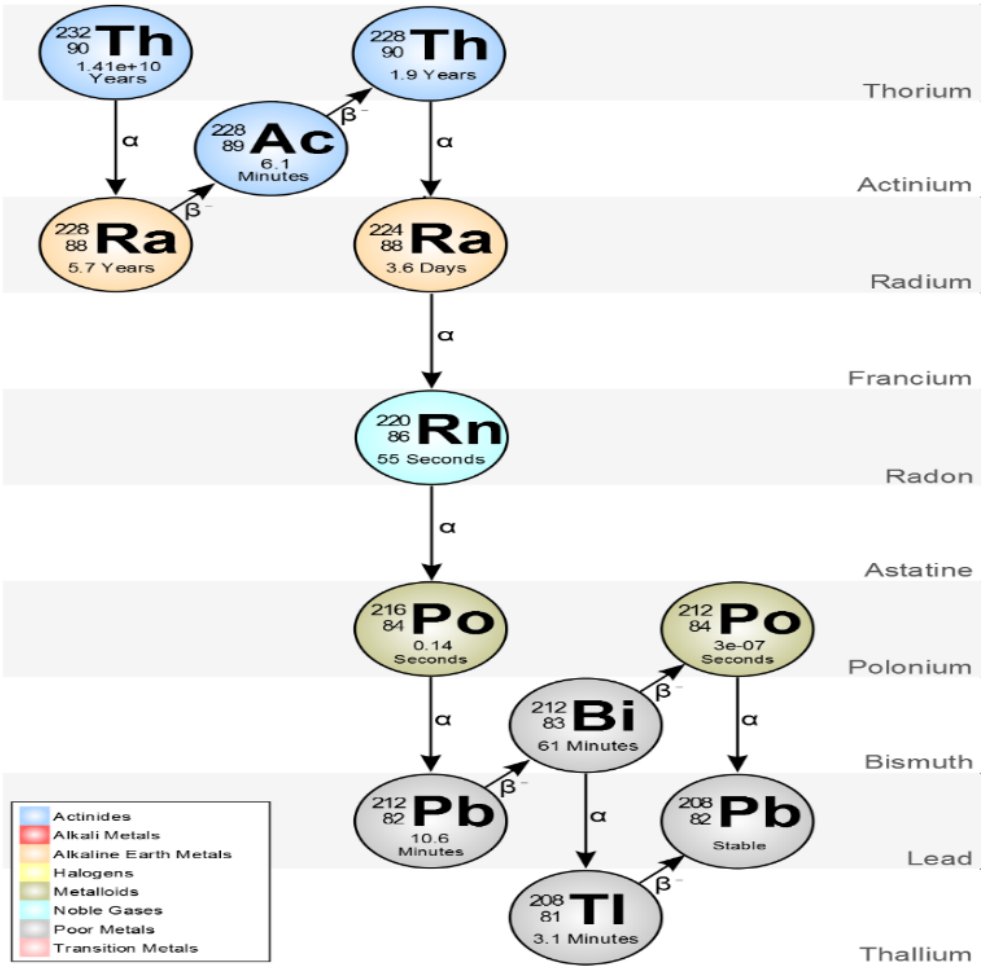

**Appendix 5: Table of radionuclides of interest with their energy and intensity**

| Radionuclide of interest | Radionuclide measured | Energy (keV) | Intensity (%) | Possibly interfering radionuclide |
|---|---|---|---|---|
| K-40 | K-40 | 1460.822 (6) | 10.55 (11) | Ac-228 (1459.131 keV; 0.87 %) |
| U-238 | Th-234 | 63.30 (2) | 3.75 (8) | Th-232 (63.811 keV; 0.259 %) |
| | Pa-234m | 766.361 (20) | 0.323 (4) | - |
| | | 1001.026 (18) | 0.847 (8) | Ac-228 (1001.69 keV; 0.0054 %) |
| Ra-226 | Ra-226 | 186.211 (13) | 3.555 (9) | U-235 (185.720 keV; 57.0 %) |
| | Pb-214 | 295.224 (2) | 18.414 (36) | - |
| | | 351.932 (2) | 35.60 (7) | Bi-211 (351.03 keV; 13.00 %) |
| | Bi-214 | 609.312 (7) | 45.59 (19) | - |
| Pb-210 | Pb-210 | 46.539 (1) | 4.252 (40) | Lanthanide x-rays |
| Ra-228 | Ac-228 | 338.320 (5) | 11.4 (4) | Ra-223 (338.282 keV; 2.85 %) |
| | | 911.196 (6) | 26.2 (8) | - |
| | | 968.960 (9) | 15.9 (5) | - |
| Th-228 | Pb-212 | 238.632 (2) | 43.6 (5) | Ra-224 (240.986 keV; 4.12 %) |
| | Tl-208 | 583.187 (2) | 85.0 (3) | Ac-228 (583.391 keV; 0.120 %) |
| U-235 | U-235 | 143.787 (3) | 10.94 (6) | Ra-223 (144.27 keV; 3.36 %) |
| | | | | Th-230 (143.872 keV; 0.049 %) |
| | | 163.356 (3) | 5.08 (3) | - |
| | | 185.720 (4) | 57.0 (3) | Ra-226 (186.211 keV; 3.555 %) |
| | | 205.316 (4) | 5.02 (3) | Th-227 (204.14 keV; 0.22 %) |
| | | | | (204.98 keV; 0.16 %) |
| | | | | (206.08 keV; 0.25 %) |
| | | | | Th-228 (205.99 keV; 0.0188 %) |
| Ac-227 | Th-227 | 235.96 (2) | 12.6 (6) | - |

## Appendix 6: Global cancer control

# Kenya

Source: Globocan 2020

### Number of new cases in 2020, both sexes, all ages

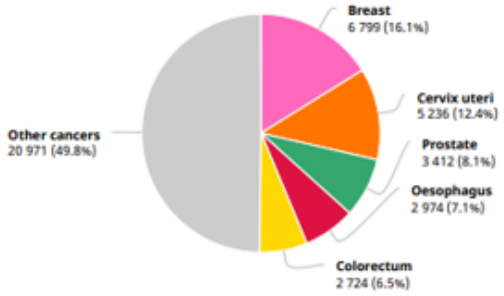


Total: 42 116

### Number of new cases in 2020, males, all ages

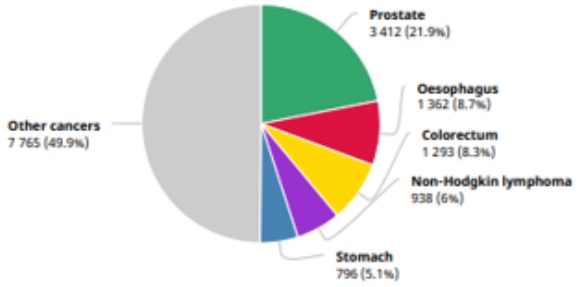


Total: 15 566

### Number of new cases in 2020, females, all ages

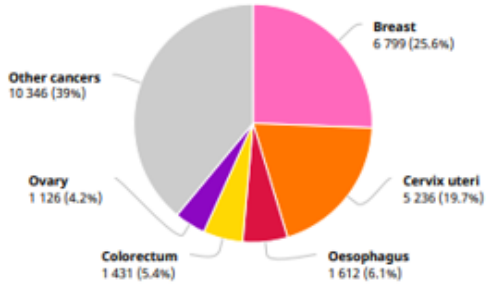


Total: 26 550

Total population

**53 771 300**

Number of new cases

**42 116**

Number of deaths

**27 092**

Number of prevalent cases (5-year)

**82 620**

**Appendix 7: Cancer cases from West-Pokot County (2019)**

D22

| | A | B | C |
|---|---|---|---|
| 1 | **MTRH CANCERS WEST POKOT - 2019** | **COUNT** | |
| 2 | CA BREAST | 14 | |
| 3 | CML-CHRONIC MYELOID LEUKAMIA | 8 | |
| 4 | HL-HODGKIN'S LYMPHOMA | 7 | |
| 5 | CA CERVIC | 7 | |
| 6 | AMMACUTE MYELOID LEUKAMIA | 2 | |
| 7 | CA COLON | 2 | |
| 8 | NHL NON HODGKIN'S LYMPHOMA | 2 | |
| 9 | RETINOBLASTOMA | 2 | |
| 10 | ALL-ACUTELYMPHOBLASTIC LEUKAMIA | 2 | |
| 11 | CA ANAL-RECTAL | 1 | |
| 12 | CA RECTUM | 1 | |
| 13 | CA NASOPHARYNGEAL | 1 | |
| 14 | DERMATOFIBROSARCOMA | 1 | |
| 15 | KS-KAPOSIS SARCOMA | 1 | |
| 16 | CA TESTICULAR | 1 | |
| 17 | SARCOMA | 1 | |
| 18 | MULTIPLE MYELOMA | 1 | |
| 19 | CA OESOPHAGUS | 1 | |
| 20 | GLIOMA | 1 | |
| 21 | CA OVARY | 1 | |
| 22 | **TOTAL** | **57** | |

## Appendix 8: Research permit

THIS IS TO CERTIFY THAT:
*MR. FELIX WANJALA OMONYA*
of KENYATTA UNIVERSITY, 0-100
Nairobi,has been permitted to conduct
research in *Westpokot County*

on the topic: *ASSESSMENT OF HUMAN EXPOSURE TO NATURAL RADIOACTIVITY AND ITS RADIOLOGICAL IMPACT IN ORTUM REGION IN KENYA*

for the period ending:
*15th January,2018*

Permit No : NACOSTI/P/15/7793/4722
Date Of Issue : 19th January,2015
Fee Recieved :0000

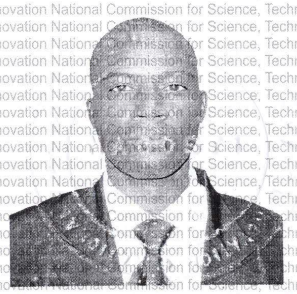

.....
*Applicant's Signature*

.....
*Secretary*
*National Commission for Science, Technology & Innovation*

**CONDITIONS**

1. You must report to the County Commissioner and the County Education Officer of the area before embarking on your research. Failure to do that may lead to the cancellation of your permit
2. Government Officers will not be interviewed without prior appointment.
3. No questionnaire will be used unless it has been approved.
4. Excavation, filming and collection of biological specimens are subject to further permission from the relevant Government Ministries.
5. You are required to submit at least two(2) hard copies and one(1) soft copy of your final report.
6. The Government of Kenya reserves the right to modify the conditions of this permit including its cancellation without notice

REPUBLIC OF KENYA

NACOSTI

National Commission for Science, Technology and Innovation

**RESEARCH CLEARANCE PERMIT**

Serial No. A 4016

CONDITIONS: see back page